TECHNISCHE UNIVERSITÄT MÜNCHEN

Institut für Maschinen und Fahrzeugtechnik, Lehrstuhl für Fahrzeugtechnik

METHODS FOR IMPROVING THE CONTROL OF TELEOPERATED VEHICLES

Tito Lu Tang Chen

Vollständiger Abdruck der von der Fakultät für Maschinenwesen der Technischen Universität München zur Erlangung des akademischen Grades eines

Doktor-Ingenieurs

genehmigten Dissertation.

Vorsitzende:	Univ.-Prof. Dr. rer. nat. S. Berensmeier
Prüfer der Dissertation:	1. Univ.-Prof. Dr.-Ing. M. Lienkamp
	2. Univ.-Prof. i.R. Dr. rer.nat.habil. H. Bubb

Die Dissertation wurde am 11.12.2014 bei der Technischen Universität München eingereicht und durch die Fakultät für Maschinenwesen am 22.04.2015 angenommen.

Kurzfassung

Ein fahrerloses Wegparken und Laden sowie die fahrerlose Bereitstellung von privaten Elektrofahrzeugen würde den Komfort von E-Fahrzeugbesitzern ohne eigene Ladestation erhöhen. Auch Car-Sharing Systeme würden – gerade mit Elektrofahrzeugen – von der Möglichkeit profitieren, die Fahrzeuge fahrerlos im Stadtgebiet zu verteilen, zu laden oder den Kunden bereitzustellen. Das Teleoperierte Fahren ist eine Lösung für diese Aufgabe. Hierbei wird die Umgebung des Fahrzeugs mittels Kameras erfasst und über eine Mobilfunkverbindung videokomprimiert an einen entfernt sitzenden Operator übermittelt. Dieser tätigt aufgrund der am Operatorarbeitsplatz dargestellten Bilder die geeigneten Lenk- und Pedalvorgaben, um das Fahrzeug zu steuern.

Da die Datenübertragung zwischen Fahrzeug und Operatorarbeitsplatz über eine Mobilfunkverbindung stattfindet, können Verbindungsabbrüche nicht vollkommen ausgeschlossen werden. Auch kann der Zeitpunkt des Verbindungsabbruchs nicht vorhergesagt werden. Um bei solchen Situationen trotzdem ein sicheres Fahren gewährleisten und das Fahrzeug in einen sicheren Zustand führen zu können, wurde das Konzept "Freier Korridor" entwickelt. Der "Freie Korridor" stellt den Bereich dar, den das Auto durchfahren würde, wenn zum aktuellen Zeitpunkt eine Vollbremsung eingeleitet werden würde. Die Aufgabe des Operators ist es, den Korridor stets frei von Hindernissen zu halten. Die Anzeige dieses Korridors wird direkt im Videobild eingezeichnet.

Ein weiteres bekanntes Problem bei teleoperierten Fahrzeugen ist das fehlende Situationsbewusstsein des Operators, wodurch die Fahrzeugführung erschwert wird. Um die richtigen Handlungsentscheidungen treffen zu können, ist eine möglichst vollständige Repräsentation des Verkehrsgeschehens und des aktuellen Fahrzeugzustands nötig. Einer der wichtigsten Faktoren ist das richtige Einschätzen der Geschwindigkeit, damit diese entsprechend der Verkehrssituation angepasst werden kann. Um die Fahraufgabe des Operators zu erleichtern, wurden Methoden für die Verbesserung des Geschwindigkeitsempfindens durch optische, auditive und haptische Rückmeldungen mittels "Unschärfe" (engl. Blur), synthetischer Motorgeräusche und Vibrationen am Sitz erforscht.

In dieser Dissertation wurden sowohl die Berechnungsmethoden und die Umsetzung des "Freien Korridors", als auch die Untersuchung der Methoden zur Erhöhung des Geschwindigkeitsempfindens am Operatorarbeitsplatz behandelt. Für den "Freien Korridor" wurden verschiedene Methoden zur Berechnung des Korridors und die entsprechenden Steuerungs- bzw. Regelungskonzepte in der Simulation untersucht, die für die Umsetzung am Realfahrzeug dienten. Es wurde nachgewiesen, dass das teleoperierte Fahrzeug mit Hilfe dieses Konzeptes in einen sicheren Zustand gebracht werden kann.

Für die Erhöhung des Geschwindigkeitsempfindens am Operatorarbeitsplatz wurden mehrere Probandenstudien durchgeführt, um die Wirksamkeit der vorgestellten Methoden zu belegen. Die Ergebnisse zeigten, dass Blur, synthetische Motorgeräusche und Vibrationen am Sitz das Geschwindigkeitsempfinden positiv beeinflussen und den Fahrer bei der Fahraufgabe unterstützen können.

Die Teleoperation ist eine Möglichkeit, unbemanntes Fahren in den öffentlichen Straßenverkehr zu bringen. Die in dieser Dissertation vorgestellten Methoden tragen zur Erreichung dieses Zieles bei.

Abstract

Owners of an electric vehicle without a personal charging station would greatly benefit from driverless parking, charging and provision of their vehicles. Similarly, car-sharing systems would benefit from the possibility of distributing vehicles throughout the city driverlessly. The teleoperation of vehicles is a solution for this task, where the vehicle's environment is captured using cameras. The information is video compressed and transmitted through a mobile connection to a remote sitting operator. The operator executes commands according to the depicted video through the steering wheel and the driving pedals to drive the vehicle.

Since the transmission of the information between the vehicle and the operator's working station takes place via mobile networks, connection losses cannot be completely ruled out. Furthermore, the exact time of connection loss cannot be predicted. Thus, in order to guarantee a safe driving in such situations, the safety concept "Free Corridor" was developed. The "Free Corridor" represents the area through which the vehicle would travel if an emergency braking was triggered at that moment. The task of the operator is to keep the corridor continually free of obstacles. The corridor is displayed directly on the video images.

In addition, a known problem with teleoperated vehicles is the situation awareness with the operator not being in the vehicle, which complicates the driving task. In order to make the right decisions, it is necessary to have a representation of the participating traffic and the vehicle's own state as complete as possible. One of the most important factors is the correct estimation of the vehicle's speed so that it can be adapted according to the traffic situation. In order to facilitate the operator's driving task, different methods to improve the speed perception were developed and studied. These include optical, auditive and haptical feedback using blur, artificial motor sounds and vibrations at the driver's seat.

Both the calculation methods and the implementation of the "Free Corridor" and the analysis of the methods to improve the speed perception at the working station are covered in this dissertation. For the "Free Corridor", different calculation methods and their corresponding control strategies were analyzed in the simulation. This served as the basis for the implementation at the experimental vehicle. Results showed the feasibility of the concept and its ability to bring the teleoperated vehicle to a safe state whenever the connection is lost.

For the analysis of the speed perception at the working station, several studies with test persons were conducted to verify the effect of the proposed methods. Results showed the positive effects of blur, artificial motor sound and vibration at the driver's seat on speed perception, allowing the operator to better fulfill the driving task.

Teleoperation is a way to achieve unmanned vehicles in the near future. The methods proposed in this dissertation further contribute to achieve the goal.

Vorwort

Die vorliegende Dissertation entstand während meiner Tätigkeit als wissenschaftlicher Mitarbeiter am Lehrstuhl für Fahrzeugtechnik der Technischen Universität München in den Jahren 2010 bis 2014.

Ganz besonders möchte ich meinem Doktorvater Prof. Dr.-Ing. Markus Lienkamp danken, der meine Arbeit betreuet hat und durch fachliche Anregungen und Diskussionen zum Gelingen dieser Dissertation beigetragen hat. Ich konnte durch die von ihm gewährte Freiheit und das Vertrauen wertvolle Erfahrungen sammeln.

Bei Herrn Prof. Dr. rer. nat. habil. Heiner Bubb möchte ich mich für die Zweitprüfung herzlich bedanken und für sein Interesse an dieser Arbeit. Weiterhin bedanke ich mich bei Frau Prof. Dr. rer. nat. Sonja Berensmeier für den Prüfungsvorsitz.

Meinen Kolleginnen und Kollegen am Lehrstuhl für Fahrzeugtechnik danke ich ebenfalls für die Unterstützung und die anregenden Diskussionen. Ein spezieller Dank gilt meinen Kollegen in der Gruppe Fahrerassistenz, vor allem bei den Kollegen Sebastian Gnatzig und Frederic Chucholowski möchte ich mich bedanken. Die Zusammenarbeit im Projekt war eine sehr wertvolle Erfahrung für mich. Ich möchte mich ebenfalls bei Herrn Dr.-Ing. Frank Diermeyer bedanken, der mich als Gruppenleiter während meiner Arbeit immer unterstützt und sich für Diskussionen bereit gestellt hat.

Ich danke auch allen von mir betreuten Studenden, die mit ihren Arbeiten und persönlichem Engagement das Forschungsprojekt unterstützt haben.

Ein herzlicher Dank gebührt meiner Familie, die mir volles Vertrauen geschenkt und mich bei meinen Plänen und Zielen unterstützt hat. Ganz besonders danke ich meiner Frau Yen-Wen für ihr volles Verständnis.

München, im Dezember 2014
Tito Tang

Symbols and Abbreviations

Symbols

a_{brake}	[m/s²]	Braking Deceleration
a_{max}	[m/s²]	Maximal Acceleration
a_y	[m/s²]	Lateral Acceleration
α	[rad]	Slip Angle
α_f	[rad]	Slip Angle at Front Wheels
α_r	[rad]	Slip Angle at Rear Wheels
b_{ego}	[m]	Ego-Vehicle Width
b_{obstacle}	[m]	Obstable Width
b_t	[m]	Track Width
b_w	[m]	Free Corridor Width
β	[rad]	Sideslip Angle
$\dot{\beta}$	[rad/s]	Sideslip Rate
c_0	[1/m]	Initial Curvature of a Clothoid
c_1	[1/m ²]	Constant Curvature Changing Rate
c_f	[N/rad]	Cornering Stiffness at the Front Wheels
c_r	[N/rad]	Cornering Stiffness at the Back Wheels
CoG	[-]	Center of Gravity
d	[m]	Length of each Segment used in the Calculation of Clothoids Braking Distance
d_{brake}	[m]	Braking Distance Needed To Avoid Frontal Collision with Obstacle
d_{evasion}	[m]	Minimal Needed Distance in Moving Direction to Obstacle for Evasion without Collision
δ_A	[rad]	Ackermann Steering Angle
δ_H	[rad]	Steering Wheel Angle
δ_f	[rad]	Steering Angle
Δv	[m/s]	Difference in Wheel Speed of Non-driven Axis
EG	[-]	Self-Steering Gradient
F_{res}	[N]	Resulting Transferable Tire Force
$F_{\text{X,W}}$	[N]	Longitudinal Wheel Force
$F_{\text{Y,W}}$	[N]	Lateral Wheel Force
$F_{\text{Z,W}}$	[N]	Vertical Wheel Force

g	[m/s²]	Gravity
γ	[rad]	Slope
J_{zz}	[kg m ^{2}]	Moment of Inertia with respect to the z-axis
K_{actuator}	[-]	Actuator Correction Factor in Experimental Vehicle for the Prediction of Braking Distance
i	[-]	Index
i_S	[-]	Steering Ratio
k_I	[-]	Integral Gain
k_P	[-]	Proportional Gain
κ	[1/m]	Curvature
κ_{tar}	[1/m]	Target Curvature
$\kappa(s)$	[1/m]	Curvature Progression
l	[m]	Wheelbase
l_f	[m]	Distance from CoG to Front Wheel Center
l_r	[m]	Distance from CoG to Rear Wheel Center
ICR	[-]	Instantaneous Center of Rotation
ICR_A	[-]	Instantaneous Center of Rotation for Ackermann Steering Angle
m_{veh}	[kg]	Vehicle Mass
μ_{max}	[-]	Maximal Available Coefficient of Friction
n	[-]	Index
ψ	[rad]	Yaw Angle
$\dot{\psi}$	[rad/s]	Yaw Rate
ρ	[m]	Radius of Curvature with Center at ICR
ρ_A	[m]	Radius of Curvature with Center at ICR_A
s	[m]	Traveled Distance
s_b	[m]	Braking Distance
$s_{b,r}$	[m]	Increase in Braking Distance Due to Time to Detection of Connection Loss
s_{evasion}	[m]	Distance Perpendicular to Moving Direction to be covered for Evasion
S_{res}	[-]	Slip
S_x	[-]	Longitudinal Slip
S_y	[-]	Lateral Slip
t_{evasion}	[s]	Needed Time for evasion
t_{brake}	[s]	Needed Time for Stopping
t_{r}	[s]	Time to Detection of Connection Loss
v	[m/s]	Absolute Value of Velocity at Wheel Center Point
ϑ	[rad]	Tangential Angle of Clothoid

v_0	[m/s]	Initial Velocity
v_{CoG}	[m/s]	Velocity Center of Gravity
v_{ego}	[m/s]	Ego-Velocity
v_f	[m/s]	Velocity Front Wheel
v_{limit}	[m/s]	Limit Velocity for a full collision avoidance
v_r	[m/s]	Velocity Rear Wheel
v_x	[m/s]	Longitudinal Velocity
$v_{\text{X,W}}$	[m/s]	Wheel Longitudinal Speed
$v_{\text{Y,W}}$	[m/s]	Wheel Lateral Speed
v_W	[m/s]	Wheel Speed
ω	[rad/s]	Wheel Rotation Speed
ω_0	[rad/s]	Wheel Rotation Speed of Straight Free-Rolling Wheel
$\bar{x}$	[-]	Arithmetic Mean

Abbreviations

ABS	Anti-lock Braking System
AEBS	Advanced Emergency Braking System
ACC	Adaptive Cruise Control
ADTF	Automotive Data and Time-Triggered Framework
BAS	Brake Assistance Systems
BASt	Bundesanstalt für Straßenwesen; English: (German) Federal Highway Research Institute
CAN	Controller Area Network
CAV	Collision Avoidance
CMS	Collision Mitigation System
DARPA	Defense Advanced Research Projects Agency
DFG	Deutsche Forschungsgemeinschaft; English: German Research Foundation
ESP	Electronic Stability Program
fps	Frames per Second
FTM	Lehrstuhl für Fahrzeugtechnik; English: Institute of Automotive Technology
GFOV	Geometric Field of View
HMI	Human-Machine-Interface
HUD	Head-Up-Display
ILD	Interaural Level Difference
ITD	Interaural Time Difference
LDW	Lane Departure Warning System
LKS	Lane Keeping System
ROV	Remotely Operated Vehicle
RPV	Remotely Piloted Vehicle
RTT	Round Trip Time
SRB	Speed Reduction Braking
TPTA	Telepresence and Teleaction
TTC	Time to Collision
UAV	Unmanned Air Vehicle
UGV	Unmanned Ground Vehicle
VPN	Virtual Private Network

Contents

1 Introduction

In the last decades, safety levels in personal transportation methods have increased. Because of the advantages of driver assistance systems, the development of such systems has become a central topic in the automobile industry. Examples of such systems include Adaptive Cruise Control (ACC), Lane Departure Warning Systems (LDW), Lane Keeping System (LKS) and Advanced Emergency Braking Systems (AEBS). The main goal of such systems is to support the human driver in the driving task as much as possible, especially because technical systems possess a very low reaction time and can reduce the risk of accidents. Among automobile manufacturers, German premium manufacturers have been developing driver assistance systems for several years with the goal of series production [Hoe11] [Sch09]. A long term goal is to further develop such systems to further reduce the driving task of a human driver. For this same reason, a known vision of many researchers and developers is to operate vehicles completely autonomously, where human errors could be reduced or even completely eliminated.

Alongside the increased safety provided by driver assistance systems, new mobility concepts can be developed with autonomous vehicles. Moreover, an increase in efficiency can be expected through optimization of traffic flow. The world's population is growing rapidly and, therefore, the number of megacities with more than 10 million inhabitants is also increasing rapidly [Uni11]. This will have a huge impact on daily mobility, making integrated mobility concepts the future for urban mobility. The automobile will become one mean of transportation among others and be used in joint ways in the form of car-sharing [Can09, pp. 16 ff.].

A possible scenario would be a person traveling with luggage from one megacity to another. The customer orders a vehicle to travel from his hotel to the main station. This vehicle is provided at a pre-arranged time directly to the customer. He is then able to transport the luggage easily with the vehicle to the station. Ideally, after arriving at the train station, the customer gets off the vehicle and does not need to find a parking space. He goes directly to its train connection and travels to his destination city. After arriving, another vehicle would be available for him to travel from the train station to his final destination. After reaching the destination, the vehicle is driven away.

This leads to an important question: How will the vehicles be provided to and distributed among the customers or driven back to a charging station? Ideally, the optimal use-oriented vehicle would be driven autonomously to the customer, for example using the *Link & Go* concept [AKK14]. After usage, this autonomous vehicle would be driven to the next customer or parked. Nevertheless, as later discussed in sections 1.2 and 1.3, fully autonomous vehicles are not yet possible. Therefore, teleoperation presents a possibility to solve the abovementioned problem in the near future.

1.1 Unmanned Vehicles

While it is common to discuss unmanned vehicles as a whole, according to ENDSLEY [End12, pp. 219–220], there are at least four different classes of control that differ in terms of their implications for the human performance:

- Exocentric teleoperation: the operator sees the vehicle directly.
- Egocentric teleoperation: the operator does not see the vehicle directly, but controls the vehicle through cameras inside looking through the windows, as if he were on-board.
- Exocentric semi-automated or automated control.
- Egocentric semi-automated or automated control.

There are several steps to be achieved before autonomous vehicles become a reality. These steps include the development of sensors and driver assistance systems to allow highly automated functions in vehicles. A roadmap of the development of driver assistance systems and their sensors towards automated cooperative driving is depicted in Figure 1.1 [Ben14, p. 8]. Current technologies allow assistant systems in longitudinal and lateral control. With the introduction of more advanced sensor systems, such as multisensor platforms and distributed sensors through a network, assistance systems will become capable of autonomous vehicle control.

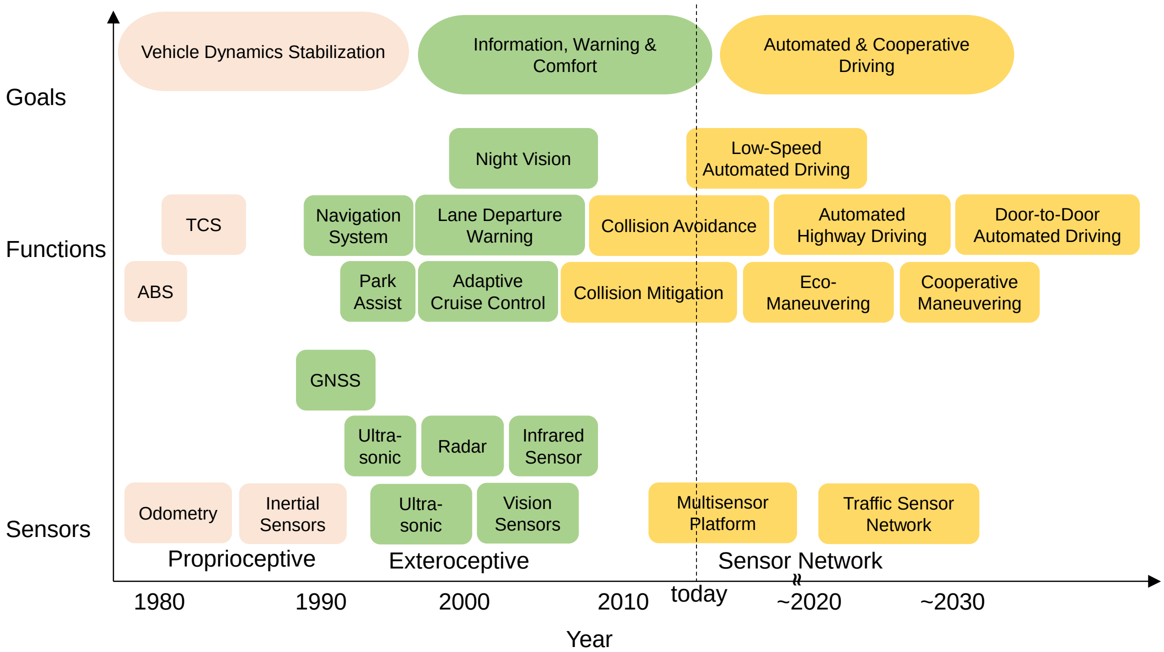

Figure 1.1: Roadmap of past and potential future evolution towards automated cooperative driving (adapted from [Ben14, p. 8])

The automobile manufacturers predicted highly automated vehicles on highways before the year 2020 [Aud13] [Con13]. During the Consumer Electronics Show (CES) 2013 in Las Vegas, Audi announced that they plan to introduce a highly automated system to the market in this decade which will allow the driver to perform additional activities [Aud13]. Similarly, BMW has been working in cooperation with Continental to bring multiple highly automated experimental vehicles on European highways in the year 2014. Here, the time frame for allowing additional activities in highly automated vehicles lies in this decade, whereas semi-automatic vehicles should be possible in the next few years [BMW13].

The different categories towards autonomous vehicles can be reflected on the different levels of automation pictured in Figure 1.2. In the case of semi-automatic vehicles, the system assumes the task for longitudinal and lateral control. However, the human driver must supervise the system and be prepared to completely overtake the vehicle control at all times. On the other hand, in a highly automated vehicle, the human driver is not required to supervise the system and is allowed to perform additional activities.

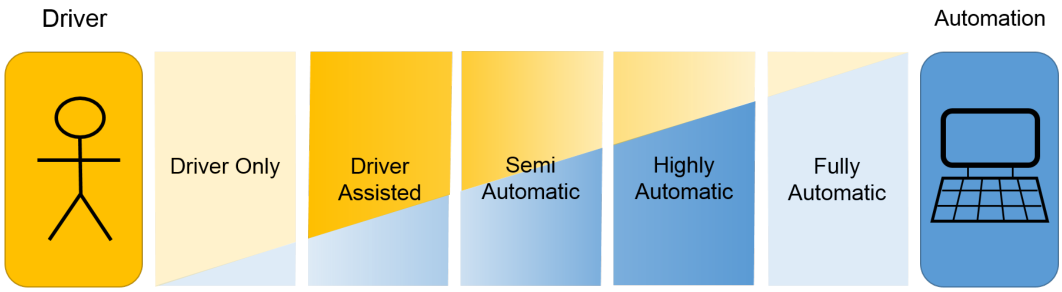

Figure 1.2: One dimensional scale of assistance and interaction (figure adapted from [Fle11, p. 273], based on BASt classification [Gas12])

1.2 Autonomous Vehicles

Autonomous or fully automatic vehicles belong to the highest level of automation according to the BASt (Bundesanstalt für Straßenwesen) classification [Gas12] and the vehicles are capable of moving through mixed traffic without additional infrastructure. Autonomous control systems need to be able to perform well under the influence of uncertainties in the system and in the environment for long periods of time. Furthermore, these systems need to be able to compensate for system failures without external intervention using techniques from the field of artificial intelligence [Ant90, p. 21].

An extensive range of research programs is engaged in researching this topic, with a significant increase since the 1980s. Some of the areas of interest include the fields of autonomous vehicle navigation [Nga11] and control [Tra06]. Alongside the early successes of the EU-Project PROMOTHEUS from the 1990s, the competitions organized by the Defense Advanced Research Projects Agency (DARPA), the DARPA Grand Challenges and the DARPA Urban Challenge, which took place in the years 2004 and 2005 and in the year 2007, respectively, are probably the best known [Jun05] [Sch08] [Nef05].

Figure 1.3 shows autonomous vehicles developed by different institutions. Research on autonomous vehicles at the Univesität der Bundeswehr München started with the *VaMoRs*, a Mercedes DB 508 vehicle, being one of the first vehicles to drive autonomously in closed streets. The vehicles *VaMP* and *Vita II* were developed together with Daimler-Benz and were equipped with different sensors, such as cameras and inertial sensors, which were able to measure accelerations and angular rates. They were capable of driving automatically over 1000 kilometers on the highway between Senlis - Parc Asterix, reaching speeds of $130\,{}^{km}/_{h}$ [Mau00, pp. 125 ff.]. Nevertheless, human interventions were necessary, for example in the cases of a lane change, a human driver was necessary to initiate the maneuver. The autonomous vehicle *Leonie*, developed by the Technische Universität Braunschweig, was able to show in 2010 that driving autonomously in normal daily traffic scenarios was possible [Wil12, p. 148]. However, additional assistance from a human was necessary to input the states of the traffic lights into the system. Within the DARPA Challenges, the team from Stanford University with *Stanley* became the winner of the 2005 Grand Challenge after completing the whole course and crossing the finish line using different sensors to interpret the surroundings [Thr06] [Nef05]. Research continued after the success of the DARPA Grand Challenges, with several teams, such as *Team AnnieWAY* [Kam08] or *Team Urbanator* [Ros07], participating in the Urban Challenge in 2007. An extensive description of different autonomous vehicles can be found in [Mau00] [Wil12].

Figure 1.3: Autonomous vehicles: *VaMoRs* (top left) [Mau00, p. 114]; *VaMP* (top center) [Mau00, p. 115]; *Leonie* (top right) [Wil12, p. 94]; *Team AnnieWAY* (bottom left)[Kam08]; *Stanley* (bottom center) [Nef05]; *Urbanator* (bottom right) [Ros07]

1.3 Motivation: Autonomous Vehicles only in determined scenarios possible

The Institute of Automotive Technology (FTM; German: Lehrstuhl für Fahrzeugtechnik) at the Technische Universität München also devoted itself to the research on the field of autonomous vehicles as part of a research topic of the German Research Foundation (DFG; German: Deutsche Forschungsgemeinschaft) Collaborative Research Center with the project "Cognitive Automobiles" [Goe08]. It is known that autonomous driving is possible on public roads in urban traffic, but only with certain constraints [Pin12]. This is mainly because of other traffic participants and confusing road topologies [Die11] [Pud11]. "Cognitive Automobiles" also showed that driving autonomously was possible in clearly defined environments [Goe08]. RAUCH ET AL. [Rau12, pp. 12–13] confirmed these results showing that autonomous driving is technically possible on a highway, completing the route on the German A9 highway from München to Ingolstadt in June 2011 without intervention of the safety driver. However, this study also showed the limitations of the present-day technologies and mentioned some situations in real traffic that cannot yet be mastered autonomously, such as construction sites, lost cargo or a burst tire. These situations require a fast, cautious and situation-specific reaction. Therefore, the safe controllability of such special events will become one of the essential challenges for the development of automatic systems.

In contrast, the time frame for the introduction of a fully automated vehicle in combined traffic with human-driven vehicles is not yet foreseeable, especially in arbitrary scenarios outside the highways [Sti05, p. 5] [Win09c, p. 667] [Gas12, p. 7]. Nevertheless, a need for new mobility concepts can be already seen: finding a parking lot in megacities is becoming harder and very time consuming; providers of car sharing services need solutions for distributing the fleet efficiently; owners of electrical vehicles do not have a private charging station and need to drive the vehicle to public charging stations.

Therefore, a suitable solution to achieve the goal of unmanned vehicles in mixed traffic situations and address the abovementioned changes in mobility would be through teleoperation. Due to large amounts of experience and the ability to anticipate, detect objects and recognize driving pathways, especially under different and changing environment conditions, the human driver is capable of performing well in relevant driving tasks [Sti05, p. 9] [Dic05, p. 204] [Abe09, p. 13]. Additionally, because of the high density in traffic, non-verbal communication is needed in order to function properly [Jür97, p. 34]. This non-verbal communication cannot be achieved by current machine approaches. Furthermore, an autonomous system requires a relatively high implementation and computational cost, whereas performance and efficiency equivalent to those of humans cannot yet be achieved [Win09c, p. 667] [Ber08]. Compared to autonomous systems, the costs of a teleoperated system are assessed to be lower, in which case only the implementation of actuators is necessary to translate the inputs from the human operator into actions. It is therefore meaningful to keep the human driver in the control-loop, while not necessarily being physically present in the vehicle. A more detailed discussion is provided in section 2.4.

For this reason, the Institute of Automotive Technology devoted itself to the research of teleoperated road vehicles. For a teleoperated system to work appropriately, there are multiple problems to be solved [Gna13]. This dissertation focuses on improving the control of teleoperated vehicles, both on the technical and on the human aspects and focuses on two aspects, described in section 2.6.

1.4 Structure of the Dissertation

The structure of this dissertation is shown in Figure 1.4. Chapter 1 presents an introduction to the topic and unmanned vehicles are described. Chapter 2 introduces teleoperation, along with the classification and the applications of teleoperated systems. Additionally, human-machine-interaction is shortly described and the system of the teleoperated vehicle of the Institute of Automotive Technology at the Technische Universität München is presented. At the end of the chapter, the motivation for this dissertation is shown and the problem statement is presented.

Based on the presented topics in chapters 1 and 2, chapter 3 addresses one important aspect for the development of methods to improve the control of teleoperated vehicles. It presents the relevant current state of the art regarding safety of vehicles and introduces the development of the "Free Corridor" as an emergency contingency strategy. The concept is analyzed in the simulation before being implemented and analyzed in the experimental vehicle. Results of the concept are shown and discussed.

Chapter 4 addresses the second aspect to improve the control of teleoperated vehicles. The term *Situation Awareness* is introduced and its relevance for the driving task is explained. Methods are proposed to improve the speed perception of the operator at the working station. These influence the situation awareness. The methods are analyzed using studies with test subjects and the results are presented and discussed.

The accomplished results of both aspects are presented and discussed in chapter 5. Finally, chapter 6 summarizes the dissertation, presents conclusions and provides an outlook.

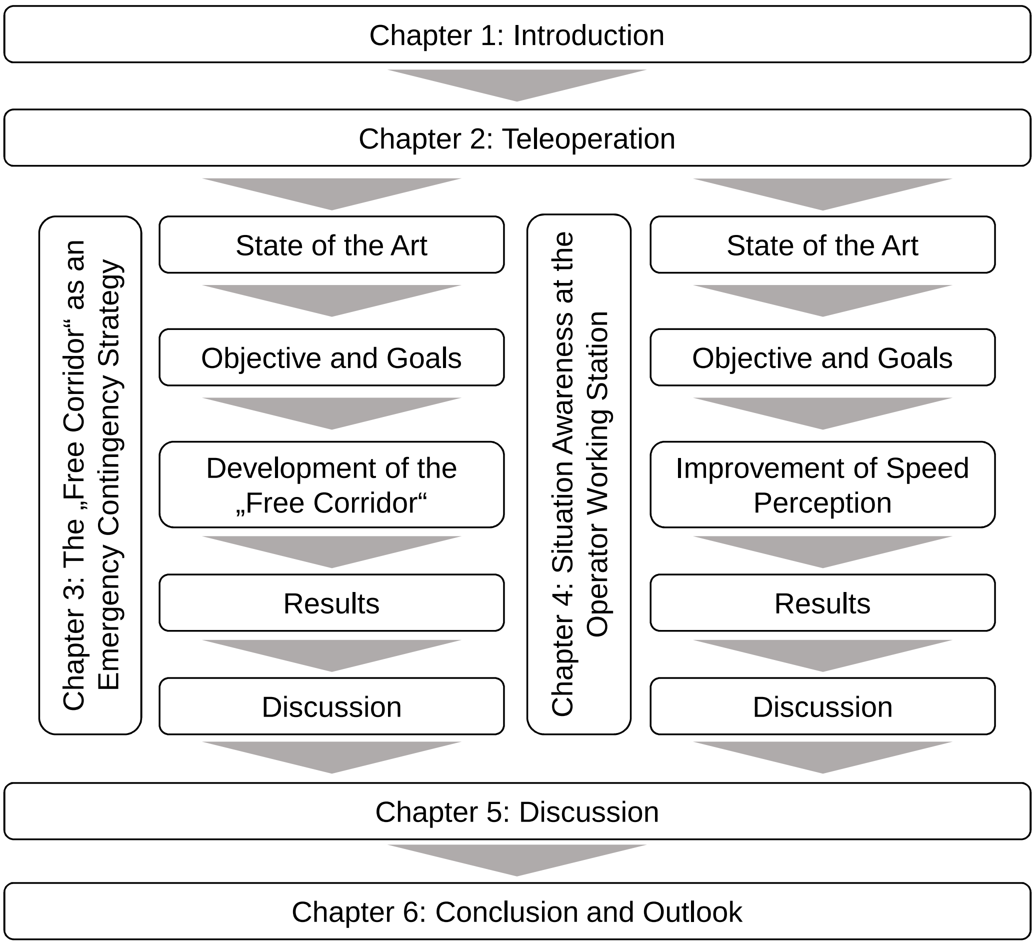

Figure 1.4: Structure of the dissertation

2 Teleoperation

Already since the beginning of the 20^{th} century, teleoperation has found great use in scenarios that are deemed too hazardous, remote or inaccessible for human beings, who could not or should not be physically present for safety reasons. However, such scenarios are too complex for (current) fully autonomous systems [Win00, p. 148]. Because of that, teleoperation has found great application in aerial, underwater and ground robots.

2.1 Definition of Teleoperation

A teleoperation system is a multimodal *Telepresence and Teleaction* (TPTA) system [Hir05, p. 3430], where a human operator commands a remote robot, known as *teleoperator*, through an interface. TPTA usually refers to the remote interaction between the human operator with a mobile robot to perform physical manipulation tasks [Rad12, p. 5]. SHERIDAN [She92, p. 4] defined teleoperator as:

> "a machine that extends a person's sensing and/or manipulating capability to a location remote from that person."

Furthermore, a *telerobot* is an advanced form of teleoperator, which uses its own artificial intelligence and sensing capabilities to carry out the tasks received from the human operator, who supervises its behaviour through a computer intermediary. The *human operator* is the person responsible of monitoring and controlling the telerobot [She92, pp. 3–7]. In teleoperated systems, a human expert or human operator is needed to interpret the objects, make judgments and direct actions. This all must be done remotely. Therefore, a teleoperated system can be regarded as an extension of the senses and (perhaps) of the hands [Win00, p. 148]. A teleoperated vehicle in this context means a vehicle that is driven remotely by an external operator using a live-streaming video [Fon01c]. Simply put, it means operating a vehicle at a distance [Fon01a, p. 121].

According to the levels of automation proposed by the BASt (Figure 1.2), a teleoperated system would be located beneath the level "Highly Automation". However, teleoperated systems were excluded from consideration [Gas12, p. 32].

2.2 Classification of Teleoperated Systems

In order to clarify the wide concept of "normal teleoperation", according to SUOMELA [Suo01, pp. 21–22], teleoperation can be split into three categories (Figure 2.1):

- Closed Loop Control (Direct Teleoperation): the operator uses direct signals to control the teleoperator and receives real-time feedback.

- Coordinated Teleoperation: the operator controls the actuators, but the teleoperator has an internal control loop (represented by the blue arc). No autonomy is present in the teleoperator. The remote loop is responsible for closing the loops that the operator cannot because of delays.
- Supervisory Control [She92]: this type of teleoperated system possesses a certain autonomy. The teleoperator is capable of performing some tasks autonomously, while the operator is only responsible for giving high-level commands and monitoring the system. The red dashed arc represents a feedback from the interface.

Even though the term *teleoperation* is often used for direct control, teleoperation can also be considered to cover the broader spectrum from direct control to supervisory control, as used by FONG [Fon01a, p. 121].

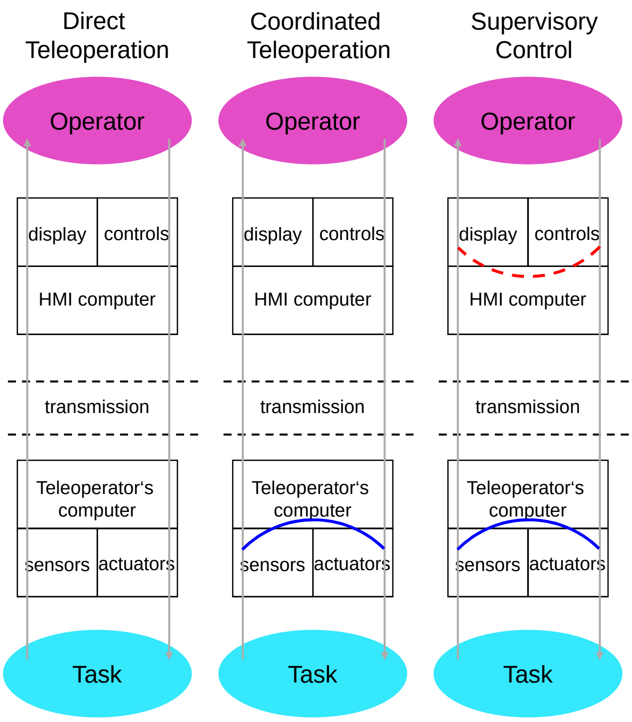

Figure 2.1: Categories of teleoperation (adapted from [Suo01, p. 22]). The blue arc represents a local control loop at the teleoperator and the red dashed arc represents a feedback from the interface.

A typical teleoperation system may consist of multiple elements. However, there are three main elements that are part of every teleoperation system [Win00, pp. 148–149]:

- The Operator Interface.
- The Communications.
- The Robot.

The *Operator Interface*, also called *Workstation*, usually consists of display elements to illustrate the images coming from the robot's on-board cameras and other sensors and to show status information. Additionally, it consists of input devices that allow the human operator to input commands for controlling the robot [Kay95] [Win00, p. 149].

The interface provides the displays to help the human operator understand the remote environment and allow him to keep situational awareness. At the basic level, maps and videos belong to the interface, but it is not required that both are visible simultaneously [Ste04, p. 2753]. For the teleoperation of vehicles, in order to be allowed to participate in public traffic, an angle of view of $140°$ is necessary [Heb61, p. 23] [Neg07, p. 11]; however, because of the importance of peripheral vision, especially for speed perception, an horizontal angle of view of $180°$ without optical distortion must be accomplished [Ara82, p. 47].

The input devices may consist of various types of devices, such as touch devices or joysticks [Fon01b] [Fon01c]. A general assessment concept regarding input devices for teleoperated systems is discussed in [Ack11]. Different input devices according to cost effectiveness and feedback representation are evaluated. ACKER [Ack11, pp. 54–57] comes to the conclusion that frequently a joystick from the user-consumer sector is enough, since it is affordable and robust against environmental influences. An investment in higher cost devices becomes necessary only when accurate force-feedback in special applications is needed.

The *Communications* might be a wired or a wireless connection, depending on the application, either if it is a fixed or mobile robot. A two-way (full duplex) communication link is needed so that surrounding information (video, sensor, etc.) can be sent from the robot to the operator interface and command data sent the other way around. The requirements on the communication link may vary with respect to bandwidth and delays [Win00, p. 149].

The *Robot*, on the other hand, may vary enormously according to the different applications and operating environments. However, the robot generally requires on-board power and energy management systems for operation, one or more communication transceivers so as to communicate with the operator interface via the communication link, computational units and program storage for local control systems and to interpret the commands sent from the operator interface and translating them into control signals for the actuators, and video cameras and sensors to perceive the surroundings [Win00, p. 149].

Since a human operator acts as a sensor to understand and interpret the surroundings, it is often sufficient to use only a camera system. Therefore, the use of additional sensor systems is optional [App10, pp. 242–243]. However, it is important to note that the loading for the human operator while controlling a teleoperated system is not lower than in manual control [Fon01a, p. 2].

2.3 Application of Teleoperated Systems

Historically, teleoperated aerial vehicles were mostly used in military applications. The first teleoperated aerial vehicles were the so called *Remotely Piloted Vehicles* (RPV), used for air defense training of the U.S. Air Force. The first teleoperated air vehicles were radio-controlled target drones, such as the US Army's Radioplane RP-5A and the US Navy's Culver PQ-14, depicted in Figure 2.2. These planes flew pre-programmed flight plans but could also be controlled remotely. Nowadays, teleoperated air vehicles are better known as *Unmanned Air Vehicles* (UAV) and are basically used for reconnaissance flights [Fon01c] [Fon01a]. As a result of developing systems which were cheaper than manned aircraft and which did not risk human lives, numerous UAVs were developed, such as the US Navy Pioneer and the US Air Force Predator, developed by General Atomics Aeronautical. These are able to excel in combat focusing on intelligence, surveillance, reconnaissance, targeting, etc. [Gen14].

Figure 2.2: Radio-controlled target drones. Radioplane RP-5A (left) [Fon01a, p. 124], Culver PQ-14 (center) [Fon01a, p. 124] and US Air Force Predator (right) [Gen14]

Underwater robots, the so called *Remotely Operated Vehicles* (ROV), are the most important industrial application of teleoperated vehicles. These robots are normally operated from a control ship and are connected through cables. The commercial success of ROV is primarily due to the boom in deep-water oil production. ROVs are now used for many different purposes. Examples include applications in oceanography, rescue work, drilling support, site survey, debris clearance, structure cleaning and exploration [Fon01c] [Fon01a] [Mar12]. Figure 2.3 shows examples of ROVs used for exploration which possess features like auto heading and depth control and are equipped with sensors such as compass and rate gyro systems [Dee14].

These teleoperated systems have taken over roles of submersibles and divers, since they are generally cheaper to operate, are able to work for longer periods, achieve deeper regions and no humans are put at risk. It is however argued, especially from deep sea oceanographers, that ROVs will never completely replace humans since electronics do not have the overall performance of human senses [Fon01a, p. 127].

Figure 2.3: Underwater Remotely Operated Vehicles ROVs: ROV from the Marine Technology Society (left)[Mar12], T4N ROV (center) and L4N ROV(right) from the Deep Ocean Engineering, Inc. [Dee14]

A further type of teleoperated vehicle consists of reconnaissance vehicles, vehicles for hazardous locations and *Unmanned Ground Vehicles* (UGV). Reconnaissance vehicles are developed to fulfill research tasks, such as collecting samples. An example is the Mars-Rover Robot sent to Mars by the NASA [NAS12], as shown in Figure 2.4 (left). Vehicles for hazardous locations are used for extremely life-threatening places, such as the Chernobyl Nuclear Power Plant. The term *Unmanned Ground Vehicles* includes a wide range of systems and technologies and refers to any piece of equipment that moves on the ground without a human present on it [Fon01a, p. 125]. This includes systems focused on remote navigation and control with applications such as reconnaissance, surveillance and target acquisition, landmine detection, road clearing and monitoring tasks. The research and development of such vehicles took place primarily in the US military, developing the Advanced Teleoperator Technology TeleOperated Dune Buggy (Figure 2.4 (center)) which used head-coupled stereo video, stereo audio and replicated controls to operate the vehicle. The US Marine Corps developed the TeleOperated Vehicle, which was controlled via fiber-optic tether (Figure 2.4 (right)) [Fon01a, p. 126] [Fon01c].

Figure 2.4: Remote Ground Vehicles RGVs: Mars Rovers (left) [Jet14], Advanced Technology Tele-Operated Dune Buggy (center) and TeleOperated Vehicle (right) [Fon01a]

A detailed description of different teleoperated systems can be found in [Fon01a] [Fon01c] [Kay97] [Rad12].

2.4 Human-Machine-Interaction

A teleoperated system is based on the interaction between humans and machines. The human is kept in the control loop and is responsible for making decisions on how the telerobot should act. This is achieved with the help of information about the telerobot's environment. According to CHARWAT [Cha92, pp. 227–228], in Human-Machine-Interaction, the human and the machine form the alternately influencing units. For the case of a (tele)robot and based on spatial region, Human-Machine-Interaction systems can be classified into two main categories [Goo07] [Yan04] [Hel06] [Rad12, p. 3]:

- *Proximate interaction*: humans and (tele)robots are co-located, where they share a common or overlapping workspace.
- *Remote interaction*: humans and (tele)robots are not co-located and are separated in two different workspaces.

The different interaction channels between human and machine through human senses related to driving are presented by HIESGEN [Hie11, p. 21] and shown in Figure 2.5. More information related to these human senses can be found in [Abe09, p. 5] [Bub01, p. 156].

To better understand the importance of teleoperated systems and accordingly, Human-Machine-Interaction, it is relevant to understand their advantages and disadvantages. Already at the beginning of vehicles capable of perceiving the environment, it was clear that in order to approach the human's performance in a general natural environment, very high computational power is needed [Dic95]. DICKMANNS mentions for example that, in order to bring the machine vision near human's performance, it is relevant to be able to evaluate color and texture of different classes of objects. This must happen under the knowledge of a huge amount of possible appearances of the objects under different conditions, such as lighting, weather, distances and perspective. Worth mentioning is the small machine cognitive performance, especially in the decision-making flexibility and it is especially difficult to recreate the human's learning-process [Win09c, p. 670]. The reasons humans are better at decision making is that they possess a more complete representation of the surroundings and are capable of reaching out for knowledge from past experiences [Abe09, p. 13].

Furthermore, there are aspects where the machine is already superior compared to the human performance, such as in the latency of the processing chain "perception-decision-action" and not being subjected to distraction and fatigue [Sti05, p. 9]. Additionally, machines

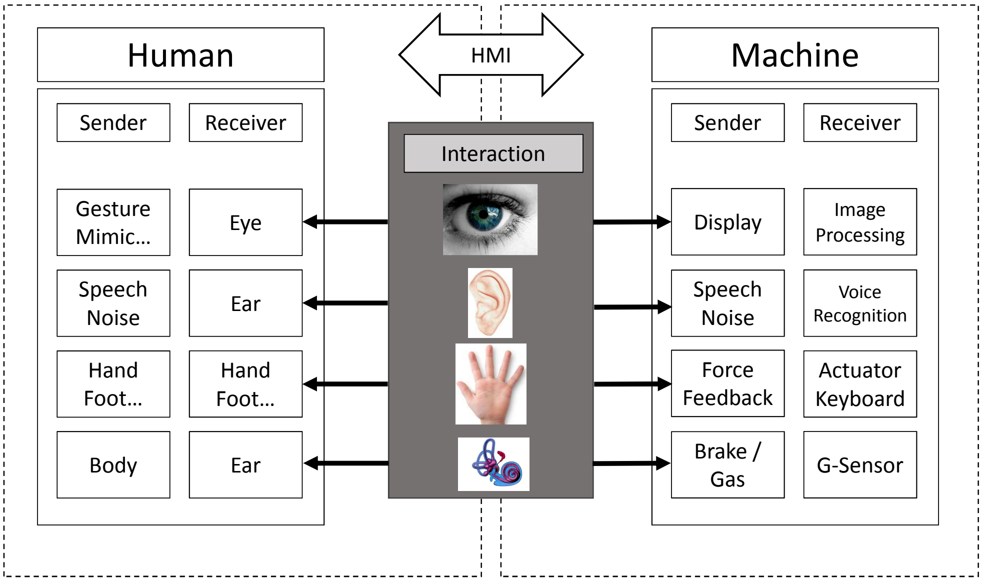

Figure 2.5: Interaction channels between human and machine (adapted from [Hie11, p. 21])

posses sensors for measuring distances to a resolution in centimeter-range [Stu04, pp. 7–11], whereas human beings are not used to estimate distance in metrical units and are usually not able to do so accurately [Cav01, p. 446].

According to FITTS [Fit51, p. 10], humans appear to surpass machines with respect to detection of small amounts of visual or accoustic energy, perception of patterns of light or sound, improvisation and usage of flexible procedures, storage of large amounts of information for long periods and recalling relevant facts at the appropriate time, inductively reasoning and exercise judgment. Machines, on the other hand, appear to surpass humans when it comes to responding quickly to control signals and applying great force smoothly and precisely, performing repetitive, routine tasks, storing information briefly and then erasing it completely, reasoning deductively and handling highly complex operations, for example doing many things in parallel.

Combining the advantages of humans and machines can bring new concepts for flexible systems and new applications can be achieved. Instead of machines directly replacing humans, they can assist humans through close interaction, especially in the areas of precision, speed of execution and their capacity for huge achievable load-bearing [Rad12, pp. 1–3], leaving the decision making to the humans, where they excel. For example, as machine image acquisition and processing often suffer from changing conditions in lighting [Rat07], it is meaningful to use complementary sensing principles, which would lead to a drastic improvement of system robustness [Thu09, p. 532]. These sensing principles can be complemented by the human operator.

Nevertheless, in order to completely exploit the potential of Human-Machine-Interaction and cooperation systems, an "optimum line" between robot autonomy and human operator control has to be found. One of the most challenging tasks for current designers of teleoperation systems is to find this "optimum line" [Tza06, p. 447]. There is always debate about what should be automated and what should be executed by humans [She02, p. 14] and it is important to keep in mind that humans are not the most appropriate at monitoring automated systems [She02, p. 147].

2.5 Teleoperation at the Institute of Automotive Technology

In the context of the project *Tele-Operated Driving* at the Institute of Automotive Technology, a concept for a teleoperated system was designed. The basic structure was conceptualized from the requirements for a human driver to be able to perform the driving task.

2.5.1 System Structure

Figure 2.6 gives an overview of the overall concept implemented. According to section 2.2, every teleoperated system consists of three main elements: *Operator Interface*, *Communications* and *Robot*. In this case, the robot consists of an experimental road vehicle, an Audi Q7. This vehicle was adapted in the predecessor project *Cognitive Automobiles* to have the capability to drive autonomously [Goe09] [Goe08] [Thu08] [Kra12]. It is connected to the internet through a mobile connection. The operator interface, which consists of a statical operator working station, is also connected to the internet. This allows the communication between the vehicle and the working station, sending control signals to the vehicle and information about the surroundings through cameras and sensors the other way around. A more detailed description can be found in [Die11] [Gna13] [Tan14b].

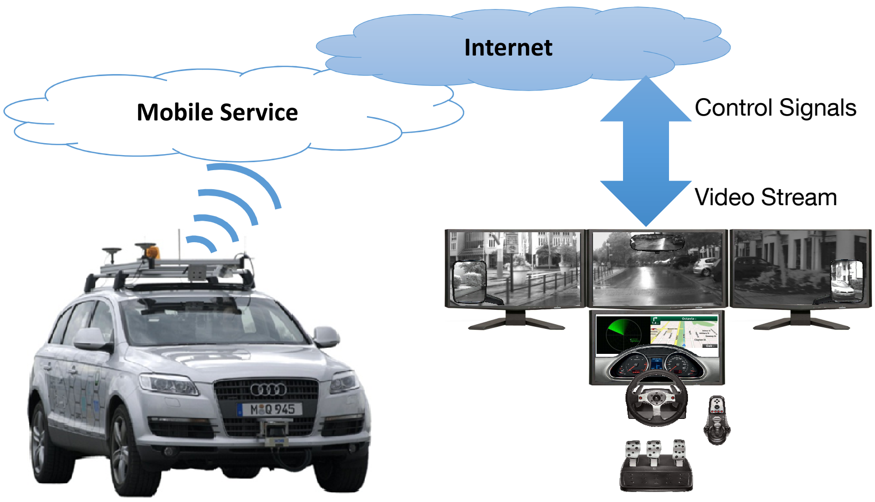

Figure 2.6: Scheme for teleoperated road vehicles at the Institute of Automotive Technology

2.5.1.1 Vehicle Architecture (Robot)

In order for the human operator to be able to drive the car, information about the surroundings must be provided. Different human senses are related to the driving task, including visual, auditory, haptical and vestibular senses [Abe09, p. 5]. Since the visual sense plays a dominant role [Jür01, p. 17], a camera system is built into the vehicle to capture the surroundings. A static camera setup was chosen against a panning system, since a panning system would need a fast enough mechanism [Kay97, pp. 131 ff.]. Cameras provide a horizontal angle of view of approximately $240°$ to the front and additional cameras provide side mirror views and rear view perspectives, fulfilling the needed requirements regarding driver's field of view [The77] [The04] (Figure 2.7 left).

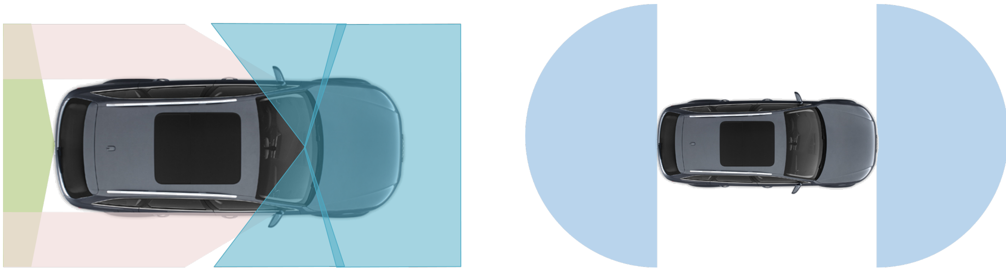

Figure 2.7: Camera concept for the Audi Q7 (left) and laser scanners range (right)

In addition to the cameras, a long range radar scanner and three single layer laser scanners are built in the vehicle to measure the environment. The laser scanners are mounted on the front, on the back and on top of the vehicle (Figure 2.7 right). The combination of all sensors allows the creation of a surround view with help of sensor fusion approaches. Two central processor units are responsible for the processing of sensors, actuators and the communication. The video streams coming from the cameras are encoded by an automotive suitable *CarPC* running a data processing framework with Windows 7 operating system. The CarPC is also responsible for the communication between the vehicle and the operator interface. The second processor unit is a real-time capable rapid prototyping unit responsible for handling the information coming from sensors and the execution of the control signals coming from the operator interface, called *Autobox*. The primary driving task is controlled via this rapid prototyping unit.

The actuators consist among others of a hollow shaft motor directly built in the steering column behind the steering wheel in order to achieve steering functionality. During operation, the hollow shaft motor can be overridden anytime by a safety driver. To achieve acceleration and braking functionality, the electronic interface of the motor control unit is used. Furthermore, to be able to guarantee a safe state at any time, an additional pneumatic system in the vehicle has the ability to brake by using a loaded air tank that directly presses on the braking pedal. A shift-by-wire system is implemented in the vehicle instead of the conventional gear selector lever. Further secondary driving tasks, such as windshield wipers, vehicle's horn or turning indicators are also controlled by the rapid prototyping unit through CAN-Bus[1] communication.

2.5.1.2 Communication

It is desired for the application of teleoperated vehicles that the operation range should cover as much as possible. Since the communication between the vehicle and the operator interface is achieved wirelessly, the already established mobile network and its infrastructure provide an interesting solution to the abovementioned requirement. This technology and its coverage are constantly growing and their available transmission speeds are equally increasing, reaching nominal peak download and upload rates of up to 300 and 75 Mbps[2], respectively. However, the actual bandwidth depends greatly on the signal strength and the number of users on the same cell, influencing the real speeds [Ten10]. Since video transmission requires a much higher bandwidth than control signals, the upload rate is the limiting factor in the present system [Chu14].

[1]CAN: Controller Area Network - an established communication protocol in automobiles
[2]Megabits per Second

Depending on the current available networks, a connection over 3G or over 4G is selected. Since the actual transmission rate is not sufficient to transmit all video images at the best quality, the videos are transmitted with lower quality and only specific areas of interest are transmitted with higher quality. Additionally, the rear cameras are transmitted selectively, according to the current driving situation. The videos are encoded using the established H.264 video codecs, where the constant rate factor and image size can be adapted constantly to assure a smooth transmission.

Due to the properties of a mobile connection, a transmission time is present in the system. According to KRENIK [Kre08], the transmission time for a 3G HSPA connection is around 50 milliseconds in each direction and for 4G networks, it could be reduced to 5 milliseconds in each direction for small packets. Own measurements of the LTE mobile networks with current system configuration showed an average round trip time (RTT)[3] of 138 milliseconds, with values ranging from 102 milliseconds up to 445 milliseconds [Chu15]. In order to keep the time delay of the video transmission as low as possible, the connectionless UDP-based protocol is used. However, UDP does not guarantee a secure transmission nor a flow control and it does not guarantee that data packets sent actually arrive at the designated receiver [Mei12, p. 650]. For safety reasons, the communication occurs over an encrypted VPN[4]-connection. An overview of important aspects to guarantee a safe and robust connection is provided by CHUCHOLOWSKI [Chu14] and in section 3.1.

To solve the influences of time delays caused by the transmission and processing of information, two different approaches have been developed by GNATZIG and CHUCHOLOWSKI and are briefly discussed in sections 2.5.2 and 2.5.3.

2.5.1.3 Operator Interface

The operator interface, also called the working station, can be compared to a static driving simulator. In order to give the human operator the feeling of presence, it was assembled according to a vehicle cockpit. It is built with a driver's seat and is equipped with conventional driver input devices such as steering wheel and pedals. Three monitors are arranged next to each other in the front and can be arranged according to the driver's or the situation's needs. The videos from the front cameras are displayed on the entire area of the monitors and the videos from side and rear mirror cameras are overlaid when necessary. Even though gray-scale images would slightly reduce the amount of necessary bandwidth, MILLER [Mil88, p. 41] showed that color is preferred while driving teleoperated land vehicles and even provides a detection-range advantage and gray-scale images would make it difficult to drive in special situations, such as driving through shadows.

An early version of the working station was built with simple components, which consisted of three 24" computer monitors and a Logitech G25 steering wheel and pedals for computer games (Figure 2.8a). The successor working station was equipped with three 55" monitors. Furthermore, in order to be able to create a better feeling of driving, a force-feedback steering system is selected. The SENSODRIVE GmbH SENSO-Wheel SD-LC was chosen for the system since it is a commonly used high-end solution for simulators. It allows for nearly perfect simulation results of physical effects and end stops [SEN14]. The steering wheel is controlled via CAN-Bus. Additionally, pedals from the same company which can be con-

[3]RTT: Time needed to transmit a video image to the operator interface and transmit the control signals back to the vehicle including processing times

[4]Virtual Private Network

trolled through the same controller were chosen. A 5.1 surround sound system is integrated in the working station to provide playback of auditory information, either directly acquired at the vehicle and sent to the working station, or motor sound simulation using vehicle's information such as engine revolution or motor load. Additionally, to simulate vibrations, an amplifier module *mivoc AM80* [Spe13] is used in combination with two bass-shakers integrated under the seat and directly behind the backrest. The working station is built based on MayTec® profiles on matching wheels, making it mobile. Figure 2.8b shows the operator interface. Throughout this dissertation, the working station refers to the second version.

(a) Version I of the operator interface [Gna13]

(b) Version II of the operator interface

Figure 2.8: The operator interfaces

Figure 2.9 shows an illustration of the environment tools used in the system. A central processing unit runs the self-developed interface and communicates directly with the CarPC on the experimental vehicle running the tool Automotive Data and Time-Triggered Framework (ADTF) via the communication channel. Control signals and information regarding the vehicle's surroundings are exchanged. Additionally, the CarPC communicates with the rapid prototyping unit, which communicates with the additional sensors and actuators in the vehicle.

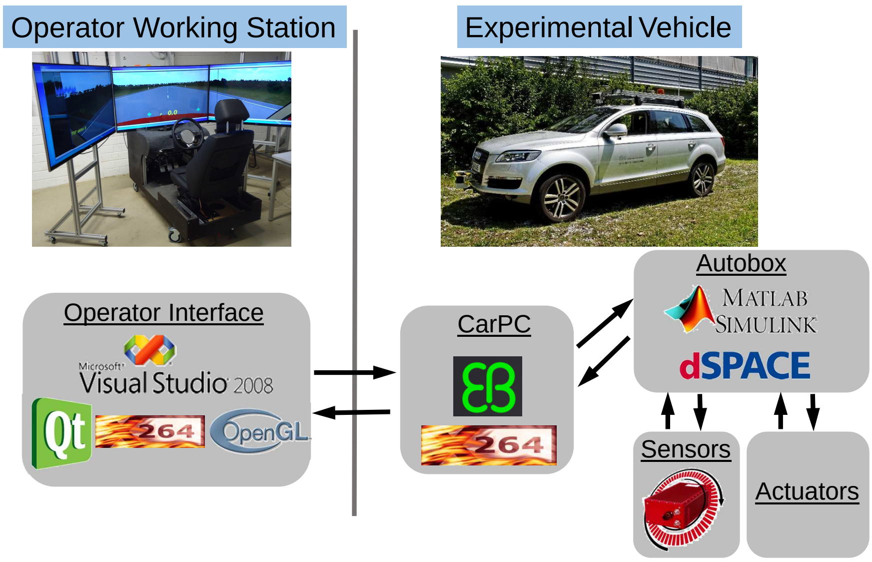

Figure 2.9: Environment tools used in the system for the teleoperated vehicle

Although direct teleoperation could be problematic because of control decisions and system performance directly depending on human capabilities, it is cheap and easy to implement, at least compared with other system models [Fon01a, p. 15]. Even though the system presented above is capable of operating in different modes, *Direct Teleoperation/Control* is used in context of this dissertation.

2.5.2 Trajectory-Based Driving

GNATZIG [Gna12a] [Gna12b] proposed a shared-control approach based on the supervisory control method as a solution for a safe and unmanned ground vehicle. Control of the vehicle is based on automated driving along predefined paths, using trajectories as command variables, which consist of parameterized curves overlaid by velocity control.

This approach possesses the advantage of being independent of the system's latency. Two control loops are closed locally. The human operator plans the trajectories along the desired path and after confirmation by the operator, the trajectory is transmitted to the vehicle. After receiving new trajectories, the vehicle is responsible for following the confirmed trajectory and for its stabilization. If no new trajectories are received, the vehicle comes to a stop at the end of the last confirmed trajectory, allowing the vehicle to come to a safe state if, for example, the connection between vehicle and working station is lost [Gna15]. Figure 2.10 shows the concept in the simulation framework.

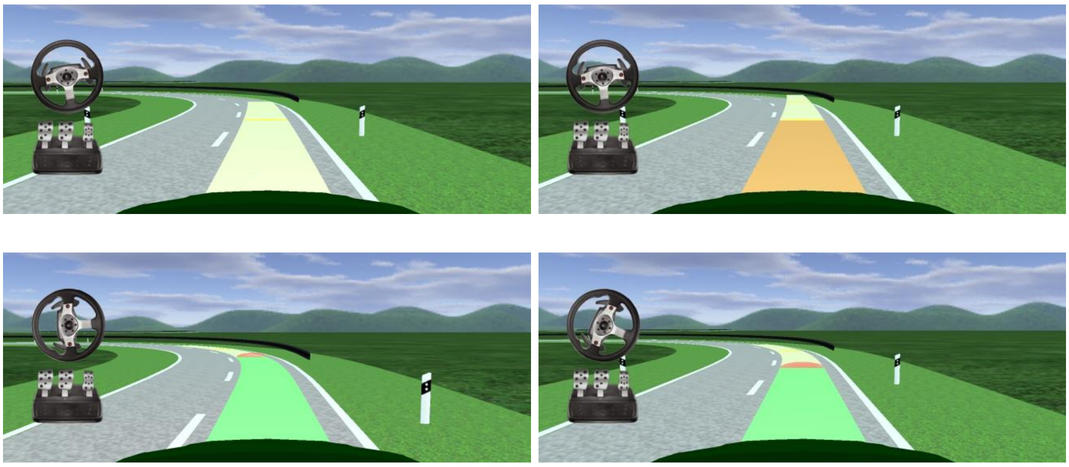

Figure 2.10: Visualization of trajectory-based driving in the simulation. The already confirmed path is presented in green and the orange path is the path awaiting confirmation [Gna15]

2.5.3 Predictive Display

Another approach for dealing with time delays while driving in direct teleoperation mode is the *predictive display* proposed by CHUCHOLOWSKI [Chu15]. To mitigate the effects of time delays, a prediction model considers the current system delay together with the control signals from the operator to calculate the position of the vehicle. This predicted position is displayed to the operator as a "third-person view". Different methods for the prediction of the vehicle are investigated [Chu13b] and a suitable one is selected. Furthermore, the corresponding display methods are investigated and the effect on driving performance is studied [Chu13a]. Additionally to the prediction of the ego-vehicle, the effects of time delay on other traffic participants are also studied. In order to predict their movements, a robust detection is necessary [Wit14]. The *Predictive Display* system is shown in Figure 2.11.

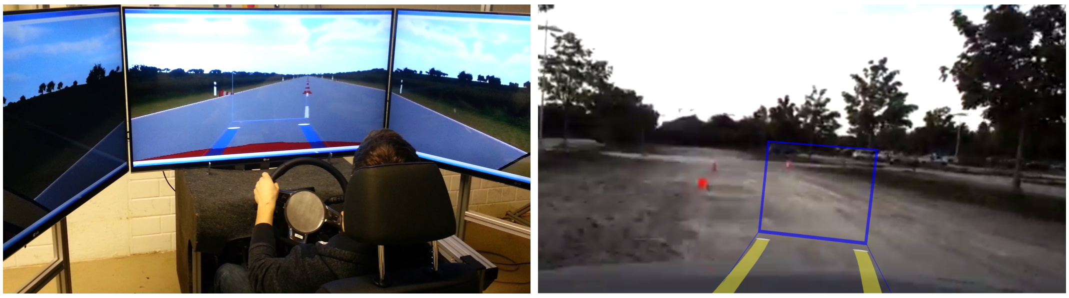

Figure 2.11: Predictive display as an approach for dealing with time delays shown at the operator working station in the simulation (left) and on the experimental vehicle (right) [Chu15]

2.6 Problem Statement

In order to improve the control of teleoperated road vehicles, two important aspects of teleoperated vehicles are addressed in this dissertation and solutions are proposed. The first one focuses on the technical aspect of the teleoperated vehicle where a strategy is developed, implemented and analyzed for the situation of a connection loss during teleoperation. This is presented in chapter 3. The second one focuses more on the human features and its capability to perceive speed correctly while driving. Its analysis is presented in chapter 4. Since the two aspects are not directly related, they are considered in terms of state of the art, results and discussion separately.

2.6.1 Connection loss of mobile connection

For the teleoperation of road vehicles, a wireless connection is needed in order to allow the exchange of information between the operator working station and the vehicle. The mobile communications network presents an interesting solution since it provides a virtually unlimited range of coverage. Nevertheless, a continuous and permanent connection cannot be guaranteed and a loss of connection could occur anytime, without the possibility to accurately predict the exact time of occurrence. Therefore, a suitable emergency contingency strategy needs to be developed that guarantees the safe state of the teleoperated vehicle. A controlled braking maneuver can be achieved in order to safely bring the vehicle to a stop.

2.6.2 Bad or Missing Situation and Risk Awareness

During teleoperation of road vehicles, the operator is physically separated from the vehicle. Therefore, a large amount of information normally available when being physically present at the vehicle is missing. This causes bad situation- and risk awareness, which affects the driving performance and the task at hand. Therefore, it is important to address this problem and develop systems that increase the feeling of driving a real vehicle so that driving performance is improved.

3 Development of an Emergency Contingency Strategy: The "Free Corridor"

Teleoperated vehicles work on the principle of wireless communication between the vehicle and the operator interface. However, this connection cannot be guaranteed to work constantly without interruptions. Furthermore, the exact time when a loss of connection might occur is unknown and cannot be predicted. Hence, it is essential to develop a contingency strategy capable of dealing with sudden loss of connection and bringing the vehicle into a safe state.

Section 3.1 gives an overview of mobile network connections related aspects and section 3.2 shortly discusses time delays, which greatly influence teleoperated systems. Section 3.3 introduces safety aspects from vehicles, with special emphasis in intervention strategies and the emergency braking decision making, explained in sections 3.3.1 and 3.3.2, respectively. From the gathered information, the goals and objectives of the development of the emergency contingency strategy are presented in section 3.4. Section 3.5 follows with the explanation of the principles of the "free corridor", the proposed contingency strategy for teleoperated vehicles. The theory is outlined and analysed. Two different calculation methods for trajectories are presented and used to determine the behaviour of the path. In order to guarantee the vehicle following the predicted trajectory, open-loop control and closed-loop control strategies are proposed and analysed in section 3.6. Sections 3.7 and 3.8 explain the implementation of the "free corridor" in the simulation and in the experimental vehicle, respectively. The concept is tested in simulation and in the experimental vehicle using different standard maneuvers where a connection loss is simulated and their results are presented. Finally, section 3.9 discusses the obtained results.

3.1 Mobile Communication Network

Communications is one of the three main components of a teleoperated system introduced in section 2.5.1. Mobile networks and their infrastructure currently have a wide coverage, especially for 3G. The fourth generation of mobile communications is already available throughout different locations and its infrastructure is continuously in development. Moreover, further generations are also in the development stage, such as LTE Advanced [Kis13]. Even though current network coverage is continuously expanding, there are still some areas where there is no or poor reception, such as tunnels and remote areas. The quality of connection depends greatly on concurrent users on the same network cell [Ten10, p. 272].

Another aspect to consider is that network cells adapt their "range" depending on the amount of concurrent users. Whenever smaller amounts of users are connected to the same cell, it expands its range and whenever it becomes heavily loaded, its range shrinks. In this case, the traffic is then redirected to neighboring cells. This effect is called *"cell breathing"* [Dol05]. Additionally, since the application of teleoperated vehicles consists of a moving vehicle, cells have to be changed regularly. All these mentioned aspects may cause an unstable connection, not being able to guarantee a constant network quality or service without interruptions, greatly influencing the communication between the vehicle and operator in terms of bandwidth, time delay or even connection loss.

3.2 Time Delays

Time delays are present in mobile networks when exchanging information. Delays pose a problem for the teleoperation. SHERIDAN [She93, p. 592] noticed restraints in the continuous teleoperation in earth orbit or deep space by human operators on earth's surface because of transmission delays imposed by limitations on speed of light or computer processing, concurring with FERRELL [Fer64, pp. 16–17], who showed that the existence of delays in the control loop causes instability. Different approaches have been proposed to avoid the instability caused by delays, such as the *Move-and-Wait* method when operating in direct teleoperation mode, sacrificing completion time, or the *Supervisory Control* when time delays are very large and the tasks are not previously defined in detail [Fer67, p. 88]. Time delays affect the human performance, but the amount of influence depends on the type and difficulty of the task [Pon08, p. 190]. Interestingly, it is basically irrelevant in which transmission direction the time delays originate, since the effect remains the same: an asynchrony between the internal and external stimuli [Pon08, p. 188] [Arn63, p. 43].

Furthermore, it has been shown that variable time delays can cause instability problems in a teleoperated system [Cho03, p. 156]. To solve this problem, different research works have been done to develop control methods that consider varying time delays [Yok99] [Cho03] [Ryu07] and discrete-time communication [Sec03] [Ber04]. Variable time delays affect the performance more than constant time delays [Pon08, p. 219].

A more detailed analysis of time delays in the current system is presented in [Chu15].

3.3 State of the Art: Safety of Vehicles

In order to better understand what safety of unmanned vehicles means, it is important to define a safe state for automobiles. According to the standard EN50129, a safe state is defined as a state, where the safety is preserved further on. A safety relevant system is located in a safe state when functioning in error- and failure-free mode, or in other words, during normal operation or initial state [Fen04, p. 147] [Hoe11, p. 32].

According to occupational safety, an accident is a sudden and unintentional event based on external influence that causes injuries. This event takes place based on external influences through the interaction between humans and objects belonging to the environment and is caused by the release of energy [Ski91, p. 28]. When trying to quantify the danger, the risk of accident can be seen as the product of the expected frequency of accident events and its expected severity [Ski91, p. 30].

For automobiles, ISERMANN [Ise06, p. 352] defines that (usually) a safe state is stand still (or low speed) at a nonhazardous place. However, it is important to know that if there is no mechanical back-up after failure of electronics, only an action of switching to a still operating alternate electronics can bring the moving vehicle to a safe state, or to reach a stop through active fail-safe systems. When dealing with the "stop" maneuver in traffic, it should be noted that in some cases, it is a very critical maneuver with a high damage potential, even though it is one of the most frequently used maneuvers in certain scenarios, such as urban traffic [Kau10, p. 1220].

Many vehicles on the market are already equipped with modern sensor technologies. An adaptive cruise control (ACC) system normally possesses the basic elements necessary for a simple collision avoidance through braking, but without steering. It detects when a collision would occur and activates the brakes to avoid it. For low speed traffic, collision avoidance systems can be already seen on the market, either providing limited automated braking capability or automatically avoiding collisions. In the future, collision avoidance systems could include steering actions. To accomplish full collision avoidance systems, besides the need for more advanced and multiple sensors, further development is required. This type of action is likely to have the highest potential benefits but is also the approach with the highest risk, since activating the system falsely could increase the risk to other road participants [Gro13, p. 1].

Driver assistance systems can be categorized according to their types of functions. Table 3.1 summarizes different systems that are available on the market accordingly. There are different systems that are categorized according to their function, such as only informing the driver or even intervening to avoid accidents.

Accidents in the longitudinal traffic belong to the biggest type of accidents and cause a considerable amount of deaths and severe injuries [Sta14, pp. 66–77] [Win09a, p. 522]. To try to minimize these, frontal collision protection systems are integrated into vehicles. Such systems include for example the *Brake Assistance Systems (BAS)*. These systems should achieve the maximal deceleration as soon as an intention for emergency braking is detected. This maximal deceleration should be kept until a withdrawal of the braking intention is detected [Win09a, p. 522] [Wei03]. This type of system could be classified according to table 3.1 as an intervening system.

Figure 3.1 shows the schematic sequence of brake pressure versus time for a hesitant driver (1), for an average driver (2), for an experienced driver (3) and for the optimal pressure rise (BAS). Two main aspects can be identified that lead to the less-than-ideal deceleration of the vehicle. First, even experienced drivers build the brake pressure hesitantly and only trained drivers in emergency brakings are able to approximate the optimal rise. Second, there is

Table 3.1: Categories for driver assistance systems according to their types of functions [Hol04]

Category	**Examples**
Informing systems	LDW (Lane Departure Warning) CMS1 (Collision Mitigation System)
Automatically acting systems (comfort)	Cruise Control, ACC
Autonomous intervening systems	ABS, ESP CMS2, Automatic Emergency Brake CAV (Collision Avoidance)
Autonomous systems	

a relatively long delay between the event and the beginning of the brake pressure build-up, or the reaching of the maximal brake pressure. A clear advantage of the brake assistance system can be seen.

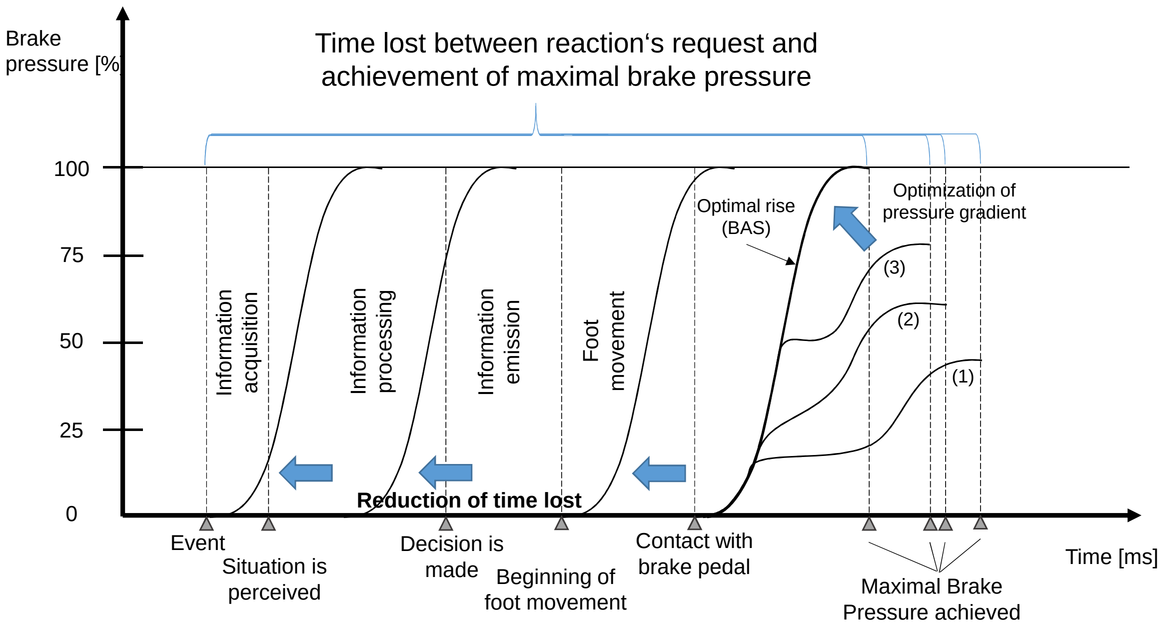

Figure 3.1: Functionality brake assistance systems for a hesitant driver (1), for an average driver (2), for an experienced driver (3) and for the optimal rise (BAS) (adapted from [Wei03, p. 4])

Additionally, accident research showed that most of the drivers do not use the braking and the deceleration potential to its full extent. Figure 3.2 shows the statistical analysis of an accident database. In each of the injury classes MAIS (*Maximum Abbreviated Injury Scale*), a certain percentage of drivers who reacted with a comfortable deceleration ($\sim 3\,\mathrm{m/s^2}$) could at least have reduced the accident's consequences by applying a higher deceleration [Mau09, p. 48].

Important in frontal collision protection systems is the warning and intervention time. *Collision Warning* systems include the widely spread auditive warning with short warning tones supported by a blinking optical display with a warning symbol. The collision mitigation system CMS1 shown in table 3.1 belongs to this type of systems [Hol04]. Vehicles with a reversible seat-belt tensioner offer the possibility to use this as a warning system, such as Honda (Legend), Lexus (LS) and Mercedes-Benz (S-Class W221, CL-Class W216). Additionally, vehicles with an active accelerator pedal from Continental are able to trigger a haptic feedback [Win09a, p. 536].

At the same time or shortly after the warnings, conditioning measures can intervene to support the driver during the emergency maneuver. The CMS1 collision mitigation system would belong to this category [Hol04]. Almost already as a standard feature is the brake's *pre-fill*. This system applies a small pressure into the brake system that allows a faster response of the braking system. This causes a slight deceleration not noticeable for the driver. Additionally, a slight modification in the chassis parameters, if possible in the vehicle, could benefit the emergency braking or evasion maneuvers. Examples of preconditioning systems are the PRE-SAFE of Mercedes-Benz (without preconditioning for evasion maneuvers) and the Advanced Pre-Crash Safety (A-PCS) system from Lexus [Win09a, p. 536] [Sta08].

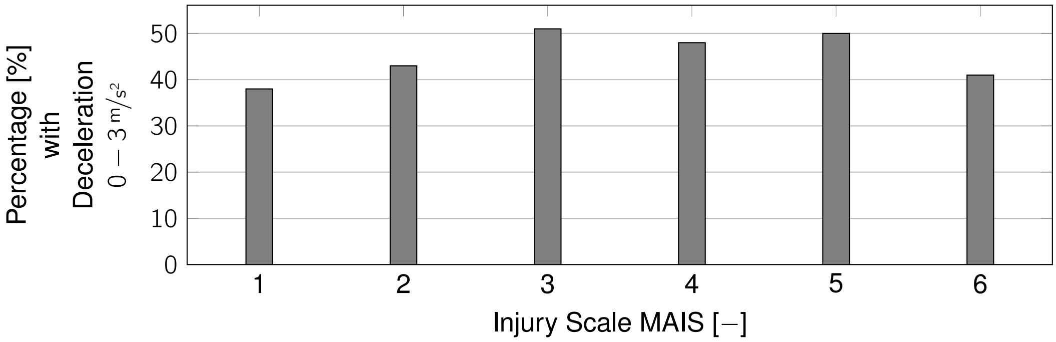

(a) Deceleration by accidents according to injury scale without emergency brake system

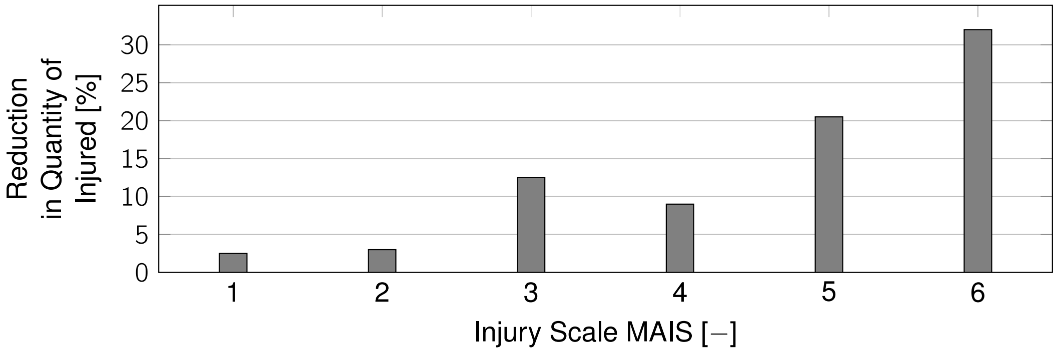

(b) Potential for reduction in injury scale with emergency brake system

Figure 3.2: Theoretical potential of an emergency brake system according to MAURER (adapted from [Mau09, p. 47])

Furthermore, small braking interventions can be applied to warn the driver. There are two possibilities: *Warning Braking* or *Speed Reduction Braking (SRB)*. The main effect of the *Warning Braking* is to induce a haptic warning to the driver. A braking with a deceleration of $4\,\mathrm{m/s^2}$ for a period of typically 0.3 seconds and a braking pressure build up time and pressure reduction time of 0.2 seconds induces a reduction in speed of approximately $2\,\mathrm{m/s}$ and therefore a reduction of kinetic energy and braking distance of approximately 20% at a velocity of $20\,\mathrm{m/s}$. This reduction of kinetic energy does not lead to a critical change of driving state, apart from the case of an already started overtaking maneuver.

During *Speed Reduction Braking*, a partial braking of $30-40\%$ of the maximal deceleration induces a higher warning with a higher reduction of kinetic energy. Such a braking maneuver with $4\,\mathrm{m/s^2}$ deceleration and 1.5 seconds Time-to-Collision (TTC) towards a static obstacle would cause a reduction of approximately $6\,\mathrm{m/s}$. Nevertheless, such a premature intervention could be overridden by the driver.

3.3.1 Intervention Strategy

The intervention strategy of a brake assistance system greatly depends on the respective area of activity. In this section, the relation between decisive parameters for the emergency braking is discussed, such as deceleration, time of intervention and initial speed. The calculations are based on the intervention strategy proposed by KOPISCHKE described in [Kae07, pp. 189 ff.] and also used in [Jan02] [Sta08] [Wal14]. According to the own velocity v_{ego} towards a static obstacle, the ideal time for the brake intervention is discussed. Figure 3.3(a) depicts the idea schematically.

If the time to deploy the maximum braking effect is not considered, through a constant braking deceleration a_{brake}, the necessary braking distance d_{brake} to avoid collision can be calculated as:

$$d_{\text{brake}} = \frac{{v_{\text{ego}}}^2}{2 \cdot a_{\text{brake}}} \tag{3.1}$$

For a collision-free evasion maneuver, at least the evasion distance s_{evasion} perpendicular to the moving direction needs to be covered:

$$s_{\text{evasion}} = \frac{b_{\text{ego}} + b_{\text{obstacle}}}{2} \tag{3.2}$$

where b_{ego} represents the width of the ego-vehicle and b_{obstacle} represents the width of the obstacle.

Using s_{evasion}, a constant lateral acceleration a_y, the needed time for evasion t_{evasion} and the minimal evasion distance d_{evasion} to the obstacle to avoid collision can be calculated:

$$t_{\text{evasion}} = \sqrt{\frac{2 \cdot s_{\text{evasion}}}{a_y}} \tag{3.3}$$

$$d_{\text{evasion}} = v_{\text{ego}} \cdot t_{\text{evasion}} \tag{3.4}$$

For the cases of $a_{\text{brake}} = 8\,{}^{\text{m}}/_{\text{s}^2}$, $a_y = 8\,{}^{\text{m}}/_{\text{s}^2}$, where depending on tire type, the maximal lateral acceleration reaches between $80 - 100\%$ of the maximal deceleration of $10\,{}^{\text{m}}/_{\text{s}^2}$ on dry roads [Win09a, p. 529], $b_{\text{ego}} = 2m$ and $b_{\text{obstacle}} = 2m$, Figure 3.3(b) is obtained. It can be recognized that up to a certain velocity, pure braking is able to avoid collisions. Furthermore, the limit velocity v_{limit} for a full collision avoidance is calculated as [Web12, p. 43]:

$$v_{\text{limit}} = 2 \cdot a_{\text{brake}} \cdot \sqrt{\frac{2 \cdot s_{\text{evasion}}}{a_y}} \approx 40.7\ {}^{\text{km}}/_{\text{h}} \tag{3.5}$$

An evasion maneuver would only make more sense at velocities over this limit value, which corroborates the same results as JANSSON [Jan02, p. 4], that braking is the most efficient countermeasure maneuver for low speeds and steering away (evasion maneuvers) for high speeds.

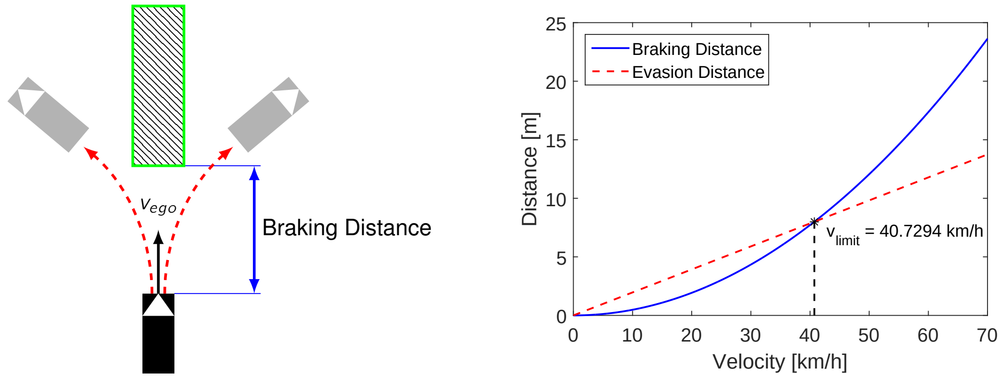

(a) Sketch of a drive towards a static obstacle

(b) Relationship of evasion distance and braking distance for different velocities

Figure 3.3: Relationship of evasion distance to braking distance for different velocities according to the KOPISCHKE intervention strategy [Kae07, pp. 189 ff.] [Jan02] [Sta08] (adapted from [Wal14])

3.3.2 Emergency-Braking Decision Making

For the decision making of an emergency braking system, the understanding of the surroundings plays an important role. Such an emergency braking system could either completely avoid the collision or reduce its consequences.

For example, LAGES [Lag01] conducted experiments on an Fuzzy-based active system for accident avoidance, where measurement uncertainties were considered. For the acquisition of the surroundings, laser scanners were used. Here, it was important to determine if and when an emergency braking was necessary. With the help of different sensors, such as radar, laser scanners and video systems, the surroundings can be interpreted. Another system, developed by JANSSON [Jan05], attempts to reduce the accident's consequences by applying a reduction in speed through the brakes once a collision becomes unavoidable. The system provides a maximum reduction of speed of $15\,{}^{\mathrm{km}}/_{\mathrm{h}}$ and an average reduction of speed of $7.5\,{}^{\mathrm{km}}/_{\mathrm{h}}$, which is estimated to reduce all injuries classified between moderate and fatal for rear-end collisions by 16%. For the decision making, if and when an emergency-braking is necessary, three approaches are discussed.

The first approach is based on a deterministic decision making based on the current state estimate of the host vehicle and those of other objects. The state estimate uncertainty is neglected, putting the focus on determining the threat of a collision when the state of other objects is known. Different decision-making functions are defined for single obstacles, such as *time to collision (TTC)*.

The second approach, which focuses on multiple obstacles, consists of searching for admissible maneuvers. When there is no admissible maneuver available, it is determined that a conflict is unavoidable and an emergency braking action is necessary.

The third approach is based on statistical methods. In this approach, the measurement uncertainties are considered. Furthermore, several actions could be considered and the collision avoidance strategy is described by a rule database, which determines the action to be taken depending on each possible state. The problem is to determine the state since they are uncertain. Using statistical methods, a probability of collision is calculated, which determines if an emergency braking is necessary or not.

For the development of an active hazard braking system, BOUZOURAA [Bou10, p. 14] specifies relevant aspects for the situation analysis, shown in Figure 3.4. It is important to know that the intervention of an emergency-braking system can only be allowed at the point when objectively an evasion maneuver becomes impossible, otherwise it could contradict the desires of the driver [See06]. This leads to the conclusion, that at the point where an evasion maneuver with comfortable lateral acceleration becomes impossible, the condition for an automatic partial braking is given. When an evasion maneuver with maximal lateral acceleration becomes impossible, the condition for an automatic emergency braking is given [Bou10, p. 18].

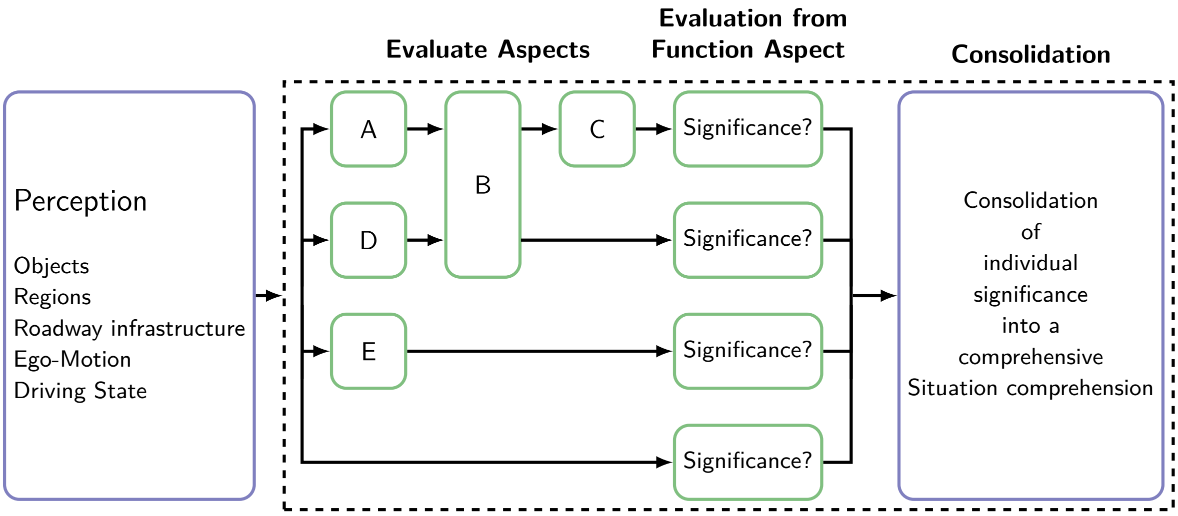

Figure 3.4: Strategic solution for the situation analysis (adapted from [Bou10, p. 14])

The state-flow for behaviour generation of an emergency braking system [Bou10, p. 22] is depicted in Figure 3.5.

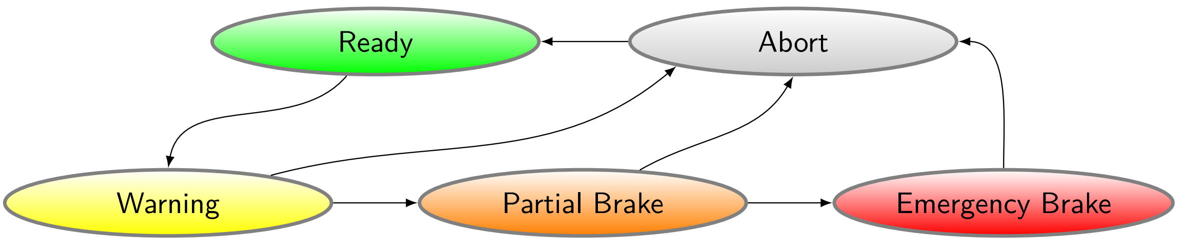

Figure 3.5: Behaviour creation for emergency braking systems (adapted from [Bou10, p. 22])

A similar approach is also proposed by KIVRIKIS AND TJERNSTRÖM [Kiv04, pp. 29 ff.]. As soon as there is no available trajectory for an evasion maneuver (or escape route), the system alarms.

A further possibility to represent the evasion maneuvers with different lateral accelerations is the *Collision Prediction Algorithm* proposed by KÄMPCHEN [Kae07, pp. 190 ff.]. Trajectories of maximal overall acceleration are considered for all possible driving maneuvers. It then checks all different combinations of trajectories between the ego and the opponent vehicles. These trajectory combinations are defined by angles in the friction circle (or Kamm's circle). These are then used to assess the situation and to predict a collision.

Another possibility is the usage of *Virtual Bumpers*, which consists of a virtually defined safe zone around the vehicle [Ros07, p. 22]. It can act as a layer of defense against impending collisions. As soon as the safe zone is breached, the vehicle is brought to a stop immediately. Even though this approach does not consider moving obstacles, it provides an easy and effective mean to avoid collisions at low speeds.

WALLNER [Wal14] developed an emergency braking system for teleoperated vehicles based on lidar sensor data at raw data level. A combination of an adapted particle filter algorithm and an intervention concept derived from the Kamm's circle is used to track moving objects and assess the situation, respectively.

The crucial part by the development of collision avoidance systems is the decision making and their conflicting considerations. These include the fact that all collisions should be avoided but never should a faulty intervention be done. The design of such systems is therefore a compromise between these two mutually exclusive conditions [Jan02, p. 1].

3.4 Objective and Goals

Section 3.3 discussed different collision avoidance systems and their importance for safe driving. It is important to guarantee that a safe state can be reached at any time. The above mentioned systems are not only valid for normal vehicles driven manually but also for teleoperated vehicles. The systems could assist the operator in the driving task. They are also capable of preparing or preconditioning the vehicle for a maneuver. However, an important situation during teleoperation is still unsolved, which is the time after the connection between operator and vehicle is lost. During this period, intervention strategies and the decision making would be difficult to determine.

According to section 3.1, the quality of the mobile connection cannot be guaranteed and a connection loss cannot be predicted accurately. Therefore, it is important to develop a contingency strategy to bring the teleoperated vehicle into a safe state.

By the definition of the different levels of automation considered for public traffic [Gas12, p. 16], the emergency stop assistant takes over the control of the vehicle exclusively in case of driver's incapacity to act or unconsciousness, either because of medical conditions or falling asleep, so that the driver is not capable of controlling the vehicle actively. The driver is informed of the taking over and is allowed to overtake the control anytime in case of recovery.

The above mentioned situation, in which the vehicle is left on its own, can be compared to the moment where the connection is lost during operation of teleoperated vehicles. As shown before, while driving at low speeds, the most efficient countermeasure is braking [Jan02, p. 4] because it is normally less dangerous and have less consequences in comparison to evasion maneuvers [Wel09] [Web12, p. 85].

An important task while driving is the compliance to hold a determined distance to the vehicle in front [Kra08, p. 76]. This distance must be large enough such that stopping behind it does not become impossible, even if it suddenly brakes [Bun13, pp. 3–4]. On roads inside built-up areas, the safety distance equals the distance driven in 1 second (approximately 15 meters when driving at 50 km/h or 3 times the vehicle's length) and outside built-up areas, the distance driven in 2 seconds (approximately half of the shown speed on the speedometer or 50 meters when driving at 100 km/h) [KFZ14].

Concepts considering safe stopping zones and travel zones have already been proposed by GIBSON [Gib38]: A field of safe travel consists of the field of possible paths which the vehicle may take unimpeded at any time. This area shifts and bends continuously. Furthermore, a minimum stopping zone, which is within the field of safe travel, is defined by the minimum braking distance required to stop the vehicle. Its size depends on the driven speed, the brakes and also on the condition of the road-surface.

Taking the above discussed aspects into consideration, it is necessary and essential to develop a suitable safety concept. The *free corridor* is proposed as a solution to the problem of connection loss in teleoperated vehicles. Following sections describe its theory, implementation and validation.

3.5 The "Free Corridor" as an Emergency Contingency Strategy

According to the aspects presented in section 3.3, bringing the teleoperated vehicle to a stop would correspond to a safe state. The "free corridor" proposes a possibility to achieve this when the connection between vehicle and operator is lost. This corridor is displayed to the operator at all times and it is the operator's responsibility to drive the vehicle in such way, that the corridor constantly remains free of obstacles. This way, it can be guaranteed that in case of a connection loss, a safe state can be reached without colliding with any objects. This makes sense, since displaying the braking distance has been shown to be meaningful and helpful for the driver in the control of longitudinal dynamics [Bub75]. However, the current proposed strategy is only capable of avoiding a collision with static objects. Currently, the human operator is responsible for also predicting the movement of other traffic participants so as to avoid collision with them. A local automated system in the teleoperator could enhance the limitation of static objects towards dynamic objects. In order to display a reliable corridor, the path and the predicted braking distance must be calculated precisely. This predicted trajectory depends on current speed, friction coefficient between tires and road and momentary radius of curvature, among others.

3.5.1 Path Generation

In order to generate the path of the corridor, different methods such as circular arcs, spline curves, polynomial curves or clothoids can be used. Since circular arcs and clothoids are typical elements used in the construction of roads, these are introduced, implemented and analyzed:

Circular arc:
The curves of the path are represented using circular segments, using smaller or bigger curve radii for inner or outer curves, respectively, and sharing the same center point. The path prediction can be achieved with relatively low effort. However, this method is basically only suitable for steady-state circular and straight maneuvers and has limited possibilities for representation and usage in road building. The "free corridor" would correspond in this case to the trajectory which the vehicle would follow if the steering wheel angle was held fix.

Clothoids:
A clothoid, or Euler Spiral, is an easy mathematical representation of a curve and very popular in road building. Its curvature changes linearly with regard to curve length. This type of curve is chosen to approximate the transitions between straight and constant radius sections since they produce a linear steering input between them [Kri12, p. 277].

MITSCHKE [Mit04, p. 616] mentions that in case a circular arc is directly connected to a straight section, the lateral acceleration would jump from zero to a particular value and the driver would have to turn abruptly. Since this is not physically possible, the vehicle would abandon the path.

Even though its mathematical representation is relatively easy, generating the path using this method would be harder because it is not possible to solve the underlying integral for the curve-definition analytically, only numerically. Using clothoids, the "free corridor" would correspond to the trajectory which the vehicle would follow if the steering wheel rate was held constant.

3.5.2 Single Track Model

For the calculation of the "free corridor", it is necessary to analyze the vehicle's dynamic behaviour correctly. For its implementation, the equations and model representation of the *Single Track Model* are used. This model was proposed in 1940 for the investigation of the dynamics of rubber-tired vehicles [Rie40].

A normal driver achieves in city traffic a maximal lateral acceleration of $\approx 3.5\,\mathrm{m/s^2}$. In the longitudinal direction, higher decelerations than accelerations are achieved. Decelerations remain under $\approx 3\,\mathrm{m/s^2}$ [Hac82]. According to WEBER [Web12, p. 74], the maximal lateral acceleration during a sharp lane change is $\approx 2\,\mathrm{m/s^2}$. Figure 3.6 shows typical accelerations for different driver types according to HACKENBERG [Hac82], BIRAL [Bir05] and WEGSCHEIDER [Weg05]. According to BÖRNER [Boe06, p. 47], the simple single track model can be used to represent the relations of lateral accelerations, a_y, of up to $4\,\mathrm{m/s^2}$ on dry road-surfaces or lateral acceleration of up to $0.5\,\mathrm{m/s^2}$ on wet ice road-surfaces. This conclusion is also reached by MITSCHKE [Mit04, p. 560] and it offers a good representation of the vehicle's dynamic behaviour [Hei11, p. 95]. Since these conditions are met for the application of tele-operated vehicles, and no advantages of a non-linear model could be determined [Söh01, pp. 144–145], the linear single track model was used.

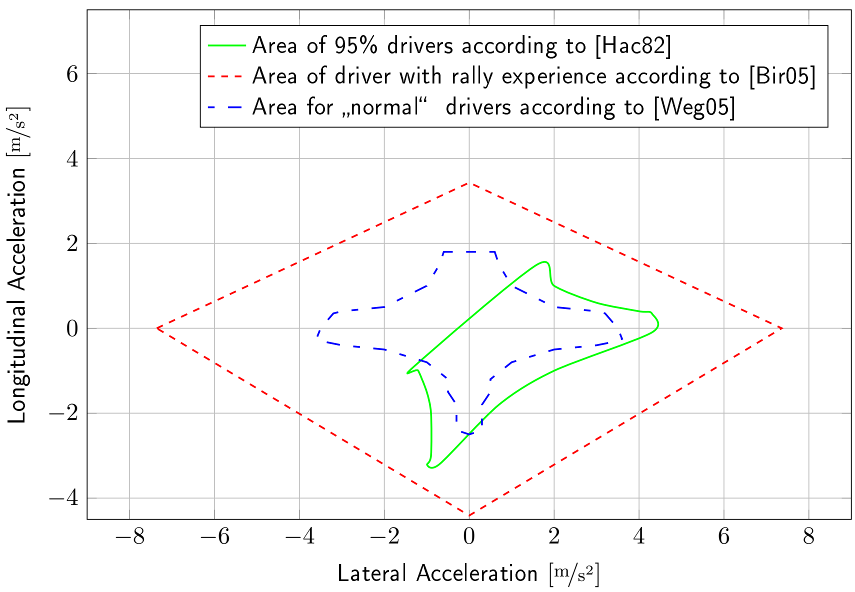

Figure 3.6: Typical lateral accelerations for different driver types according to HACKENBERG [Hac82], BIRAL [Bir05] and WEGSCHEIDER [Weg05]

This model presents some simplifications [Hei11, p. 95] [Mit04, p. 547]:

- The double track vehicle's dynamic model is simplified as a single track model. The vehicle consists of only one front and one rear wheel.
- The center of gravity is located on road level. This way, changes in loads due to pitch- and roll motion are not considered. The motion is limited to two translational degrees of freedom in the $x - y$ plane and one rotatory degree of freedom (yawing around the z axis).
- The system is linearized through small angles approximation.

Figure 3.7 shows a representation of the single track model.

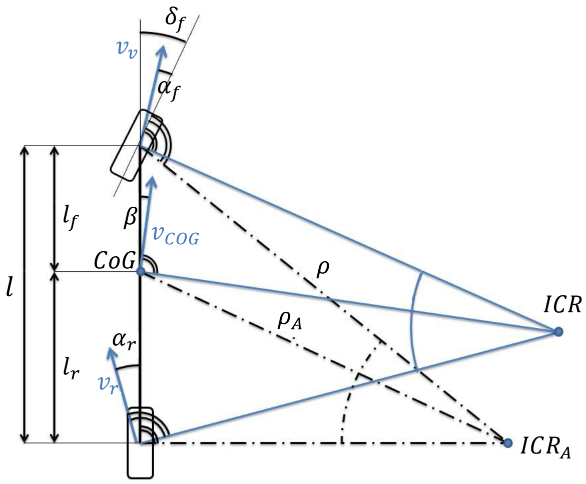

Figure 3.7: Single track vehicle's dynamic model (adapted from [Tan13b])

3.5.3 Momentary Radius of Curvature

In order to calculate the path using either circular arcs or clothoids, the momentary radius of curvature ρ needs to be calculated. WINNER [Win09b, p. 497] proposes different methods to calculate the curvature κ, which is the inverse of the radius of curvature. Detailed discussion regarding the different methods can be found in [Win09b, p. 497]:

A. Radius of curvature from lateral acceleration

This method is based on the physical law of circular movement where the centrifugal force corresponds to the side force on the vehicle due to lateral acceleration. The radius of curvature can be calculated as

$$m_{\text{veh}} \cdot a_y = \frac{m_{\text{veh}} \cdot {v_x}^2}{\rho} = m_{\text{veh}} \cdot v_x \cdot (\dot{\psi} + \dot{\beta}) \tag{3.6}$$

$$\rho = \frac{{v_x}^2}{a_y} \tag{3.7}$$

where

m_{veh}	:	vehicle mass
a_y	:	lateral acceleration
v_x	:	longitudinal velocity
ρ	:	radius of curvature
$\dot{\psi}$	:	yaw rate
$\dot{\beta}$	:	sideslip rate

B. Radius of curvature from yaw rate

Using equation (3.6), the radius of curvature can also be computed using the yaw rate as follows:

$$\rho = \frac{v_x}{\dot{\psi} + \dot{\beta}} \tag{3.8}$$

However, the sideslip angle is normally not measured because it requires expensive equipment such as optical correlation sensors [Gri09, p. 36] or has to be derived from other signals. Therefore, the assumption that $\dot{\beta} \approx 0$ is used [Win09b, p. 497]. This is valid for low dynamic vehicle states, and since the application of teleoperated vehicles is for urban scenarios, this assumption can be made. Simplifying equation (3.8), the radius of curvature can be calculated as:

$$\rho = \frac{v_x}{\dot{\psi}} \tag{3.9}$$

C. Radius of curvature from steering wheel angle

In order to compute the radius of curvature from the steering wheel angle δ_H, it is necessary to know the slip angle at the front and rear wheels. Using the single track model and calculations of slip angles according to [Hei11, pp. 95 ff.] and the steering ration i_S, the radius of curvature can be calculated as:

$$\rho = \frac{l_f + l_r}{\frac{\delta_H}{i_S} + \alpha_r - \alpha_f} = \frac{l}{\frac{\delta_H}{i_S} + \alpha_r - \alpha_f} \tag{3.10}$$

This method for calculating the radius of curvature is not convenient since a lot of effort and costs are needed to measure slip angles and estimations are not accurate enough.

D. Radius of curvature from wheel speed

The curvature from the wheel speed can be calculated as:

$$\rho = \frac{v_x \cdot b_t}{\Delta v} \tag{3.11}$$

where

Δv	:	difference in wheel speed of non-driven axis
b_t	:	track width

The different proposed methods mainly differ from their robustness towards external influences, such as cross winds, road cross slope or tolerance of tire radius, among others. Each of them is better applicable for different working conditions and their advantages are explained by WINNER [Win09b, p. 497]. He concludes that the use of the yaw rate for the computation of radius of curvature is the most suitable. However, he proposes that a combination of different methods can be used to improve quality.

In the application of the emergency contingency strategy "free corridor", the radius of curvature is calculated using the current vehicle's yaw rate.

3.5.4 Braking Distance

Additionally to the momentary radius of curvature, it is necessary to calculate the braking distance s_b until the vehicle comes to a stop. The calculation is discussed for the two methods proposed in section 3.5.1.

Circular arc:
In order to calculate the braking trajectory along a determined path, two differential equations were established by SWIK [Swi74]:

$$\frac{ds}{dv} = \frac{v}{g\sqrt{\mu_{\text{max}}^2 - \left(\frac{\kappa(s)v^2}{g}\right)^2}} \tag{3.12}$$

$$\frac{d\gamma}{dv} = \frac{\kappa(s)v}{g\sqrt{\mu_{\text{max}}^2 - \left(\frac{\kappa(s)v^2}{g}\right)^2}} \tag{3.13}$$

where

v	:	absolute value of velocity at wheel center point
s	:	traveled distance
g	:	gravity
μ_{max}	:	maximal available coefficient of friction
$\kappa(s)$	:	curvature progression
γ	:	slope

In the case of a circular arc ($\kappa = constant$), the differential equations (3.12) and (3.13) can be integrated analytically. Using the following boundary conditions

Initial values	:	$v = v_0, \gamma(v_0) = s(v_0) = 0$
End values	:	$v = 0, \gamma(0) = \gamma_b, s(0) = s_b$

the braking distance can be determined as:

$$s_b = \frac{1}{\kappa}\int_0^{v_0} \frac{v\,dv}{\sqrt{\left(\frac{g\mu_{\text{max}}}{\kappa}\right)^2 - v^4}} = \frac{1}{2\kappa}\arcsin({v_0}^2 \cdot \frac{\kappa}{g \cdot \mu_{\text{max}}}) \tag{3.14}$$

In the special case of straight-line braking (curvature $\kappa = 0$),

$$s_b = \frac{{v_0}^2}{2g \cdot \mu_{\text{max}}} \tag{3.15}$$

Clothoids:
Since clothoids do not have a constant curvature, equation (3.14) cannot be used. However, the braking distance can be computed using the maximal deceleration, which according to SWIK [Swi74] can be determined as

$$a_{\text{max}} = -g\sqrt{\mu_{\text{max}}^2 - \left(\frac{\kappa(s)\cdot v^2}{g}\right)^2} \tag{3.16}$$

The complete clothoid trajectory is split into n-segments, each of length d. The velocity at the end of each segment can be calculated as

$$v_{(i+1)} = v_i + a_{\text{max,i}} \cdot t_i \tag{3.17}$$

where the time needed to complete each segment t_i is calculated as $t_i = d/v_i$ and $a_{\text{max,i}}$ represents the possible deceleration at each segment. During the small amount of t_i, the velocity is assumed to be constant. These steps are repeated until the velocity equals 0. The braking distance s_b becomes the sum of elements:

$$s_b = i_{\text{end}} \cdot d \tag{3.18}$$

In case the curvature progression $\kappa(s)$ becomes too high, so that $\mu_{\text{max}}^2 - \left(\frac{\kappa(s)\cdot v^2}{g}\right)^2 < 0$, a complex value for the deceleration would be obtained from equation (3.16). In this case, the vehicle is not capable of following the trajectory anymore, since the maximal possible friction force of the wheels through lateral acceleration has already been exceeded. Therefore, the braking distance at the maximal allowed curve speed according to SWIK [Swi74] is used:

$$s_b = \frac{v^2}{g \cdot \mu_{\text{max}}} \cdot \frac{\pi}{4} \tag{3.19}$$

Simulation results showed that for a segment length $d = 0.05m$, this approach is sufficiently accurate for the application since the error lies below 1%.

3.5.5 Path Elements

Circular arc:
Using the calculated values of radius of curvature ρ and the braking distance s_b, a circular arc with center point ICR can be generated. Figure 3.8a shows a sketch of the vehicle-fixed coordinates, the vehicle's path at any time $t = t_{\text{brake}}$ on the xy-plane. The braking distance s_b is represented in red and additionally, the point at which the vehicle's bumper would come to a stop after the emergency brake is shown in green. If t_{brake} is the time needed to come to a stop, the elbow angle θ can be computed as

$$\theta(t_{\text{brake}}) = \frac{s_b}{\rho(t_{\text{brake}})} = \frac{1}{2\kappa\rho(t_{\text{brake}})} * \arcsin({v_0}^2 * \frac{\kappa}{g * \mu_{\text{max}}}) \tag{3.20}$$

The angle θ is defined as positive in a left-curve and negative in a right-curve, keeping the same convention of yaw angle in vehicle's coordinate system. The position of the center of mass where the vehicle would stop can be calculated as

$$\begin{bmatrix} x_{\text{CoGStop}} \\ y_{\text{CoGStop}} \end{bmatrix} = \begin{bmatrix} \rho(t_{\text{brake}}) * \sin\big(\theta(t_{\text{brake}})\big) \\ \rho(t_{\text{brake}}) * \big(1 - \cos\big(\theta(t_{\text{brake}})\big)\big) \end{bmatrix} \tag{3.21}$$

and the position of the corridor, shown in red dash dot, can be calculated using trigonometric relations with a predefined corridor width b_w. The position of the right (r) and left (l) corresponding i-elements, as shown in Figure 3.8b, becomes

$$\begin{bmatrix} x_{\text{il}} \\ y_{\text{il}} \end{bmatrix} = \begin{bmatrix} x_{\text{CoGi}} - \frac{1}{2} \cdot b_w \cdot \sin(\theta_i) \\ y_{\text{CoGi}} + \frac{1}{2} \cdot b_w \cdot \cos(\theta_i) \end{bmatrix} \tag{3.22}$$

and

$$\begin{bmatrix} x_{\text{ir}} \\ y_{\text{ir}} \end{bmatrix} = \begin{bmatrix} x_{\text{CoGi}} + \frac{1}{2} \cdot b_w \cdot \sin(\theta_i) \\ y_{\text{CoGi}} - \frac{1}{2} \cdot b_w \cdot \cos(\theta_i) \end{bmatrix} \tag{3.23}$$

However, for the driver it makes more sense to know the stopping point of the front bumper position, depicted in Figure 3.8 as the green line. Therefore, an offset from the center of mass in the vehicle's longitudinal coordinate to the bumper $\Delta CoG_{\text{Bumper}}$ is added. Using again trigonometric functions, the stopping point for the bumper can be calculated as

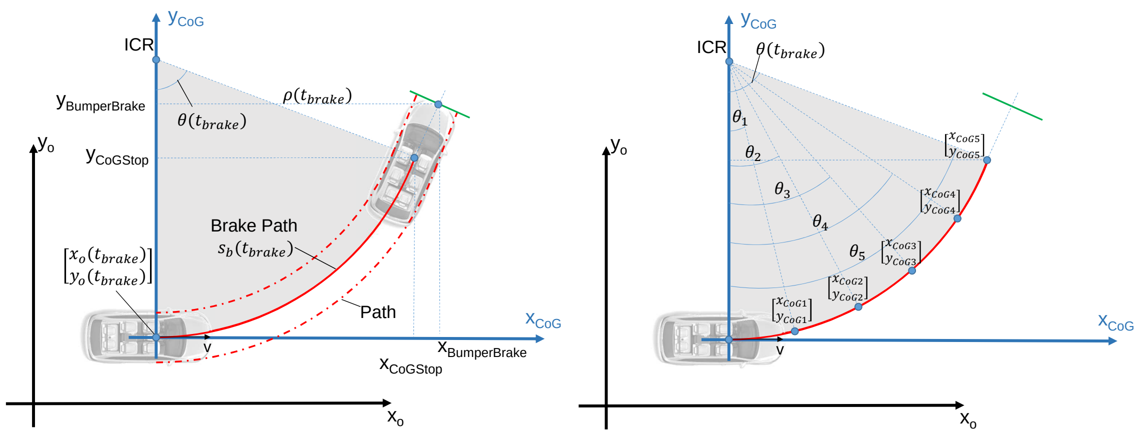

(a) Representation of path using a circular arc (b) Distribution of elements

Figure 3.8: Representation of path using a circular arc (left); distribution of elements (right) (adapted from [Tan13b] [Tan14a])

$$
\begin{aligned}
\begin{bmatrix} x_{\text{BumperBrake}} \\ y_{\text{BumperBrake}} \end{bmatrix} &= \begin{bmatrix} \rho * \sin(\theta) + \Delta x \\ \rho * \left(1 - \cos(\theta)\right) + \Delta y \end{bmatrix} \\
&= \begin{bmatrix} \rho * \sin(\theta) + \Delta CoG_{\text{Bumper}} * \cos(\theta) \\ \rho * \left(1 - \cos(\theta)\right) + \Delta CoG_{\text{Bumper}} * \sin(\theta) \end{bmatrix}
\end{aligned}
\tag{3.24}
$$

This is shown in Figure 3.9. In the case of circular arcs, a total amount of 5 elements were used for the representation of the "free corridor".

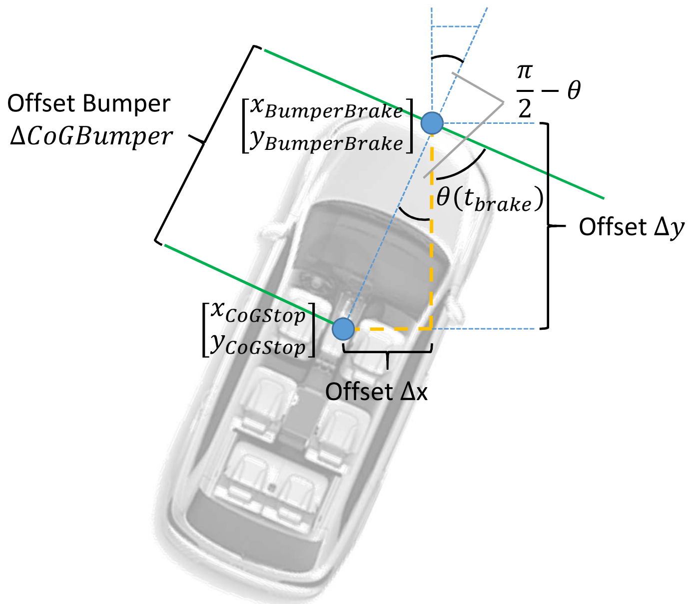

Figure 3.9: Bumper offset from the center of mass

Clothoids:
A clothoid can be seen as a spiral curve whose curvature κ is changing with a constant rate and is determined as [Cor04]:

$$\kappa(s) = \frac{1}{\rho(s)} = c_0 + c_1 \cdot s \tag{3.25}$$

where c_0 represents the initial curvature at $s = 0$ and c_1 represents the constant curvature changing rate. In the special cases of $c_1 = 0$ and $c_0 = c_1 = 0$, the curves are a circular arc and a line, respectively. Integrating equation (3.25) with respect to s, the tangential angle ϑ at any position s can be determined as:

$$\vartheta(s) = \int_0^s \kappa(\tilde{s}) d\tilde{s} = c_0 \cdot s + \frac{1}{2} c_1 \cdot s^2 + \vartheta_0 \tag{3.26}$$

where ϑ_0 represents the tangential angle at the beginning of the clothoid. For the case that a global coordinate system is used for calculation, ϑ_0 would be the yaw angle ψ and in the case of calculating using a vehicle-fixed coordinate system , $\vartheta_0 = 0$. The x- and y-coordinates can be obtained from the integral of the cosine and sine of the tangential angle $\vartheta(s)$ with respect to s:

$$x(s) = \int_0^s \cos\big(\vartheta(\tilde{s})\big) d\tilde{s} = \int_0^s \cos\big(c_0 \cdot \tilde{s} + \frac{1}{2} c_1 \cdot \tilde{s}^2 + \vartheta_0\big) d\tilde{s} \tag{3.27}$$

$$y(s) = \int_0^s \sin\big(\vartheta(\tilde{s})\big) d\tilde{s} = \int_0^s \sin\big(c_0 \cdot \tilde{s} + \frac{1}{2} c_1 \cdot \tilde{s}^2 + \vartheta_0\big) d\tilde{s} \tag{3.28}$$

These equations consist of Fresnel Integrals and can only be solved numerically [Hen79]. Since solving these implies high efforts, an approximation based on numerical integration can be used. Simulation results showed that the necessary accuracy for the application is achieved with 40 strips.

Different amounts of elements can be used for the representation of the corridor. In this application, it was determined that an amount of 10 elements was a good trade-off between computational expense and smooth representation of the corridor.

3.5.6 Circular Arc and Clothoids for the Path Generation

The proposed methods (section 3.5.1) for the path generation are analyzed in the simulation environment DYNA4, which is further explained in section 3.7.1. Two routes were selected to evaluate the performance of both methods. The first road, which includes roundabouts, consists of straight lines, circular arcs, and clothoids as transition segments. The roundabouts are designed with a radius of 28.5 meters and an overall path width of 3.0 meters. For the second road, a standard city road was built. The radii of curvature are between 8 − 25 meters. There are longer straight lines and an overall path width of 3.0 meters. Similarly, the route consists of straight lines, circular arcs and clothoids as transition segments. Figures 3.10a and 3.10b show both roads, respectively.

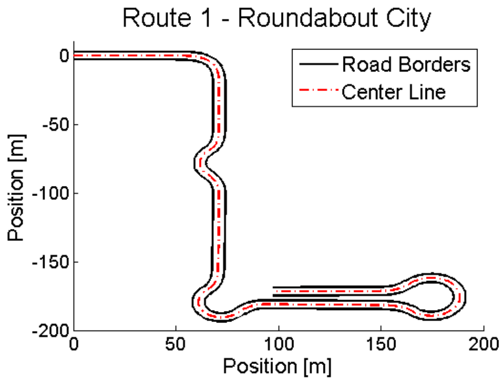

(a) Road 1 - roundabout city

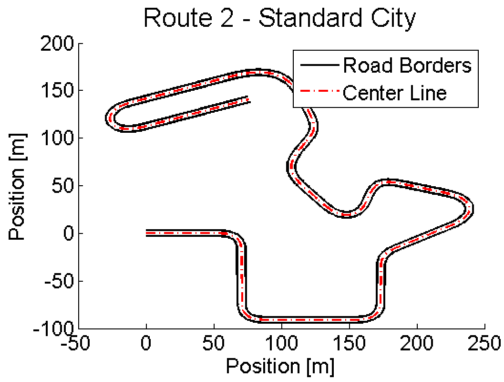

(b) Road 2 - standard city

Figure 3.10: Two different roads used for the evaluation of path generation

Both methods were tested using three different drivers, a cautious, a moderate and a more dynamic driver. These drivers are parameterized as shown in table 3.2, where the maximal allowed values for deceleration, acceleration, lateral acceleration and velocity are shown.

Table 3.2: Driver's parametrization used for the analysis of the "free corridor"

	Unit	**Cautious**	**Moderate**	**Dynamic**
Max. Deceleration	[m/s²]	−4	−5	−6
Max. Acceleration	[m/s²]	2	3	4
Max. Lateral Acceleration	[m/s²]	2.5	3.5	4.5
Max. Velocity	[km/h]	55	55	60

To evaluate the performance of the two concepts, the distance between the last element and the path boundaries was recorded. It is defined as positive if it is within the path and negative if outside. In these two scenarios, the center line serves as path boundary. The results of the simulation are shown for the dynamic driver in the two different roads in Figure 3.11. Goal is to determine if the emergency contingency concept "free corridor" would lead to an unsafe state at any point. This could happen if exactly at the moment of connection loss, the predicted trajectory was located outside the traveling path and an unsafe state would be reached when the vehicle came to a stop. The distances to the road borders of the roundabout city route (Route 1) are shown in figures 3.11a and 3.11b for the right and the left side, respectively. Similarly, the distances to the road borders of the standard city (Route 2) are shown in figures 3.11c and 3.11d.

In the case of path generation using circular arcs, there are in all the cases negative values present. On the other hand, using clothoids, the amount of negative values are much lower. Only on route 2 -standard city-, short negative values are to be seen. Looking at the results,

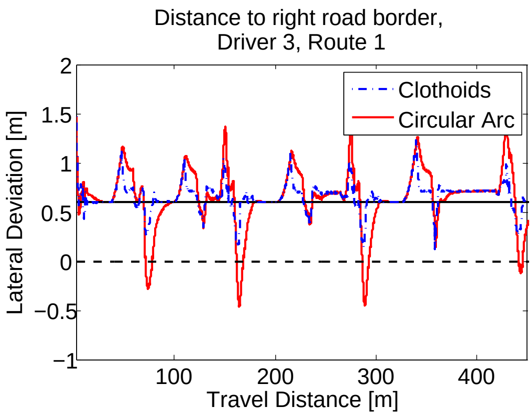

(a) Distance to right border, driver 3, route 1 roundabout city

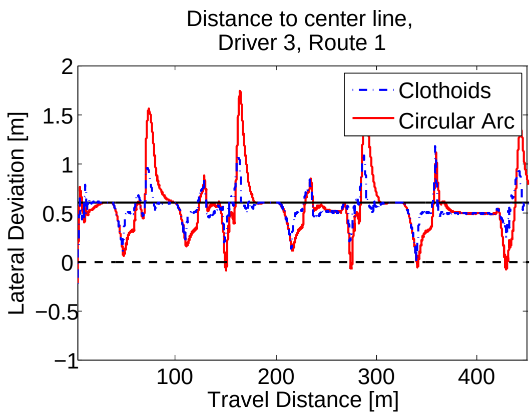

(b) Distance to left border, driver 3, route 1 roundabout city

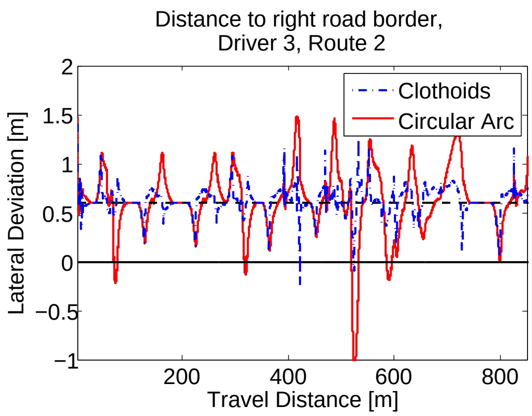

(c) Distance to right border, driver 3, route 2 standard city

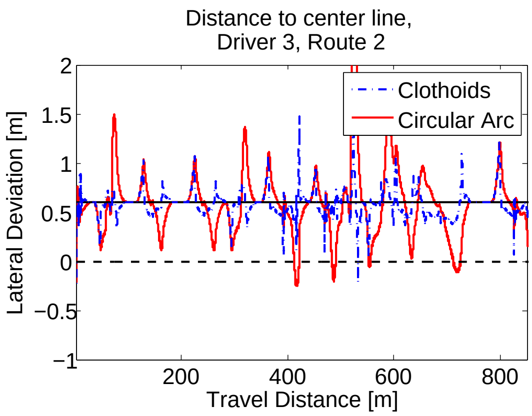

(d) Distance to left border, driver 3, route 2 standard city

Figure 3.11: Comparison of lateral deviation for the two path generation methods

it is clear that due to the structure of the road design, the path generation using clothoids is more appropriate. The creation of elements using circular arcs can be applied only conditionally, especially since the values of the lateral deviation are at some points relatively far away (at travel distance ≈ 520 meters on Figure 3.11c). Similar tendencies are to be found for drivers 1 and 2.

These results were achieved with a driver's model in the simulation framework. In reality, a human operator would be driving the teleoperated vehicle and could completely avoid the slight negative values adapting his driving behaviour.

Due to these results, it was determined that clothoids are more adequate for the "free corridor" and therefore, further development and analysis is based on path generation using clothoids only. Calculation using circular arcs is not further contemplated. Clothoids are also able to produce circular arcs when the constant curvature changing rate c_1 in equation (3.25) becomes zero.

3.5.7 Coefficient of Friction

The "free corridor" is based on an emergency brake when the connection between teleoperated vehicle and working station is lost. The vehicle behaviour depends greatly on the grip between tires and road and an accurate coefficient of friction is important for the correct calculation of the braking distance [Bub75]. Forces between tires and road are transmitted through the contact patch in both circumferential and lateral directions. In both cases, slip can occur. According to the DIN Standard 70000 [Deu94], the longitudinal slip is defined as

$$S_x = \frac{\omega - \omega_0}{\omega_0} \tag{3.29}$$

where

ω	:	wheel rotation speed
ω_0	:	wheel rotation speed of straight free-rolling wheel

The lateral slip is normally given using the slip angle α and its value lies between 0 and 1. Lateral slip depends on the relation between longitudinal and lateral speed on the tire. It can be calculated as [Hei08, p. 59]:

$$S_y = \frac{v_{\mathrm{Y,W}}}{v_{\mathrm{X,W}}} = \frac{v_W \cdot \sin\alpha}{v_W \cdot \cos\alpha} = \tan\alpha \tag{3.30}$$

where

$v_{\mathrm{X,W}}$	:	wheel longitudinal speed
$v_{\mathrm{Y,W}}$	:	wheel lateral speed
v_W	:	wheel speed

According to SCHORN [Sch06, pp. 38–39], the relation of slip S_{res} and longitudinal and lateral slip is the geometrical sum:

$$S_{\mathrm{res}} = \sqrt{{S_x}^2 + {S_y}^2} \tag{3.31}$$

With a coefficient of friction versus slip graph, shown in Figure 3.12a, the available coefficient of friction μ can be established. Besides slip, the coefficient of friction also depends on the road surface, the environment's temperature, tire pressure and mixture.

On a dry asphalt road, the coefficient of friction is $\mu \approx 1.0$, on a wet road $\mu \approx 0.6 - 0.8$ and on ice, $\mu \approx 0.05$. The resulting transferable tire force F_{res} results from the product of coefficient of friction and the vertical wheel forces $F_{\mathrm{Z,W}}$ [Sch06, p. 38]:

$$F_{\mathrm{res}} = \mu \cdot F_{\mathrm{Z,W}} \tag{3.32}$$

This force can be split into longitudinal and lateral wheel forces, $F_{X,W}$ and $F_{Y,W}$ respectively, which depend on the direction of slip:

$$F_{X,W} = \frac{S_x}{S_{res}} \cdot \mu \cdot F_{Z,W} \tag{3.33}$$

$$F_{Y,W} = \frac{S_y}{S_{res}} \cdot \mu \cdot F_{Z,W} \tag{3.34}$$

Here, the resulting tire force has to be smaller than or equal to the product of the maximal available coefficient of friction and vertical wheel forces:

$$F_{res} = \sqrt{F_{X,W}{}^2 + F_{Y,W}{}^2} \leq \mu_{max} \cdot F_{Z,W} \tag{3.35}$$

This can be represented in the Kamm's Circle, as shown in Figure 3.12b. The red circle represents the friction boundary of an isotropic[5] tire. As long as the resulting transferable tire force F_{res} remains inside the circle (green area), a transfer of force between the tires and the road can be guaranteed.

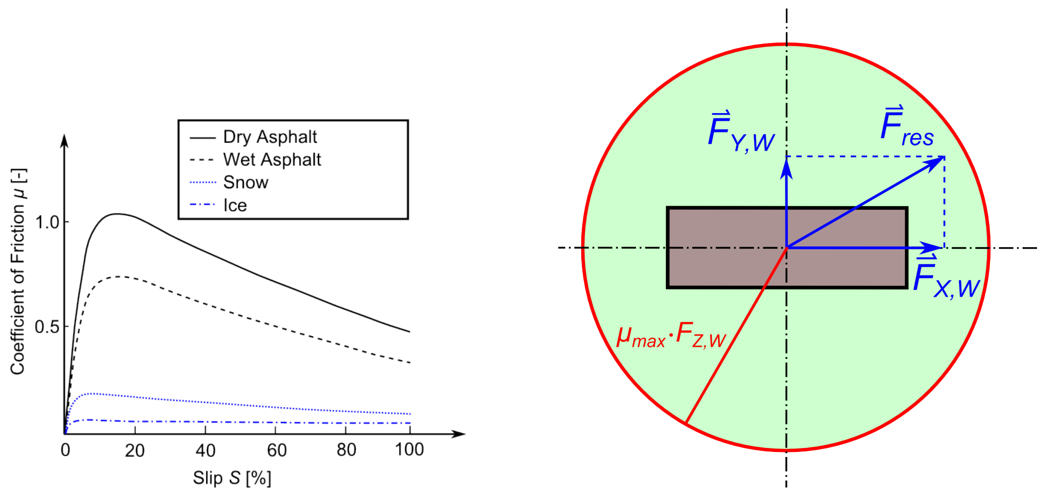

(a) Coefficient of friction vs. slip curve (adapted from [Sch06, p. 38])

(b) Kamm's circle (adapted from [Sch06, p. 38])

Figure 3.12: Coefficient of friction vs. slip curve and Kamm's circle

3.5.8 Vehicle's Behaviour when Braking in Curves

The "free corridor" triggers an emergency braking in order to bring the vehicle to a stop as soon as possible. It is possible that this emergency braking takes place while driving along curves. There are three different possible behaviours that a vehicle might exhibit: neutral, oversteer, understeer.

[5]the coefficient of friction is equal in all directions

These terms are normally used for the description of the self-steering behaviour during steady-state circular motion to determine a vehicle's understeer/oversteer tendency [Mit04, p. 570] [Hei08, p. 142]. The self-steering behaviour is defined through the relation between the steering wheel angle δ_H and the lateral acceleration a_y. In order to analyze the behaviour, a constant radius path is driven and the vehicle is accelerated incrementally. The resulting lateral acceleration is measured with each incremented step and the self-steering gradient EG can be determined using the slope of the steering angle curve, as shown in Figure 3.13. This parameter is used to determine tendency towards understeering or oversteering and is important for handling setup and tuning. Since a sudden sliding of the vehicle's rear due to strong oversteering tendency is difficult to control, modern vehicles are tuned to present a slight understeering tendency.

When $EG > 0$, the vehicle is understeered and by increasing lateral acceleration, the driver must increase the required steer angle in order to follow the path. On the other hand, if $EG < 0$, the vehicle is oversteered and the driver must decrease the required steer angle. This behaviour is of importance in order to better design the controllers.

While braking during curve-driving, the axle load distribution shifts to the front axle due to decelerations. Because of the higher vertical wheel forces, more friction potential is available and the lateral slip decreases (cmp. section 3.5.7). In other words, the slip angles at the front wheels α_f become smaller. The opposite occurs at the rear axle, where the slip angles α_r increase. This results in a change of the instantaneous center of curvature towards the front and closer to the vehicle (cmp. section 3.5.2), resulting in a smaller radius of curvature. This leads to a change of the vehicle's behaviour towards oversteering, which brings the need of a correction in steering [Hei08, pp. 138–139]. However, this effect does not occur when using the single track model, since the assumption of the center of gravity being located on road level cancels pitch- and roll motion.

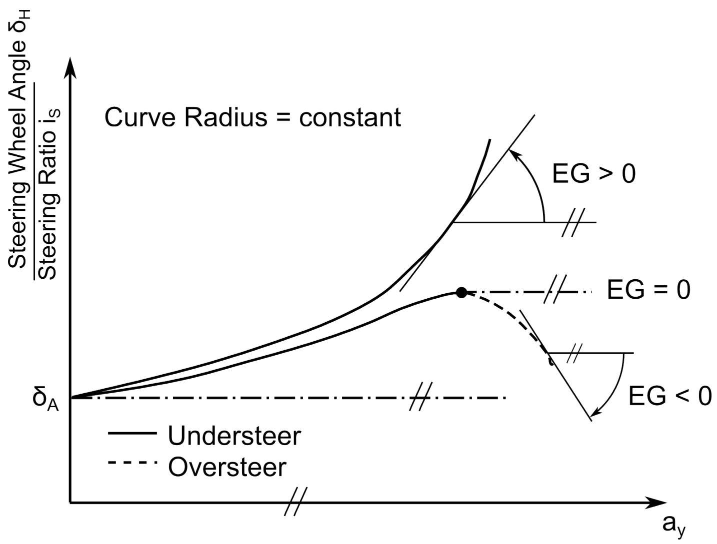

Figure 3.13: Steering characteristics and self-steering behaviour from steady-state skidpad motion (adapted from [Hei08])

3.6 Control Strategies for the "Free Corridor"

The "free corridor" uses current vehicle's states to determine the predicted trajectory. Furthermore, the environmental conditions, such as coefficient of friction, cannot be accurately determined. All these aspects lead to the question of whether the vehicle actually follows the predicted trajectory or not. In order to guarantee the vehicle following the predicted trajectory, different control strategies are analyzed to determine how good they perform in keeping the vehicle within acceptable lateral deviations after a connection loss. Following control strategies are proposed and studied:

- **Open Loop Control 1: Calculation of Control Variable using Predicted Clothoid**

  Since the vehicle's velocity changes due to the emergency braking, the traveled distance is calculated through the integration of the current longitudinal velocity $v_x(t)$:

  $$s(t) = \int_0^t v_x(\tau) d\tau \tag{3.36}$$

  which set in equation (3.25) produces the target curvature κ_{tar} at time t

  $$\kappa_{\text{tar}}(t) = c_0 + c_1 \cdot \int_0^t v_x(\tau) d\tau \tag{3.37}$$

  The relation between steering angle δ_f and curvature κ can be approximated for low velocities as:

  $$\delta_f = \frac{l}{\rho} = l \cdot \kappa \tag{3.38}$$

  and the relation between steering wheel angle δ_H and steering angle δ_f is

  $$\delta_H = i_S \cdot \delta_f \tag{3.39}$$

  where i_S represents the steering ratio. From equations (3.37) (3.38) and (3.39), the target steering wheel angle at time t is determined as:

  $$\delta_{\text{H,tar,OpenLoop1}} = i_S \cdot l \cdot \left(c_0 + c_1 \cdot \int_0^t v_x(\tau) d\tau\right) \tag{3.40}$$

Worth noticing is that the steering ratio is not constant in many vehicles, such as in the case of the experimental vehicle Audi Q7. Its steering ratio was determined by measurements and taken into consideration for the implementation.

- **Open Loop Control 2: Calculation of Control Variable using Predicted Change of Curvature**

  This open loop control uses the steering wheel angle at the time of connection loss $\delta_{H,0}$ as the initial condition. This is in order to guarantee a smooth transition between the steering wheel angles when the open-loop control is activated. The target steering wheel angle at time t becomes:

$$\delta_{\text{H,tar,OpenLoop2}} = \delta_{H,0} + i_S \cdot l \cdot c_1 \cdot \int_0^t v_x(\tau) d\tau \tag{3.41}$$

- **Open Loop Control 3: Constant Steering Wheel Rate**

  Here, the last registered steering wheel rate at the time of connection loss is kept constant. In theory, this concept is valid only when the vehicle's velocity remains constant and not in curves where acceleration or deceleration is present. It is however analyzed. The target steering wheel angle at time t becomes:

$$\delta_{\text{H,tar,OpenLoop3}} = \delta_{H,0} + \frac{d\delta_H}{dt_0} \cdot t \tag{3.42}$$

- **Open Loop Control 4: Constant Steering Wheel Angle** The steering wheel is held constant at the last registered steering wheel angle at the time of connection loss. The target steering wheel angle at time t becomes:

$$\delta_{\text{H,tar,OpenLoop4}} = \delta_{H,0} \tag{3.43}$$

- **Closed Loop Control 1: Feed-Forward with Closed-Loop Control of Curvature Error**

  The disadvantage of an open-loop control is the missing feedback of the actual states. The advantage of the open-loop control is the faster reaction towards the target value [Lun08, p. 9]. On the other hand, a closed-loop control has the advantage of compensation against interferences and robustness against uncertainties in the modeling. A possible approach is the combination of open-loop and closed-loop control into a feed-forward with closed-loop control.

  The feed-forward with closed-loop control is based on the one discussed by LUNZE [Lun08, pp. 9 ff.] and shown in Figure 3.14.

  The target curvature is calculated using the "free corridor" and the actual velocity. The anticipated needed steering wheel angle $\delta_{H,V}$ to reach the target curvature is calculated using the feed-forward. During the complete emergency braking maneuver, the

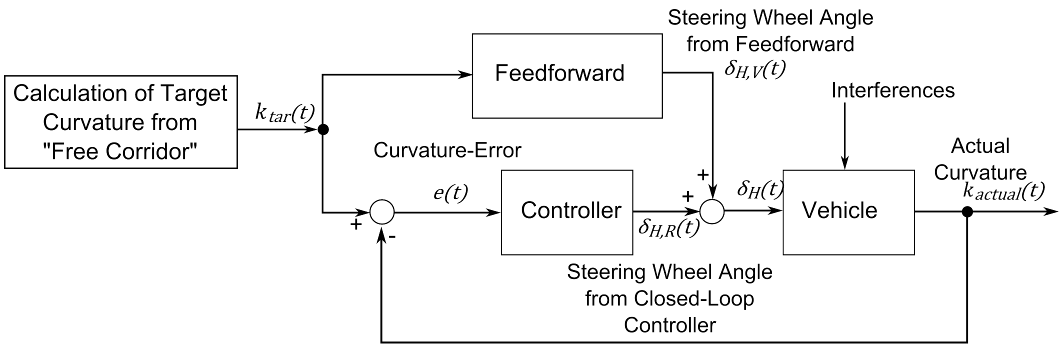

Figure 3.14: Scheme of feed-forward with closed-loop control

target κ_{tar} and actual curvature κ_{actual} values are calculated permanently. Their differences determine the curvature error $e(t)$. The closed-loop controller is then responsible of minimizing the curvature error through an additional steering wheel angle $\delta_{H,R}$. The correcting variable consists of the anticipatory and the compensatory proportions

$$\delta_H(t) = \delta_{H,V}(t) + \delta_{H,R}(t) \tag{3.44}$$

For the controller, a PI-controller is selected. The D-term of a typical PID-controller was omitted since it could cause instability when used on dynamic systems or a non-smooth behaviour in the control error. In order to minimize the control error continuously, an I-term is necessary [Lun08, pp. 373 ff.]. The transfer function results in

$$u(t) = k_P e(t) + k_I \int_0^t e(\tau) d\tau \tag{3.45}$$

Using adjustments proposed by Ziegler and Nichols [Zie42] (also cmp. [Lun08, pp. 442–443]) for this type of controllers, the optimal gains were determined.

- **Closed Loop Control 2: State Controller**

  For the control of multivariable systems, linear and time invariant systems are the most common. These systems can be depicted in the state space [Lun08, p. 74]:

$$\begin{aligned} \dot{\tilde{x}} &= A\tilde{x} + Bu + Ez \\ y &= C\tilde{x} + Du \end{aligned} \tag{3.46}$$

where

$\tilde{x}$	:	state vector
u	:	input (or control) vector
y	:	output vector
z	:	disturbance vector
A	:	state (or system) matrix
B	:	input matrix
C	:	output matrix
D	:	feedthrough (or feedforward) matrix
E	:	disturbance matrix

According to SÖHNITZ [Söh01, p. 44], the lateral control of a vehicle can be seen as a problem regarding path following. Here, the controlled variable is the lateral deviation of the vehicle's center of mass to a target trajectory. Based on the single track model, the lateral motion can be described using the lateral deviation ξ and the travel angle deviation X, which are shown in Figure 3.15 and can be calculated as:

$$\xi = [0\ 1\ 0]\ T_{\text{CoG,world}} \cdot \left(x_{\text{world,target}} - x_{\text{world,actual}}\right) \tag{3.47}$$

$$X = \vartheta_{\text{target}} - (\psi + \beta) \tag{3.48}$$

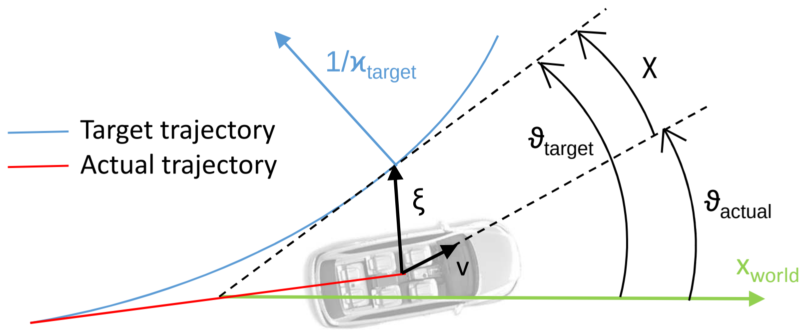

Figure 3.15: Lateral deviation for the state controller (adapted from [Söh01, p. 40])

In this dissertation, the yaw rate and the travel angle are selected together with the lateral deviation in the outputs. The manipulated variable is the steering angle δ_f, or accordingly the steering wheel angle δ_H after conversion using the steering ratio i_S.

The system can then be described as:

$$\begin{bmatrix} \ddot{\psi} \\ \dot{X} \\ \dot{\xi} \end{bmatrix} = \begin{bmatrix} -\frac{c_r {l_r}^2 + c_f {l_f}^2}{J_{zz} v} & 0 & 0 \\ \frac{-c_r l_r + c_f l_f}{m v^2} & 0 & 0 \\ 0 & v & 0 \end{bmatrix} \begin{bmatrix} \dot{\psi} \\ X \\ \xi \end{bmatrix} + \begin{bmatrix} \frac{c_f l_f}{J_{zz}} \\ -\frac{c_f}{m v} \\ 0 \end{bmatrix} \delta_f + \begin{bmatrix} 0 \\ v \\ 0 \end{bmatrix} \kappa_{\text{target}} \tag{3.49}$$

where

J_{zz}	:	moment of inertia with respect to the z-axis
c_f	:	cornering stiffness at the front wheels
c_r	:	cornering stiffness at the back wheels

Here, some assumptions are made [Söh01, pp. 40–44]:

- Driving resistance is neglected.
- X is assumed to be small.
- Actual and target velocities have the same absolute value.
- The steering angle δ_f is assumed to be small, so that the influence of the driving force on the lateral motion can be neglected.

The target yaw rate is obtained from equation (3.9) and in order to calculate the target curvature, the values for the initial curvature c_0 and its derivative c_1 are saved at the moment of the emergency brake. The target lateral and travel angle deviations ξ and X are set to zero. For the determination of the current lateral and travel angle deviations, equations (3.26)(3.27)(3.28) in combination with equations (3.47) and (3.48) are used.

The state controller is designed using the *Linear Quadratic Regulator (LQR)* to minimize the quadratic cost function

$$J = \int_0^\infty (\tilde{x}^T(t)Q\tilde{x}(t) + u^T(t)Ru(t))dt \tag{3.50}$$

where Q and R are the symmetric, positive semidefinite weighting matrices of the state variables and the manipulated variables, respectively. Using the feedback law

$$u(t) = K\tilde{x}(t) \tag{3.51}$$

with the optimal LQR state feedback gain K

$$K = R^{-1}B^TP \tag{3.52}$$

where P is the symmetric positive definite solution of the algebraic Riccati equation

$$A^TP + PA - PBR^{-1}B^TP + Q = 0 \tag{3.53}$$

Since the state space model is velocity dependent, the controller gains are also determined according to the current speed. The controller was designed in $5\,\text{km/h}$ steps from $5\,\text{km/h}$ to $60\,\text{km/h}$ and using interpolation for values in between. In order to be able to affect the complete dynamics of the system, it must be controllable. The system can be shown to be controllable.

The LQR state feedback gain K is then composed as:

$$K = \begin{bmatrix} K_{\dot{\psi}} & K_X & K_{\xi} \end{bmatrix} \tag{3.54}$$

Normally, the output vector y contains all measurable state variables. All other variables can be estimated, provided the system is observable. In the current configuration, the yaw rate is the only variable that can be measured, and therefore, the other variables need to be estimated. However, the system is not observable without the measurement of vehicle's position. Therefore, in order to implement this controller, the position of the vehicle needs to be determined.

To determine the current vehicle's position without a high-precision positioning system, the yaw rate $\dot{\psi}$ and the vehicle's velocity measured by the ESP can be used. The yaw angle ψ is then calculated from the time of connection loss through integration of the yaw rate with respect to time:

$$\psi = \int_{t_{\text{brake}}}^{t} \dot{\psi}(\tau) d\tau \tag{3.55}$$

The discrete-time vehicle's position measured from the point of connection loss is calculated for $n \in \mathbb{N}$ with initial conditions $x[n=0] = y[n=0] = 0$:

$$x_{\text{brake}}[n+1] = x_{\text{brake}}[n] + v_x[n] \cdot t_s \cdot cos(\psi[n]) \tag{3.56}$$

$$y_{\text{brake}}[n+1] = y_{\text{brake}}[n] + v_x[n] \cdot t_s \cdot sin(\psi[n]) \tag{3.57}$$

where x_{brake} and y_{brake} are the x and y vehicle's positions with respect to the braking point, and t_s is the sample rate. During the short period between each discrete-time value, it is assumed that the velocity and the yaw angle remain constant. The vehicle's position is then determined by the traveled distance with respect to the old position. Because of the difficulty to determine the sideslip angle and the sample rate is very short, the sideslip angle and the lateral velocity are neglected. This, however, influences the accuracy of the predicted traveled distance.

It can be expected from the control strategies that the closed-loop controllers would deliver the best results. Especially the state controller would deliver optimal results if the prediction of the current position can be achieved accurately. In simulation, the real position of the vehicle can be determined easily and used to corroborate the effects of the state controller when having perfect position. Nevertheless, the closed-loop controllers would require a

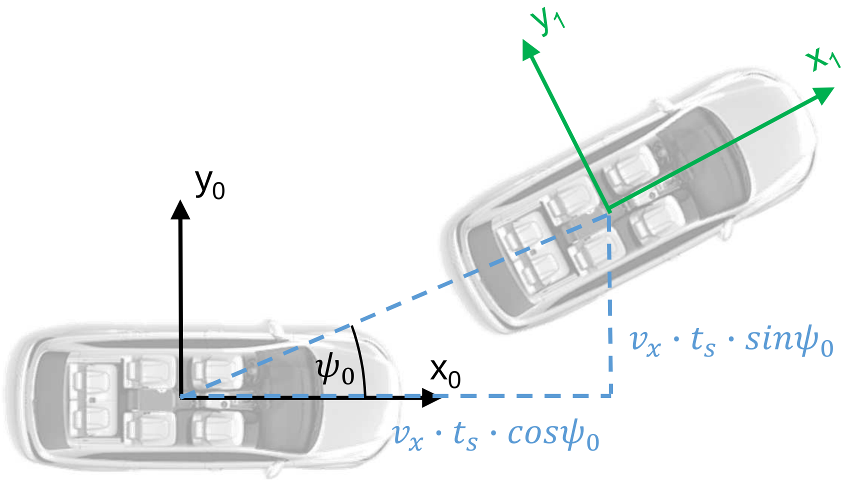

Figure 3.16: Calculation of vehicle's position using velocity and yaw angle

higher effort in the implementation. Open-loop controllers are on the other hand easy to implement. Since they don't possess any feedback on the vehicle's state and no correction is performed accordingly, it cannot be expected to deliver the best results.

3.7 Simulation Results

3.7.1 Simulation Environment

For the analysis of the emergency contingency strategy "free corridor", the modular simulation framework for simulation models in vehicle development processes DYNA4 version 2.3 from the company *TESIS DYNAware GmbH* was used. DYNA4 is based on MATLAB/Simulink® and the vehicle's components, environment parameters, etc. are defined in a Simulink model [Tes12]. DYNA4's user interface provides the possibility to create different maneuvers, vehicle's parameters and environments for the virtual test drives. These parameters and settings can be varied after each simulation iteration in order to test different settings automatically.

This model can be adapted and extended according to the respective purposes. For the development and analysis of the "free corridor", the Simulink model is extended with components for the calculation of the strategy's parameters, as described in section 3.5, and their depiction in DYNAanimation. Additionally, the model is extended to include the control of the steering wheel angle during the emergency braking.

3.7.1.1 Coordinate System

The simulation framework DYNA4 distinguishes between world-fixed coordinate systems (also called "global-system") and vehicle-fixed coordinate systems (also called "vehicle-system"), which are depicted in Figure 3.17. The global-system (depicted with subscript 0) is fixed with the road and the center of the vehicle's front axle is set at its origin at the beginning of each simulation. The vehicle-fixed coordinate system has its origin at the center of the front axle (depicted with subscript FA). The x-axis points to the moving direction of the vehicle, while the y-axis points to the left, being the yaw angle ψ the angle of rotation between both coordinate systems.

However, the calculations of the "free corridor" are based on another vehicle-fixed coordinate system with its origin on the vehicle's center of mass (depicted with subscript CoG). This coordinate system has the same orientation as the system in the front axle. Additionally, for the evaluation of the "free corridor", a new coordinate system is defined (depicted with subscript $CoGBrake$) as the CoG-coordinate system at the time of connection loss and the beginning of the emergency braking. At this point, the coordinate system changes from vehicle-fixed to world-fixed coordinate system and both the coordinates and the prediction of the corridor are frozen. This is used to compare the predicted and the real traveled trajectories later.

The direction of the axis in DYNA4 corresponds to the typical definition of the axis in a real vehicle, where the positive x-axis points to the front of the vehicle, the positive y-axis to the left, and correspondingly, the positive z-axis upwards of the vehicle.

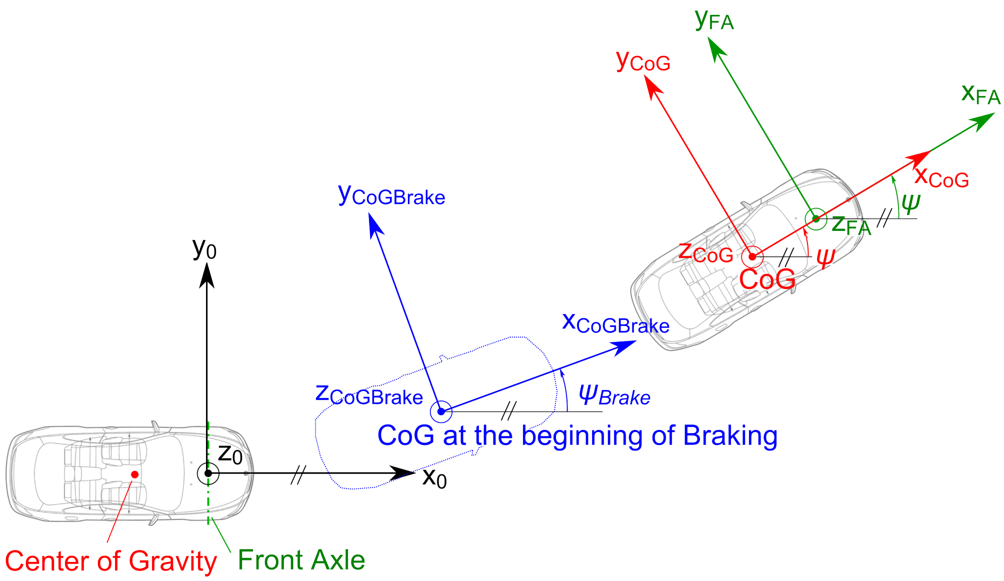

Figure 3.17: Coordinate systems in the simulation framework DYNA4

3.7.1.2 DYNAanimation

For the display of the simulation and the calculated trajectory, DYNAanimation is used. The calculated positions of the path elements are used to define the "free corridor". In order to display them correctly in the animation, the positions need to be moved and rotated accordingly. Additionally, elements in the simulation are scaled to build a closed trajectory. The DYNAanimation's user manual gives a detailed description on the necessary calculations [Tes11].

Figure 3.18 shows an example of the "free corridor" (the path elements are depicted in yellow and the braking point for the bumper in red).

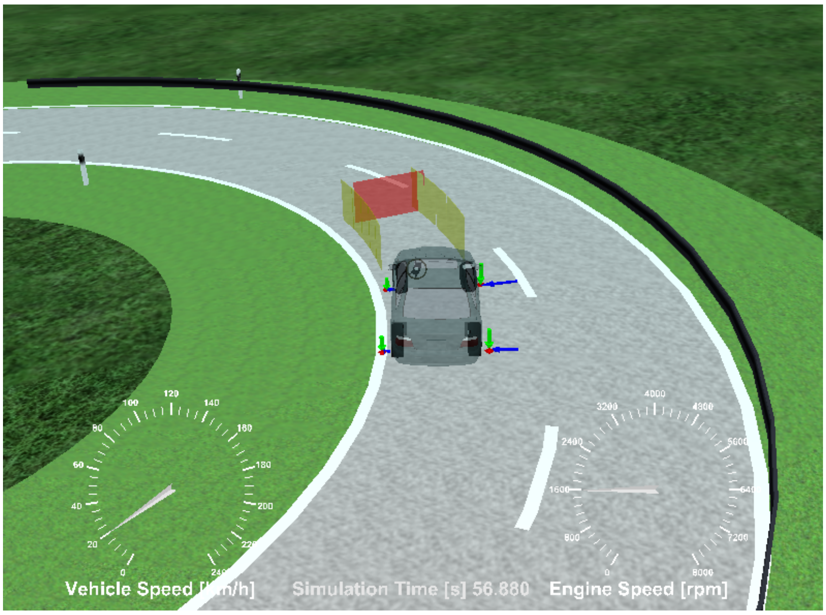

Figure 3.18: The emergency contingency strategy "free corridor" showed in DYNAanimation with the help of the simulation framework DYNA4

3.7.2 Scenarios for the Evaluation of the Safety Concept in the Simulation

In order to investigate the vehicle's behaviour during deceleration along a clothoid, a scenario consisting of a *ramp circular maneuver* for clothoidal motion was used. Figure 3.19 shows a scheme of the test scenario. The vehicle accelerates to a desired velocity v_x on a straight line and holds this velocity. Afterwards, the steering wheel angle δ_H is increased with a constant steering wheel rate $d\delta_H/dt$ until a desired lateral acceleration a_y is reached. At this moment, a connection loss is simulated and an emergency braking is activated to bring the vehicle to a stop and the different control strategies overtake the lateral control of the vehicle. Since the ABS system has a positive influence on the vehicle's stability while braking on curves, the system is active during the tests.

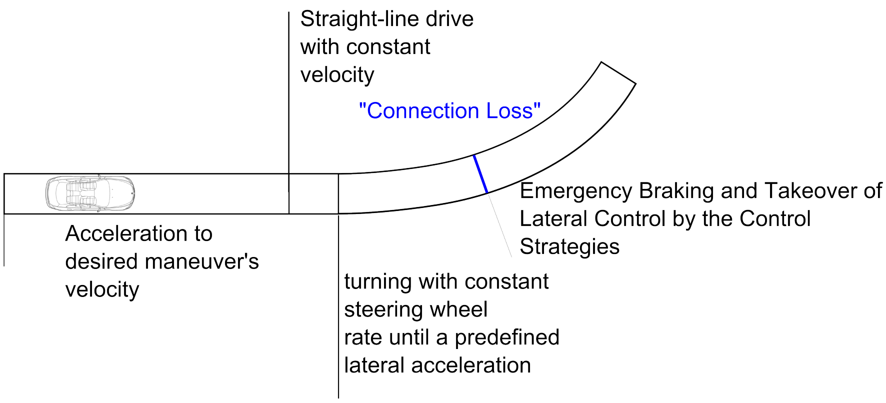

Figure 3.19: Scheme of the scenario used for testing the free corridor when decelerating after a "connection loss"

Table 3.3: Variation parameters and values used in the evaluation of the free corridor in simulation

Parameter	**Variations**		
Maneuver Velocity v_x	20 km/h	40 km/h	60 km/h
Lateral Acceleration a_y	2 m/s²	3 m/s²	4 m/s²
Steering Wheel Rate $d\delta_H/dt$	100 °/s	200 °/s	400 °/s
Maximal Available Coefficient of Friction μ_{max}	1.0	0.8	0.6

A series of tests was conducted with different variations of parameters to allow the discussion of the proposed concept properly.

These variation parameters are chosen according to the main application of teleoperated vehicles, which is driving in urban areas. The velocity limit in German cities is 50 km/h and therefore, it is covered in the tested variations. The accelerations of 95% drivers according to HACKENBERG AND HEISSING [Hac82] (Figure 3.6) show that a lateral acceleration of $a_y = 4\,\text{m/s}^2$ is not exceeded and conforms with the maximal lateral acceleration selected in the tests.

According to FISCHER [Fis09, pp. 8–9], drivers willing to take risks can achieve maximal steering wheel rates of $\approx 1100\,°/\text{s}$. However, steering wheel rates of maximal 200 °/s can be achieved in extreme situations such as evasion maneuvers and rates of maximal 400 °/s at lower velocities, especially during maneuvering [Mui09, p. 99]. Therefore, the maximal steering wheel rate of 400 °/s was chosen for the simulation tests.

Different coefficients of friction were evaluated, ranging from $\mu_{\text{max}} = 0.6$ to $\mu_{\text{max}} = 1.0$ which correspond to wet roads and dry roads, respectively. In between, a value for the coefficient of friction of $\mu_{\text{max}} = 0.8$ was tested, which would represent a humid surface (cmp. section 3.5.7 and Figure 3.12a).

Table 3.3 gives an overview of the parameters and values used for the tests in the simulation.

After each simulation, the driven trajectory of the vehicle is compared to the predicted trajectory. For comparison, the global coordinate system is used. In total, three values are calculated to help the assessment of the strategy. Figure 3.20 shows an example of the driven-trajectory (red) and the predicted trajectory (blue x-marks). First, the maximal lateral deviation during the braking maneuver (magenta) is calculated from the center of the bumper to the center point of the trajectory. Here, the value is defined as positive if it lies on the left of the predicted corridor and negative if it lies on the right (as is the case in the picture). Second, the longitudinal deviation of the bumper to the predicted braking point (green) is calculated. This is used to determine whether the predicted braking distance was overrun or not. The value is defined as negative if the vehicle stops before the braking point. Finally, the yaw angle after stopping is calculated in order to determine the vehicle's rotation.

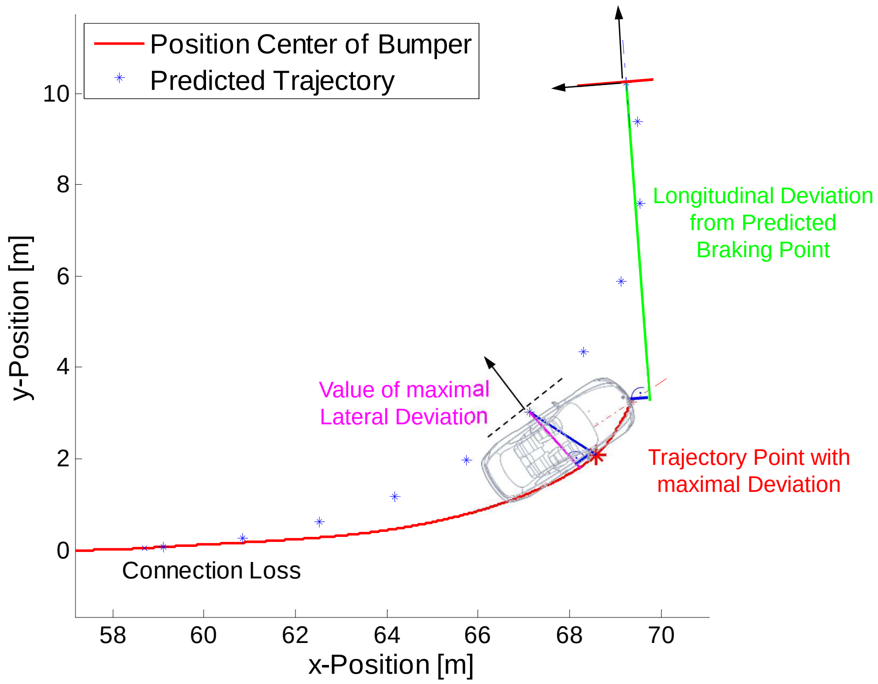

Figure 3.20: Calculation of longitudinal and lateral deviations between the driven- and the predicted-trajectory using an exemplary open-loop with constant steering wheel rate

3.7.3 Evaluation of the Control Strategies in the Simulation

Lateral Deviation:
For the emergency contingency strategy "free corridor", it is important that during the emergency braking maneuver, the vehicle stays along the predicted trajectory. As a quality criterion, the maximal lateral deviation during the complete braking maneuver is used. The smaller the maximal lateral deviation, the better the results. Three ranges were defined for the evaluation of the results:

- **Good**: the absolute values of the maximal lateral accelerations do not exceed $0.4\ m$. This area is depicted as *green* in the results.
- **Acceptable**: the absolute values of the maximal lateral acceleration occur up to $0.7\ m$. This area is depicted in *yellow*.
- **Dangerous**: the absolute values of the maximal lateral acceleration exceed $0.7\ m$. This area is depicted in *red* and represents unacceptable lateral accelerations, since a safe state cannot be guaranteed.

The ranges were selected accordingly, since roads are usually built with a width of $3\ m$. The experimental vehicle has an approximate width of $2\ m$ and assuming it to be moving in the center of the road, there is a $0.5\ m$ free space for maneuvering. The acceptable range would exceed the $0.5\ m$ free space, but it is also assumed that other traffic participants normally move in the center of their lane. Absolute values exceeding $1.5\ m$ are not discussed, since they would be completely out of scope.

Figure 3.21 shows an example of the maximal lateral deviations for different maneuvers for a dry road with $\mu = 1.0$. Comparing the different control strategies with small $d\delta_H/dt = 100°/s$, and up to a velocity of $40\ ^{km}/_{h}$, all open-loop control strategies are in the acceptable range. Merely at maneuvers with a velocity of $60\ ^{km}/_{h}$, the vehicle abandons the predicted trajectory too much. The open-loop control strategy 1 was identified as providing better results compared to the others.

With higher steering wheel rates, the maximal lateral deviations differ more. The open-loop control 3 turns too much towards the inside of the curve, and open-loop control 2, though better than control 3, also overturns. Open-loop control strategy 1 follows the predicted trajectory best and remains acceptable even at higher velocities and lateral accelerations.

Taking a look at the proposed feed-forward with closed-loop control strategy, it can be noted that the lateral deviation remains in the good areas (green) in almost all of the tested maneuvers. Especially during maneuvers at high velocities, the effect of the closed-loop control compared to an open-loop control can be noticed clearly. The only maneuver in which the maximal lateral deviation became unacceptable was at maneuvers not common during normal driving situations ($d\delta/dt = 400°/s$, 4 $^{m}/_{s^2}$ and $v = 60$ $^{km}/_{h}$).

A similar performance can be seen with the state controller for velocities up to $v = 40$ $^{km}/_{h}$ (Figure 3.21). However, when driving at higher velocities $v = 60$ $^{km}/_{h}$, especially with higher lateral accelerations, it shows slightly worse results as the feed-forward with closed-loop control.

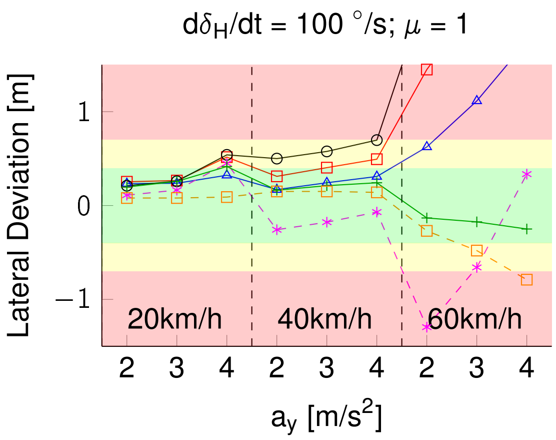

(a) $d\delta_H/dt = 100°/s$ and $\mu = 1.0$

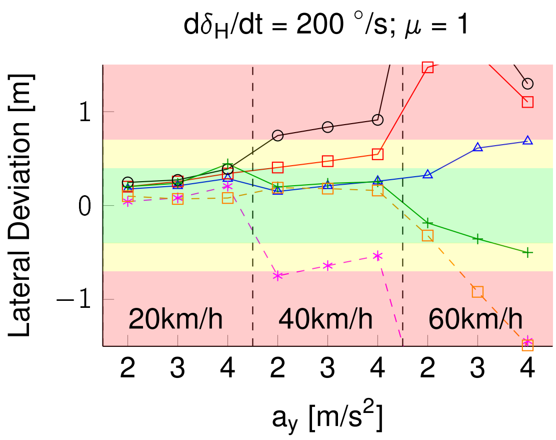

(b) $d\delta_H/dt = 200°/s$ and $\mu = 1.0$

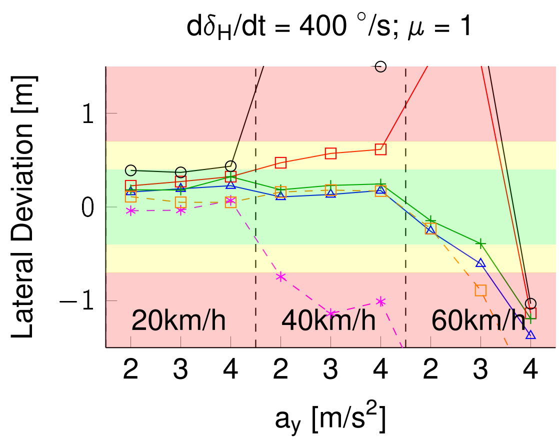

(c) $d\delta_H/dt = 400°/s$ and $\mu = 1.0$

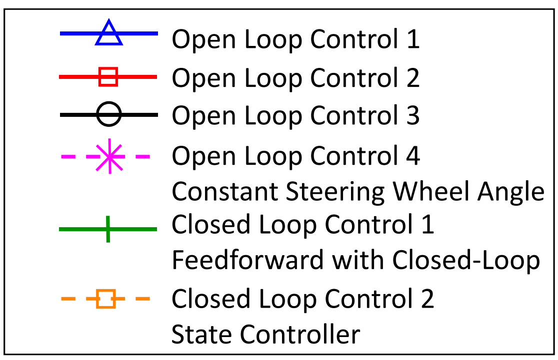

(d) Legend

Figure 3.21: Maximal lateral deviation for different control strategies during braking maneuver on a curve with $\mu = 1.0$

When testing the open-loop control strategies on a humid surface, similar behaviour was established. In general, control strategy 1 performs better for more scenarios. At higher velocities and $a_y \geq 3\,\mathrm{m/s^2}$, the vehicle abandons the lane due to low friction potential between tire and the surface. The closed-loop control strategies, compared to the different open-loop controls, also showed an improvement in the lateral deviation when testing on humid surfaces.

The limits of the "free corridor" using an open-loop control can be seen when testing on wet roads $\mu = 0.6$. Even at low steering wheel rates, the lateral deviation is acceptable only for up to $v = 40\,\mathrm{km/h}$ and $a_y = 3\,\mathrm{m/s^2}$. There is a tendency towards under-steering (Figure 3.22).

These limits can also be seen for the closed-loop control strategies. For the feed-forward with closed-loop controller, for low steering wheel rates, a lateral acceleration of $a_y = 3\,\mathrm{m/s^2}$ should not be exceeded and for middle to higher steering wheel rates, $a_y \leq 2\,\mathrm{m/s^2}$. For the state controller during low steering wheel rates maneuvers, a lateral acceleration limit of $a_y = 3\,\mathrm{m/s^2}$ should be kept.

The friction potential between tires and road in such situations is so low, that it is not possible to remain on the path. Since this effect can be seen in all analyzed maneuvers, it can be concluded that an active steering on road surfaces with a low coefficient of friction can only achieve a limited reduction of the lateral deviation.

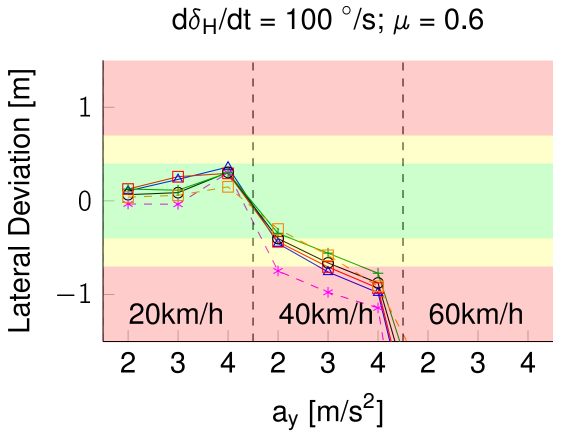

(a) $d\delta_H/dt = 100°/s$ and $\mu = 0.6$

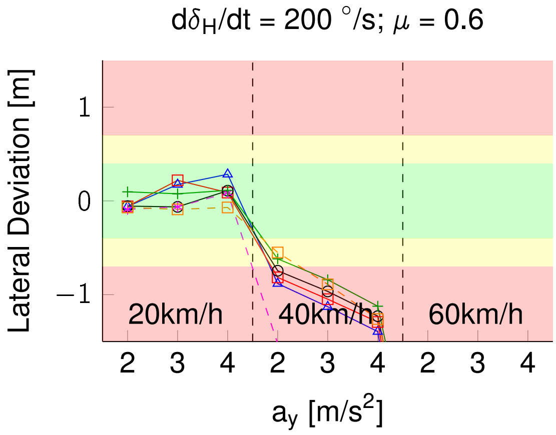

(b) $d\delta_H/dt = 200°/s$ and $\mu = 0.6$

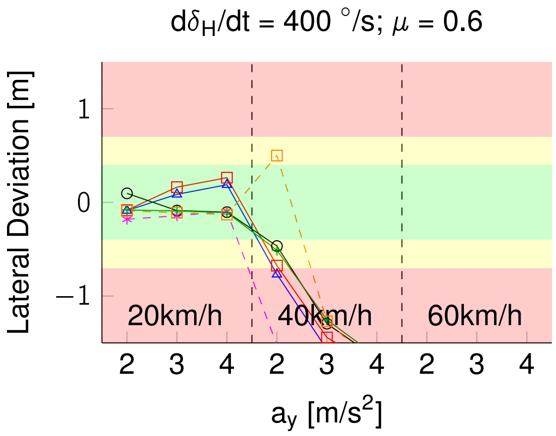

(c) $d\delta_H/dt = 400°/s$ and $\mu = 0.6$

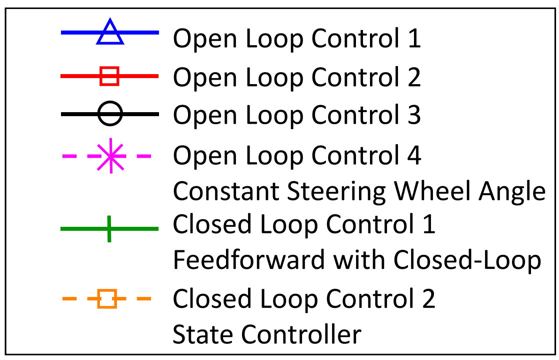

(d) Legend

Figure 3.22: Maximal lateral deviation for different control strategies during braking maneuver on a curve with $\mu = 0.6$

Longitudinal Deviation:
Results are shown in Figure 3.23. For a dry road with $d\delta_H/dt = 100°/s$, no obvious difference can be recognized between the different control strategies and the braking point is overrun from velocities of $v = 40\,\mathrm{km/h}$ on. For higher steering wheel rates, the longitudinal deviation is in most cases in the accepted ranges and the vehicle slightly overruns only in very slow velocity ranges. For higher velocities and accelerations, the vehicle stops with a large distance to spare.

In the case of a humid road ($\mu = 0.8$), the prediction of the braking distance can be judged to be accurate enough, since only at curves with small changing rate ($d\delta_H/dt = 100°/s$) is a light overrun to be seen in control strategies 1 and 2 (Figure 3.23c). Similar tendencies are to be seen when braking on a wet surface (Figure 3.23d), where at velocities of $v = 60\,\mathrm{km/h}$, the actual stopping point lies far before the predicted one.

In general it is to be perceived that the longitudinal deviation mostly depends on the prediction of the braking distance and not directly on the control strategies. However, when braking from higher velocities and lateral accelerations and having a lower coefficient of friction, the needed braking distance is over-estimated. Apparently, this could be caused due to already exceeding the limits (the term under the square root in equation(3.16) is negative) and therefore, equation (3.19) is used instead.

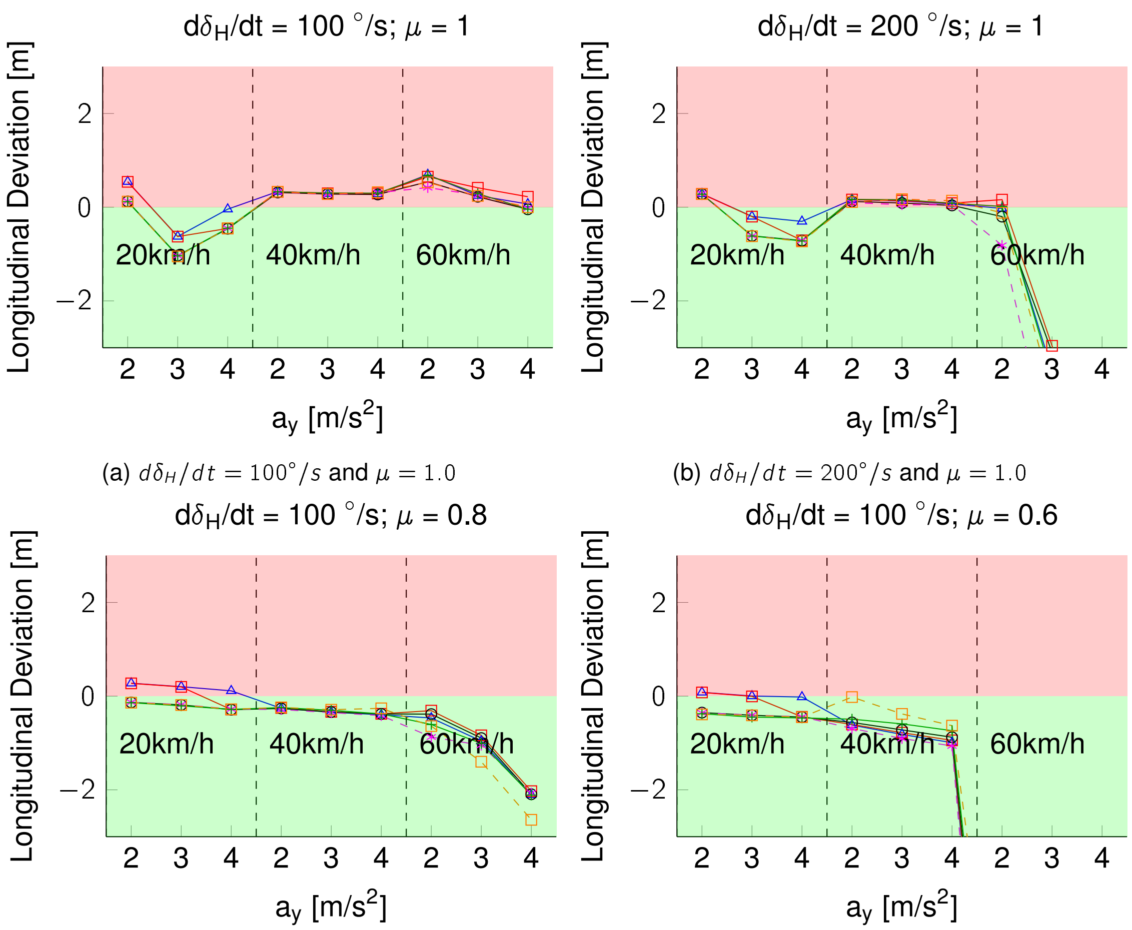

(a) $d\delta_H/dt = 100°/s$ and $\mu = 1.0$

(b) $d\delta_H/dt = 200°/s$ and $\mu = 1.0$

(c) $d\delta_H/dt = 100°/s$ and $\mu = 0.8$

(d) $d\delta_H/dt = 100°/s$ and $\mu = 0.6$

Figure 3.23: Maximal longitudinal deviation for different control strategies during braking maneuver on a curve

Figure 3.24 summarizes the maximal lateral deviations for different maneuvers for $\mu = 1.0$. Here, it can be seen that the feed-forward with closed-loop control delivers good results, whereas for dynamically higher maneuvers, the open-loop control and the fixed steering wheel are not able to perform in an acceptable range. A similar tendency can be also seen for the state controller, where the maximal lateral deviation becomes unacceptable for high accelerations at high velocities.

It is important to keep in mind that the state controller uses a prediction of the current position. This showed errors when driving at higher speeds, causing the results of the controller to become worse. When tested in the simulation using vehicle's positions provided by the simulation, results improved. Nonetheless, it was the goal to develop and test controllers that are not dependent on highly accurate position systems, since they are not available in series vehicles.

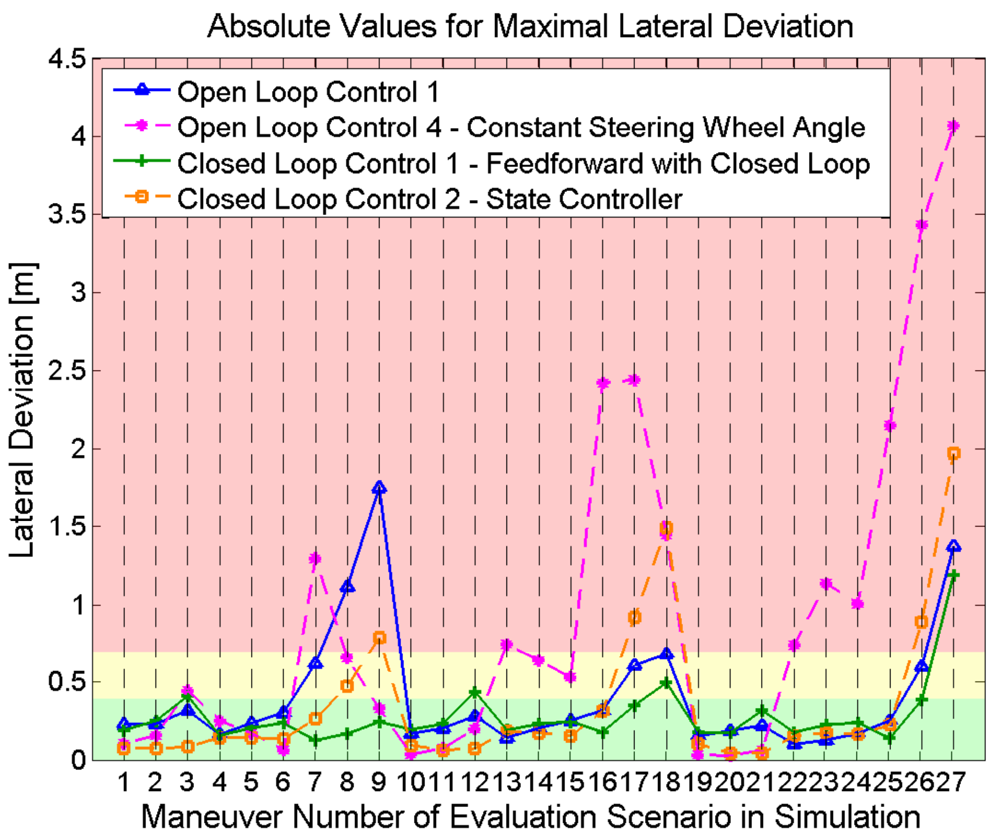

Figure 3.24: Summary of absolute values of maximal lateral deviations in simulation for $\mu = 1.0$

Results showed that when driving on a dry surface, velocities of up to $60\,\mathrm{km/h}$ but not exceeding a lateral acceleration of $3\,\mathrm{m/s^2}$ can be achieved. On humid surfaces, high lateral accelerations should be avoided ($a_y \leq 2\,\mathrm{m/s^2}$) and on wet roads, a limit in velocity and lateral acceleration of $40\,\mathrm{km/h}$ and $a_y \leq 2\,\mathrm{m/s^2}$ should be kept.

This is realistic since measurements performed during teleoperation drives showed lateral acceleration not exceeding $2\,\mathrm{m/s^2}$. If the lateral acceleration is kept withing this limit, the operator would only need to adjust the maximal velocity accordingly to guarantee that a safe state can be reached.

3.8 Results in the Experimental Vehicle

3.8.1 Experimental Vehicle's Environment

The overall development and environment tools were presented in Figure 2.9. The implementation took place using the programming language C++.

The presented "free corridor" is displayed to the operator directly at the interface. This can be compared to a contact analogue Head-Up-Display (HUD) device on a vehicle or an augmented reality system. The HUD was found to be better compared to other display methods, such as circular- or vertical-instruments [Bub75, pp. 186–202]. In order to be able to display it at the correct location on the interface, the cameras need to be calibrated. A camera depicts the three-dimensional world into a two-dimensional projection area. In order to achieve this, a set of two parameters are used: *Intrinsic camera parameters*, which depend only on the camera characteristics, such as the focal length, the pixel size in x and y direction, and the principal points in x and y. *Extrinsic camera parameters*, which depend only on the position of the camera, are determined through relations of the camera position to a known frame. A detailed description of the calculation of the parameters can be found in [Sti09, pp. 200–201].

For the determination of the intrinsic and extrinsic camera parameters, an automated calibration procedure is used. BOUGUET [Bou13] provides a toolbox for MATLAB to achieve this. It makes use of a set of pictures taken in different perspectives of a chessboard with known characteristics, which are typically used as calibration targets [Han11, p. 110]. Making use of the set of pictures, the corners of the chessboard-pattern are extracted and using an optimization, the intrinsic parameters are calculated. Another picture of a known chessboard-pattern in a known position relative to the vehicle's coordinate system is used to determine the extrinsic parameters. Taking into account the intrinsic parameters, the toolbox calculates the position of the pattern relative to the camera. Combined with the knowledge of the position of the pattern, the projection matrix of vehicle's coordinate systems can be calculated into pixel coordinates.

The information about the vehicle's state is constantly sent to the working station to calculate the position of the predicted trajectory in vehicle's coordinate system. With the help of OpenGL and the camera parameters obtained from the calibration, the "free corridor" is displayed in the interface for the operator (Figure 3.25).

Parallelly, the exact same information is used in the experimental vehicle at the Autobox to determine the target path for the control strategies. In case of a connection loss, the Autobox uses the predicted trajectory as a target path to produce an active intervention at the steering wheel angle in order to guarantee the vehicle following this path.

3.8.1.1 Coordinate System

For the implementation of the "free corridor" in the experimental vehicle and its validation using accurate navigation information, other coordinate-systems from the simulation need to be used. For the determination of the vehicle's position in the geographical coordinate system, a fusion of Differential Global Positioning System *DGPS* and the signals of the inertial and GPS measurement system's compass is used. This position is given using

Figure 3.25: Interface at the working station showing the free corridor

WGS84: World Geodetic System. The direction of the vehicle is given using the heading-angle Θ, measured clockwise from the north (Figure 3.26a).

Furthermore, the inertial and GPS measurement system is capable of giving the information using the North-East-Down coordinate system [Oxf11], where the x-axis always points to the north, the y-axis to the east and the z-axis points down perpendicular to the WGS84 reference ellipsoid. The direction of the vehicle is determined by the heading-angle Θ. The origin on the system is defined in the settings of the inertial and GPS measurement system (Figure 3.26b).

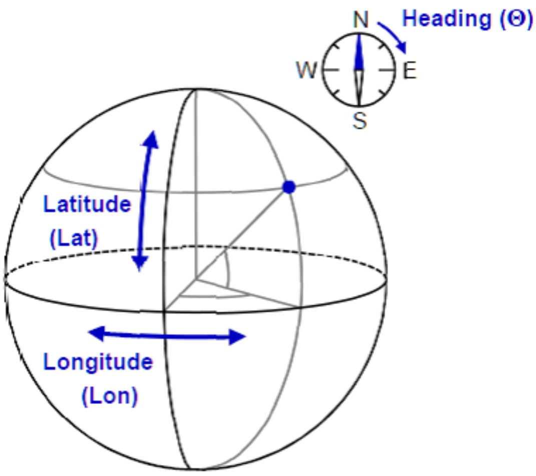

(a) Geographical coordinate system

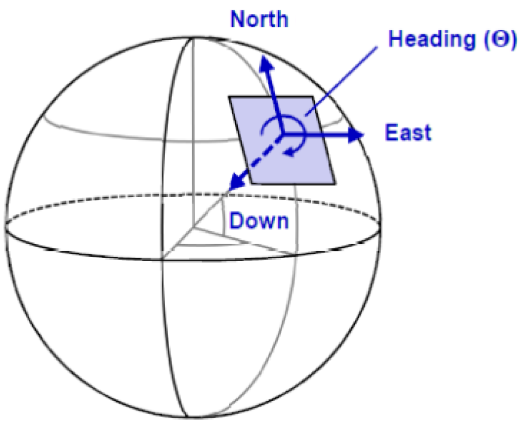

(b) North-East-Down coordinate system

Figure 3.26: Representation of a geographical coordinate system (left) and a North-East-Down coordinate system (right)

For the comparison of the predicted and actual trajectories, the coordinate systems are rotated to correspond to the conventional vehicle's coordinate systems, also used in section 3.7.1.1. The x-axis points to the north, the y-axis to the west and the z-axis upwards (North-West-Up coordinate system) and therefore, the direction of the vehicle is measured counterclockwise from the north.

3.8.1.2 Adjustment of Prediction of the Braking Distance

Measurements conducted on the experimental vehicle during test showed lower values for the possible decelerations using the available actuators in the Audi Q7 compared to a human driver. A maximal deceleration of approximately $= 6\,{}^{m}/{}_{s^2}$ was achieved, as can be seen in Figure 3.27 during one tested maneuver. The average deceleration is even lower, since the actuator needs to build up the braking force over time. The time to deploy the maximum braking effect is not considered here.

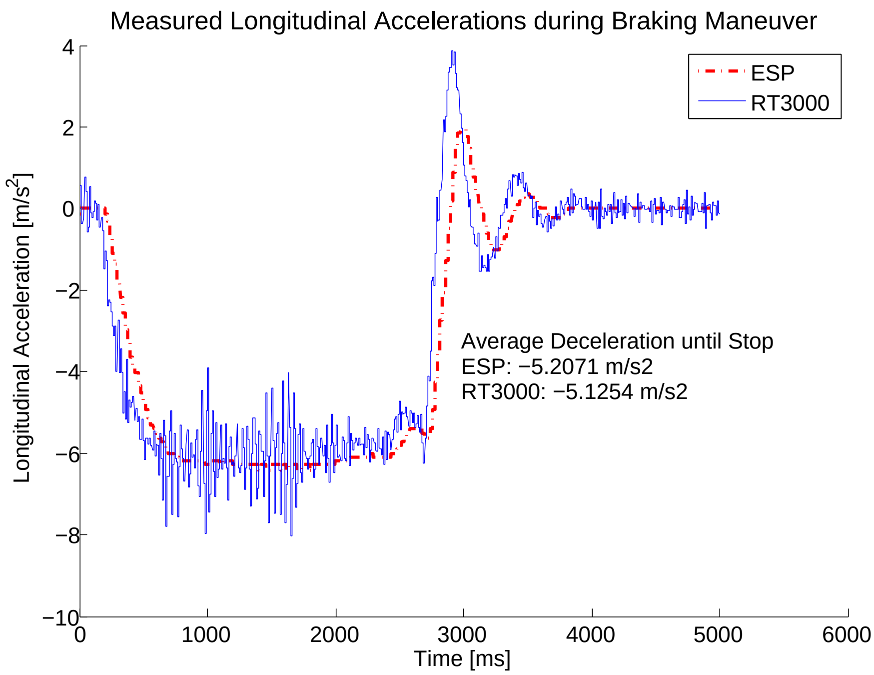

Figure 3.27: Measured longitudinal accelerations during braking maneuver with ESP sensor cluster and RT3000 inertial measurement system

In order to consider the characteristics of the available actuator in the experimental vehicle in the prediction of the braking distance, a correction factor K_{actuator} is introduced. Therefore, the possible deceleration becomes

$$a_{\text{max,actuator}} = K_{\text{actuator}} \cdot a_{\text{max}} = -K_{\text{actuator}} \cdot g \sqrt{\mu_{\text{max}}^2 - \left(\frac{\kappa(s) \cdot v^2}{g}\right)^2} \tag{3.58}$$

and the braking distance in a circular arc becomes

$$s_b = \frac{1}{K_{\text{actuator}}} \cdot \frac{1}{\kappa} \int_0^{v_0} \frac{v\,dv}{\sqrt{\left(\frac{g\mu_{\text{max}}}{\kappa}\right)^2 - v^4}} = \frac{1}{K_{\text{actuator}}} \cdot \frac{1}{2\kappa} \arcsin({v_0}^2 \cdot \frac{\kappa}{g \cdot \mu_{\text{max}}}) \tag{3.59}$$

The braking distance at limit ranges (at the maximal allowed curve speed) becomes

$$s_b = \frac{1}{K_{\text{actuator}}} \cdot \frac{v^2}{g \cdot \mu_{\text{max}}} \cdot \frac{\pi}{4} \tag{3.60}$$

The correction factor can be determined using the absolute value of the average deceleration divided with the maximal possible deceleration at good conditions ($\mu_{\text{max}} = 1.0$). Since a longer prediction of the braking distance is uncritical, the smallest measured value can be used.

$$K_{\text{actuator}} = \frac{a_{\text{max,actuator}}}{a_{\text{max}}} \tag{3.61}$$

3.8.2 Scenarios for the Evaluation of the Safety Concept in the Experimental Vehicle

From the simulation, it was determined that the open-loop control strategy 1, where the predicted clothoid was used to calculate the control variable, delivered the best results among open-loop strategies 1, 2 and 3. Therefore, the experiments in real conditions using the experimental vehicle were conducted only using strategy 1 and strategy 4, the last used only for comparison purposes.

The "free corridor" was evaluated at the testing ground of the Universität der Bundeswehr München in Neubiberg and at the old airport landing runway in Leipheim.

Three different maneuvers were tested: straight line driving, a steady state circular test and a ramp circular maneuver. The emergency braking maneuver was triggered by a simulated loss of connection. This loss of connection was triggered for straight line driving and steady state circular test after the maneuver's velocity was reached, and for ramp circular maneuver, three seconds after the begin of the steering.

According to the road surface conditions, the coefficient of friction was selected based on values discussed in as section 3.5.7. A coefficient of friction was selected as $\mu_{\text{max}} = 0.8$ for a humid surface due to previous precipitations and $\mu_{\text{max}} = 1.0$ for a dry surface.

All the tested combinations are shown in table 3.4. Each of the combinations was tested with each control strategy to measure the deviations of the predicted and the actual driven trajectories to assess the "free corridor".

3.8.3 Evaluation of the Control Strategies in the Experimental Vehicle

During emergency braking on a straight line maneuver, the vehicle is capable of following the predicted trajectory using all different control strategies mostly accurately. The maximal lateral deviation is approximately 1.5 meters with the state controller (Figure 3.29), where the lateral deviation overshoots because of the inaccuracy in the prediction of the vehicle's position.

Table 3.4: Evaluation scenarios for the "free corridor" in the experimental vehicle

	Maneuver	**Steering Wheel Angle / Steering Wheel Rate**	**Velocity**
1	Straight Line	-	$20\,\mathrm{km/h}$
2	Straight Line	-	$30\,\mathrm{km/h}$
3	Straight Line	-	$40\,\mathrm{km/h}$
4	Straight Line	-	$50\,\mathrm{km/h}$
5	Steady State Circular Test - Left	$\delta_H = 90°$	$20\,\mathrm{km/h}$
6	Steady State Circular Test - Left	$\delta_H = 180°$	$20\,\mathrm{km/h}$
7	Steady State Circular Test - Left	$\delta_H = 180°$	$30\,\mathrm{km/h}$
8	Steady State Circular Test - Right	$\delta_H = -180°$	$20\,\mathrm{km/h}$
9	Steady State Circular Test - Right	$\delta_H = -180°$	$30\,\mathrm{km/h}$
10	Ramp Circular Test - Left	$d\delta_H/dt = 50\,°/\mathrm{s}$	$20\,\mathrm{km/h}$
11	Ramp Circular Test - Left	$d\delta_H/dt = 100\,°/\mathrm{s}$	$20\,\mathrm{km/h}$
12	Ramp Circular Test - Left	$d\delta_H/dt = 50\,°/\mathrm{s}$	$30\,\mathrm{km/h}$
13	Ramp Circular Test - Right	$d\delta_H/dt = -50\,°/\mathrm{s}$	$20\,\mathrm{km/h}$
14	Ramp Circular Test - Right	$d\delta_H/dt = -100\,°/\mathrm{s}$	$20\,\mathrm{km/h}$
15	Ramp Circular Test - Right	$d\delta_H/dt = -50\,°/\mathrm{s}$	$30\,\mathrm{km/h}$

Because of the mentioned problem in section 3.8.1.2 with respect to maximal possible deceleration with the current actuators, the calculation of the lateral deviation for steady state circular tests and ramp circular tests does not represent a realistic value, since the reference points of the predicted trajectories are too far away (Figure 3.28a). Therefore, to determine the lateral deviation, the points of the "free corridor" were not directly used, but the extension of the clothoid were taken into account (Figure 3.28b). This is valid since the maximal possible deceleration only influences the length of the braking distance and not the trajectory itself.

The performance of the different control strategies can be evaluated. For the steady state circular tests with a velocity of $v = 30\,\mathrm{km/h}$, the lateral deviation of all the control strategies lies in acceptable ranges (up to +/- 0.4 meters). The best results are achieved with the open-loop control strategy with a maximal lateral deviation of 0.25 m. The state controller shows

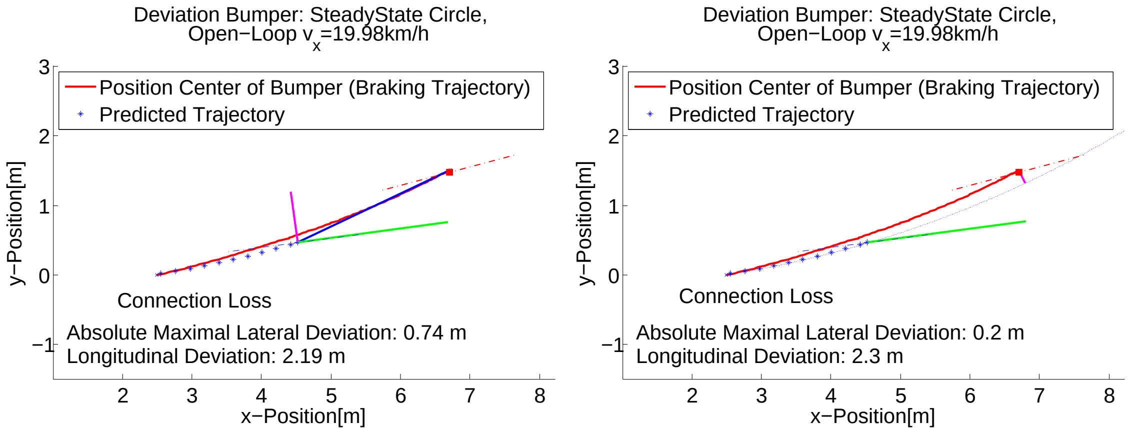

(a) Calculation of lateral deviation with predicted "free corridor"

(b) Calculation of lateral deviation with extended "free corridor"

Figure 3.28: Calculation of lateral deviation for tests on experimental vehicle

at a velocity of $v = 30\,{}^{\text{km}}/_{\text{h}}$ rather higher lateral deviations, however they are still within the acceptable range.

For ramp circular tests with a velocity of $v = 30\,{}^{\text{km}}/_{\text{h}}$ and steering wheel rate $d\delta_H/dt = 50\,{}^{\circ}/_{\text{s}}$, a safe stop can be achieved, even though lateral accelerations of $a_y = 5\,{}^{\text{m}}/_{\text{s}^2}$ were present. The feed-forward with closed-loop control showed overall very good results compared to the open loop controls. However, for maneuvers with high steering rate (numbers 11 and 15 in table 3.4 and Figure 3.29), the lateral deviation becomes unacceptable. In this case, the state controller was able to perform better and keep the lateral deviation in acceptable ranges. Such highly dynamic maneuvers do not arise during teleoperation, where lateral accelerations of approximately $7\,{}^{\text{m}}/_{\text{s}^2}$ were reached.

Figure 3.29 summarizes the maximal lateral deviations measured for the test maneuvers.

3.9 Discussion

The emergency concept "free corridor" was introduced and analyzed both in the simulation and in real conditions with the experimental vehicle. Two different methods for the calculation of the trajectory for the "free corridor" were presented. It was determined that the method using clothoids is more adequate for the application, since roads also consist of clothoid segments, which provide a smoother transition between other segments. Therefore, using clothoids for the trajectory calculation, it became easier to keep it on the roads continuously.

Furthermore, different control strategies were presented to guarantee the vehicle following the predicted trajectory. These strategies consisted of open-loop and also of closed-loop controllers and were tested in different scenarios, again both in simulation and in real conditions. From all the proposed open-loop control strategies, open-loop control 1, where the control variable was calculated using the predicted clothoid, showed the best results with the smallest lateral deviations. This is understandable, since the steering wheel angle was calculated directly using the predicted clothoid, which would correspond to the predicted trajectory. While it would have been expected that control strategy 3 (constant steering wheel rate) delivers good results, since this maneuver corresponds to a clothoid, this condition is

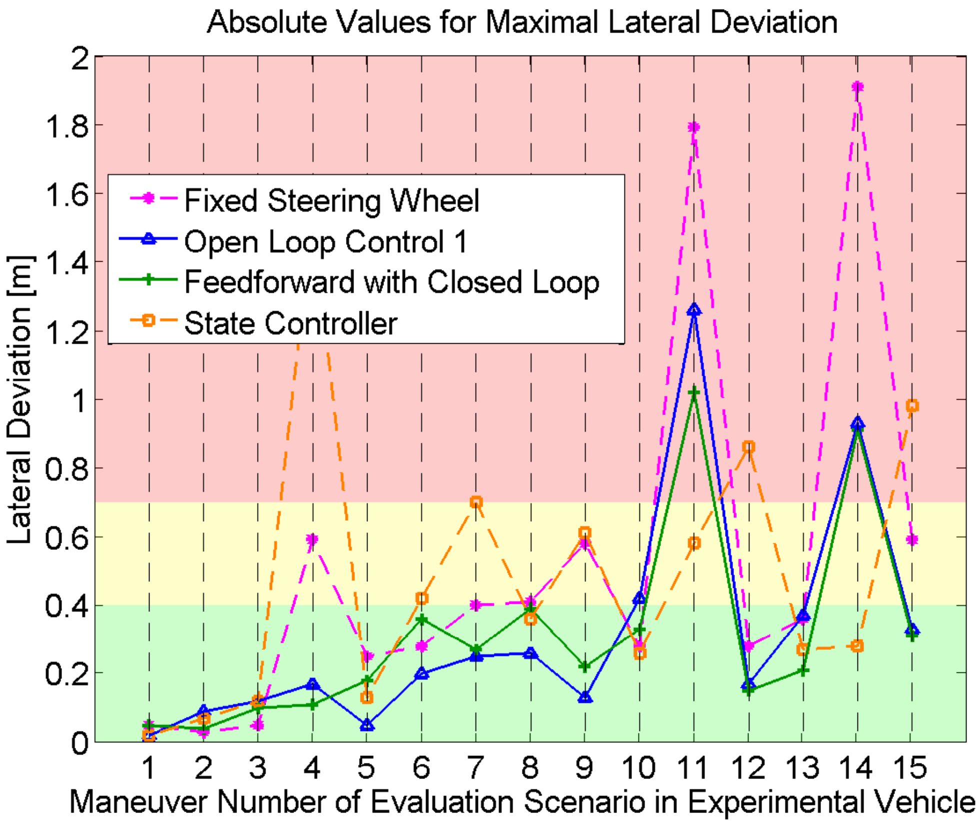

Figure 3.29: Summary of absolute values of maximal lateral deviations in experimental vehicle

only valid for constant velocities. In a braking maneuver, the velocity is reduced and therefore, the vehicle shows a tendency towards turning to the inside of the curve.

The open-loop control strategies show the advantage of being easy to implement and to test. The different proposed open-loop controls showed the applicability of those concepts, but also their limits. The open-loop control strategies showed acceptable results both in simulation and in the experimental vehicle for the dynamic ranges of interest, where a lateral acceleration of $2\,\mathrm{m/s^2}$ is not exceeded.

On one hand, when testing the feed-forward with closed-loop control, it showed very good results in the simulation. However, in the experimental vehicle, results were not so obvious. The parameters of the PI-controller used in the feed-forward with closed-loop controller can be further optimized for the experimental vehicle, allowing a more accurate controlling of the vehicle. A more detailed modeling of the vehicle would provide the possibility to better optimize the parameters.

On the other hand, the state controller neither showed clear advantages or disadvantages compared to the feed-forward with closed-loop control. For some maneuvers, the state controller achieved better results, but also for other maneuvers, worse results were achieved. For velocities of up to $v = 40\,\mathrm{km/h}$, the state controller performed in average better than the feed-forward with closed-loop controller. However, it can be expected that by having an accurate positioning system in the experimental vehicle instead of the predicted position, a better result can be achieved. The high lateral deviations seen in the results of the state controller could have possibly arisen due to errors in the calculation of the current position.

Results from the simulation showed the limits of the "free corridor" when driving in humid or wet surfaces, where the coefficient of friction is relatively low. Even though ABS system was activated during the maneuvers, unacceptable lateral deviations were determined (Figure 3.22) at higher velocities $v = 60\,{}^{km}/_{h}$, even at low lateral accelerations $a_y = 2\,{}^{m}/_{s^2}$. Additional analysis of the effect of the ABS system in the simulation framework should be conducted to determine its effect and validate the obtained results.

With respect to longitudinal deviation, no clear difference could be established between the different control strategies. Here it is to keep in mind that the calculation of the braking distance does not take into account the influence of ABS systems. This would create errors in the prediction of the needed braking distance. However, ABS provides advantages in vehicle's behaviour when braking on curves and was therefore used during the evaluation. Nevertheless, it would be of importance to take it into account.

Since no obvious advantage of the state controller could be determined, and it can further be argued that the feed-forward with closed-loop control strategy is easier to implement and no high precision position systems are currently available in series vehicles, the feed-forward with closed-loop controller is the current preferred controller. However, a combination of feed-forward with closed-loop controller and state controller could also be conceivable. Depending on the current speed, the controller to be used can be selected to guarantee the best possible results.

Results from the simulation and the tests in the experimental vehicle showed that when driving on a dry surface, the "free corridor" can bring the vehicle to a safe stop for velocities of up to $60\,{}^{km}/_{h}$ without exceeding a lateral acceleration of $3\,{}^{m}/_{s^2}$. When driving in humid or wet surfaces, the operator needs to adapt and not exceed the velocity limit of $40\,{}^{km}/_{h}$ and the lateral acceleration limit of $2\,{}^{m}/_{s^2}$ to guarantee the safe state.

Another important aspect to consider is the coefficient of friction between the tires and the road surface. As mentioned in section 3.5.4, the braking distance greatly depends on the current available coefficient of friction. This value is very difficult to measure [Bub75] and therefore, an estimation of the current value can be used. Nevertheless, since coming to a stop before the predicted braking point could be seen as uncritical, whereas stopping after the braking point becomes dangerous, a more conservative estimation of the value for the coefficient of friction can be used. This would increase the length of the predicted corridor, but stopping within the corridor could be guaranteed.

Furthermore, the workload while performing the driving task in combination with the "free corridor" should be studied to determine to which degree a human operator is capable of dealing with the extra information provided without reducing performance. The NASA-RTLX (NASA Raw Task Load Index), which is a modified version of the standard NASA-TLX (NASA Task Load Index), can be used to obtain the workload estimates of a operator while performing a task or immediately afterwards [Har06].

4 Situation Awareness at the Operator Working Station

FONG [Fon01b, p. 77] describes vehicle teleoperation as often problematic, especially for novices. Common reasons are failure to detect obstacles, poor depth judgment and loss of situational awareness. Additionally, a common problem is the difficulty to maintain spatial orientation with respect to major landmarks, map features or compass directions. It is not uncommon that operators of teleoperated vehicles, even though having landmarks and maps as support, have problems to judge their location and orientation and are not able to return to the starting location without additional assistance [McG89, p. 38-6] [Kay97, pp. 10–11]. The driving task is one of the primary mental activities that has to turn information into reactions and where the driver is normally performing a control activity while continuously processing information [Abe09, p. 4]. A representation of the traffic scenario as complete as possible is basic for the correct choice of action for the driver [Abe09, p. 6]. Nine different sensorial modalities are attributed to the human perception system. For the driving task, only the visual, the acoustic, the haptic and the vestibular perception systems are of relevance [Abe09, p. 5]. Of special importance are the visual and the aural senses, since these enable the human operator to make a timing and position-related prediction, which is very important for highly dynamic traffic situations [Ara82, p. 9] [Heb61, p. 11] [Neg07, p. 9].

Statistics show that an inappropriate speed is not only the most common cause of accidents but also the one with the most severe consequences [Sta11, p. 26]. The speed perception is one of the elements that influence the situation awareness of the operator and hence, it is essential to develop and analyze different methods to improve speed perception at the operator working station of a teleoperated vehicle. This can be achieved by influencing the sensorial modalities related to speed perception, especially the visual, the acoustic, the kinesthetic and the haptic perception [Bub77, p. 103]. This is of relevance since drivers tend to drive slower when their perceived subjective risk seems high, and similarly, tend to drive faster when the risk seems lower [Tay64], with the possibility of leading to an accident.

Section 4.1 discusses the situation awareness at the operator working station. This section begins with an overview of the driving task, presented in 4.1.1. The concepts of situation awareness together with presence and telepresence are explained in sections 4.1.2 and 4.1.3 to allow a better understanding. Following, a more detailed discussion regarding speed perception is presented in section 4.1.4, where the human senses related to speed perception are further discussed. From the above obtained information, section 4.2 derives and presents the goals and objectives of developing methods to influence the operator's speed perception to improve the performance while performing the driving task. Section 4.3 explains the different methods proposed to improve the speed perception. Different studies are conducted to examine the influence of the methods and the results are shown in section 4.4 and finally discussed in section 4.5.

4.1 State of the Art: Situation Awareness at the Operator Working Station

4.1.1 Driving Task

The driving of a vehicle can be seen as the controlling of a machine. The course of the road, other traffic participants and the surroundings determine the driving commands. In other words, the desired longitudinal and lateral positions of the vehicle are controlled. The task of the driver is to perceive this information and translate it into input controls through operating elements, such as steering wheel and accelerator or braking pedals, so that the vehicle follows the desired path [Bub01, p. 156].

The assignments of the driver can be further classified into three subcategories [Bub03]: *Primary Driving Task*, *Secondary Driving Task* and *Tertiary Driving Task*.

Driving tasks can be classified as a target-oriented activity of the human, which according to RASMUSSEN [Ras83] can be divided into three different categories: *Knowledge-based behaviour*, *Rule-based behaviour* and *Skill-based behaviour*.

This classification can be compared to the 3-level hierarchy of the driving task presented by DONGES [Don82], which is divided into three categories: *Navigation*, *Guidance* and *Stabilization*.

The guidance level plays an important role regarding safety in the driving task, since it is at this level that a decision is made as to whether the driver is capable of interpreting the sensoric input information in time and if the selected control variables are in the safe zone or not. Here, the human is equipped with the ability to interpret the traffic scenery with anticipation, allowing him to react in an anticipatory manner [Don99, pp. 116–117].

Figure 4.1 depicts the relation between the human behaviour categories and the 3-level hierarchy of the driving task.

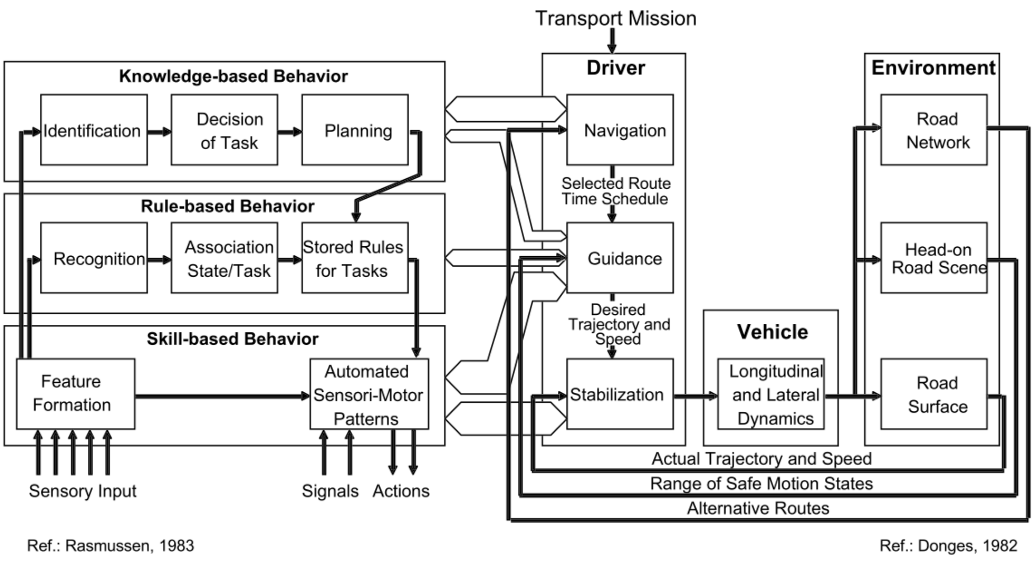

Figure 4.1: The 3-level hierarchy of the driving task according to DONGES and the categories of human behaviour according to RASMUSSEN [Don99, p. 115] (references to [Don82] and [Ras83])

The human is subjected to many stimuli and they use their attention to master these. However, not all of the information can be processed parallelly and therefore, humans need to focus on specific sources of information identified as important ones [Ras04, p. 6] and to be able to learn how to distribute this attention. Failure to distribute it properly can lead to incorrect actions, which could become critical when performing the driving task.

4.1.2 Situation Awareness

The loss of situation awareness could be problematic for the teleoperation of vehicles. What is exactly *Situation Awareness*? How can it be known that situation awareness was lost?

There are different definitions for situation awareness. One widely used definition is from ENDSLEY [End88, p. 792], who defined situation awareness as:

> "Situation Awareness is the perception of the elements in the environment within a volume of time and space, the comprehension of their meaning, and the projection of their status in the near future."

ENDSLEY [End01, pp. 4–5] [End97, pp. 14–15] proposes a model that is descriptive of the situation awareness phenomenon and synthesizes information from different areas (shown in Figure 4.2). This model provides the basis for discussing situation awareness in terms of its role in the complete process of decision making. Situation awareness involves the perception of critical factors in the environment (level 1), the understanding of their meaning, also called comprehension (level 2) and the understanding of what will happen with the system in the near future, also called the projection (level 3). It is this higher level of situation awareness that allows people to function effectively. These levels are processed one after the other and, subsequently, the actions are selected and performed. Similar definitions were reached by WICKENS [Wic95, p. K2-1] and BAUMANN ET AL. [Bau06, p. 43].

Interesting results can be seen in the study of JONES [Jon96], who studied the loss of situation awareness in dynamic flight environments and determined that 76.3% of the errors were level 1 error, 20.3% were level 2 and only 3.4% were level 3 errors, showing that most of the errors due to loss of situation awareness were caused by failure to perceive the environment correctly.

An important aspect while performing the driving task related to situation awareness is the driver's attention. RASSL [Ras04, p. 6] defines attention as the focusing on the stimuli coming to the person and processing its information. According to ABENDROTH [Abe09, p. 5], different forms of attention in the selectivity and intensity dimensions can be made. Regarding the selective allocation of attention, the human has to decide between various sources of information competing with each other. When the attention is shared, the human needs to perceive different stimuli simultaneously and change from one stimulus to the other. The intensity of the attention affects the level of activation, such as a reduced vigilance or sustained attention. Attention therefore can also be considered as a process of selection that determines which parts of the environment are included in the mental representation of the situation [Rau09, p. 9]. When the attention to activities crucial for safe driving in the absence of a competing activity is diminished, it is referred to as *Driver Inattention* [Reg08, p. 32] and it is in its various forms the most prevalent cause of traffic accidents [Wan96, p. 377]. When, however, a competing activity is present and the attention is diverted towards it, then it is referred to as *Driver Distraction* [Reg08, p. 34].

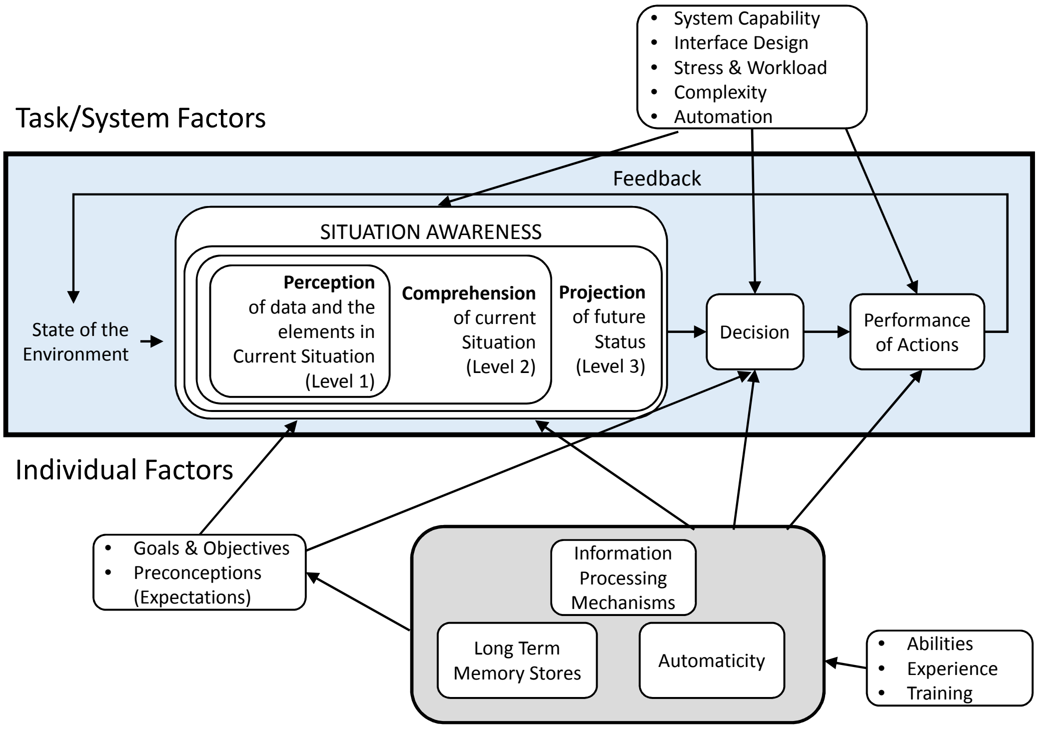

Figure 4.2: Model of situation awareness in dynamic decision making (adapted from [End95, p. 35])

4.1.3 Presence and Telepresence

Presence or *Telepresence* are important concepts for the sense of situation awareness. According to WITMER AND SINGER [Wit98, p. 225]:

> "Presence is defined as the subjective experience of being in one place or environment, even when one is physically situated in another. As described by teleoperators, presence is the sensation of being at the remote worksite rather than at the operator's control station. As applied to a virtual environment (VE), presence refers to experiencing the computer-generated environment rather than the actual physical locale."

SHERIDAN [She94, pp. 1073–1074] and NIELSEN [Nie07, p. 928], based on the definition of STEUER [Ste92, pp. 75–76], also describe presence and telepresence in a similar way. Telepresence is when a human participant feels himself to be present in a location other than the actual one, both real and immediate. Presence, on the other hand, can include feedback from the tele- or virtual environment to the human senses of vision, hearing and haptics.

In presently available virtual environments, it is not possible to completely switch off the real environment. Therefore, a form of combination between both environments or a conflict between the sensory information originates [Dar99, p. 338]. Since the sensory information does not completely come from either the real or the virtual environment, it is up to the user to decide where his attention will be focused [Hee05, pp. 49–50]. When the real environment is extensively isolated, the presence increases.

There are many different elements that influence the sense of presence, such as head-tracking, stereopsis, the geometric field of view (GFOV) [Hen94, p. 98], sound [Neg07, p. 50] and spatialized sound added to a stereoscopic scene [Hen94, p. 61].

In order to achieve perfect remote presence or telepresence, the system should enable the operator to perceive the remote environment as if he were sensing it directly, reproducing the complete multisensory flow of information experienced by humans through all their senses, even smell and taste [Rob10, p. 2809]. However, since information transfered to the driver have been decreasing in recent years due to the high efforts to reduce vibrations and noises in the vehicles, a certain decoupling between the driver and its environment arises, which leads to the driver perceiving the traffic situation emotionally as less risky [Ger02, p. 17]. This has a role in the subjective driving impression and also on the feeling of presence. According to HIGUCHI [Hig96, p. 1035], the driver subjective evaluation depends on feedbacks from the environment and the vehicle's reaction. In the driver subjective evaluation, haptical feedback from the steering wheel, visual and kinesthetic feedback from the vehicle's reaction, acoustic feedback from motor sound, wind noises and tire squeals also play a role [Hua03, p. 3]. HUANG depicts the relation between the subjective impression of the driver in the driver-vehicle-control loop, where feedback to the driver comes from the control elements and also from the vehicle's reactions (Figure 4.3).

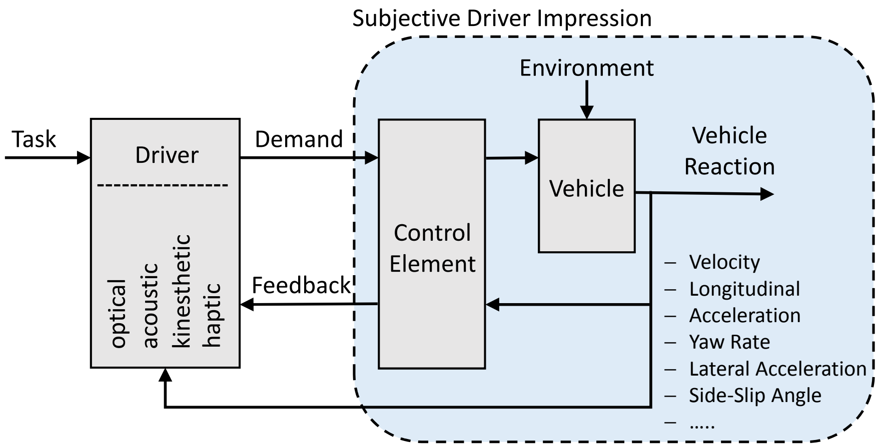

Figure 4.3: Subjective driver's impression according to HUANG (adapted from [Hua03, p. 3])

It is interesting to notice the difference described by HEERS [Hee05, pp. 54–56] between telepresence and virtual presence. This basically lies in the origin of the sensory data.

4.1.4 Speed Perception

It is known that being able to choose an appropriate speed plays an important role in the driving task and in order to achieve this appropriate choice of speed, the current driving speed needs to be perceived correctly. Furthermore, speed perception influences the situation awareness of the operator and it is related to different sensorial modalities. An increase in the ability to perceive the speed correctly would therefore help improve the situation awareness.

The human being does not possess a direct organ to perceive speed. From the human senses, basically only the visual, acoustic, haptic and kinesthetic senses have an influence on speed perception [Bub77, p. 103]. ABENDROTH [Abe09, p. 6] additionally mentions the vestibular sense to contribute in the perception of speed and accelerations of own's vehicle. From the different perception processes, the visual sense is the dominant one, whereas the acoustic, haptic and vestibular senses play a significantly smaller role [Jür01, p. 17]. However, the human is capable of using different means to deduce the speed at which he is moving in the environment. These deductions are mostly based on the feeling of intensity of determined stimuli, such as vibrations and noises. The human estimates accelerations from the perceived information over the specific duration of the acceleration process to determine the change in velocity. The visual sense, especially because of the peripheral vision, allows an accurate estimation of the differences in speeds. The acoustic sense is basically responsible for the estimation of the speed level [Bub77]. SCHWEIGERT [Sch03, p. 4] summarizes the relation between driving information and human sensory channels as in table 4.1.

Table 4.1: Relation between driving information and human sensory channels according to [Sch03, p. 4]

Information	Visual	Vestibular	Haptic	Acoustic
Lateral Velocity	x			
Driving Velocity	x			x
Longitudinal and Lateral Accelerations		x	x	
Yaw Speed	x			
Yaw Acceleration		x		

Interestingly, results of a study showed that the estimation error of the speed was between 5-8% when all the senses were involved, but with the acoustic sense turned off, the estimation errors increased to 25-30% [Heb61, p. 70]. A tendency towards overestimation could be found when subjects were deprived from the visual sense, and towards underestimation when deprived from the acoustic sense [Eva70] [Mat80].

The perceived speed shows a strong adaptation effect by continual motion [Ham00] [Smi87] [Hie08]. The effect of adaptation is to reduce the perceived speed which increased with the adaptation duration [Ham00, p. 1123]. This effect is known from drives on highways and the subsequent slower drive after the exit, which appears to be at snail's pace [Cha03, pp. 73–74]. This adaptation mechanism is described by RECARTE [Rec96] according to the initial speed prior to perception. In a study, the adjustment error was higher when decelerating and lower when accelerating. Furthermore, it was determined that there was a general underestimation of 13.0 km/h and it decreased when speeds increased. This effect was more evident in women than in men and interestingly, driving experience had no significant effect on the accuracy of the estimation [Rec96, p. 301].

Some studies provide information regarding speed perception, such as the one presented by BUBB [Bub77], which discusses speed perception in real vehicles and the relationship between sensory channels and speed perception. Additionally, the study from RECARTE AND NUNES [Rec96] offers information regarding speed perception of a driver compared to a passenger and finally, the study presented by CONCHILLO ET AL. [Con06] gives information regarding estimation of speed in different traffic scenarios.

4.1.4.1 Visual Sense

Vision is a crucial capability which makes driving possible, which according to SUOMELA [Suo01, p. 30] consists of more than 90% of the perception information. When driving, it is important to pick up information from the environment from rather great distances, so that the driver has enough time to control the vehicle's movement and react, whenever necessary. This requirement confirms the importance of the visual sense since the eye is the only long-range receptor and can be specifically oriented [Coh91, p. 153] [Abe09, p. 6]. Visual perception is timely and spatially in advance and can therefore provide an anticipatory behaviour so that the driver is able to react before the disturbances are reached [Ara82, p. 9]. The human uses the eye as the main mean for orientation in space. Without impeccable eyesight to identify objects according to form and color, it is impossible to behave in a safe way in traffic [Heb61, p. 11].

The anatomic sensors related to vision are cones and rods. Cones provide sharp visual acuity and color vision, while rods provide less visual discrimination but are more sensitive in low light conditions. The visual subsystem consists of two independent systems, each with principal functions. *Peripheral* vision is predominately responsible for spacial orientation and *Fovial* vision is involved with the recognition of objects. Both rods and cones are important for the peripheral vision [Pas94, p. 3]. The eye not only provides the perception of colors, objects and motion, but also the perception of spatial depth and size [Abe09, p. 5]. The components for depth perception can be summarized as [Gol10, pp. 230–240] [Sch77, p. 249]: *Oculomotor Cues*, *Monocular Cues* and *Binocular Depth Information*.

Binocular depth information is however effective only over a short distance of approximately 10 meters [Lee70, p. 65]. However, higher distances are typically the ones with which a traffic participant has to deal with. In this case, the adaptation takes over a major role [Heb61, pp. 17–18]. Figure 4.4a depicts the approximate progression of the human eye's accommodation with respect to the distance from the eye.

There are two variables that can be defined from which information regarding the motion state can be extracted. The first variable is the gradient of the changing field of vision. This variable is responsible for the speed perception. The second one is the vector field (radial pattern of the directions), which causes the perception of the motion's direction [Bub77, pp. 103–104]. During motion, the observer sees the environment drifting past them, as can be seen in Figure 4.4b through the vectors that flow apart and become larger as the distance to the observer decreases. Additionally, the perceived speed increases with increasing distance toward the edges. This effect is called optical flow.

There are different factors that influence speed perception related to the optical sense, for example optical flow, time-to-contact, the field of view, the angular declination, the image contrast or the weather conditions [Kem03]. MOURANT [Mou07] and DIELS [Die09] determined the relation betweeen speed perception and the geometric field of view to be a linear increase of perceived speed with the size of the geometric field of view. According to ARAND [Ara82, p. 47], because of the importance of peripheral vision on speed perception, it is necessary to design the working station with an horizontal view of at least $180°$. This should be achieved without any distortion in the image. In order to accurately perceive the vehicle speeds and distances, simulation studies showed that the use of a large field of view and the rendering of motion parallax due to observer's self-motion was recommended [Kem03, p. 36]. NEGELE [Neg07, p. 80] mentioned that using displays with a field of view of $40 - 60°$, a good speed estimation is possible for low velocities of up to $60\ ^{km}/_{h}$ but for higher velocities,

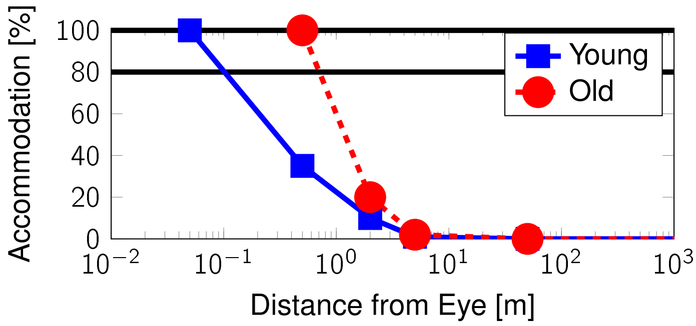

(a) Approximate progression of accommodation with respect to distance between object and human eye (adapted from [Neg07, p. 11])

(b) View of vector field perceived by an observer moving forward ([Gol02, p. 331])

Figure 4.4: Approximate accomodation progression of the human eye and the view of vector field perceived by an observer moving forward

the field of view should be increased in order to increase the optical flow. To provide a good speed perception, an horizontal field of view of $120 - 140°$ should be used [Neg07, p. 100]. Experiments also showed that driving with a field of view of $40°$ leads to operators not being comfortable while turning corners, but when increasing the field of view to $120°$, it resulted in much easier operation [McG89, p. 38-4].

According to JAMSON [Jam00, p. 63], the image resolution and also the field of view have a significant influence on the speed perception, where a reduction of the image resolution causes a worsening in the validity of speed, even if the horizontal field of view was increased. Therefore, the choice of speed will benefit from high image quality and pixel density, even at the expense of field of view. Weather conditions could also have a great influence on speed perception, especially from objects in the atmosphere such as raindrops, hailstones, or snowflakes, which influence the optical flow and depending on the direction of their flow, it could influence the speed perception [Cha03, pp. 107–108]. Additionally, the distance to objects is also an important factor that influences the speed perception. The smaller the distance to the object, the higher the angle-velocity on the retina. Close objects appear to be moving faster than farther ones [Cha03, p. 22].

Another important factor when discussing speed perception is the self-motion. The main factor for perceiving self-motion according to LAPPE [Lap99] is the optical flow. According to BERTHOZ [Ber75], the peripheral vision also plays an important role for the perception of linear horizontal self-motion. GIBSON [Gib79, p. 183] discussed the awareness of one's own motion in the world and the phenomenon of visual kinesthesis and according to him, visual kinesthesis goes along with muscular kinesthesis and concluded that vision obtaining only external information to be incorrect.

4.1.4.2 Acoustic Sense

The acoustic sense is the second sense that has a considerable influence in the perception of speed in vehicles. The frequency spectrum is characteristically determined by the vehicle's speed and the engine revolution (or engine speed), among others such as wind speed, road conditions, surfaces reflecting sound, type of tires, etc. When the engine revolution is increased, the higher edge of the spectrum shifts towards high frequencies [Bub77, p. 104], which indicates that a change in the volume of the noise is the main influence factor in the perceived speed changes.

While the visual sense only provides information regarding the surroundings at the direction where the eyes are directed, the human is capable to hear all the noises coming from the front, sides and rear. This is possible independently of the current position of the head. The auditive sense is capable of delivering a representation of the surroundings in a spatial structured form that compensates the visual sense. Objects that are not visible to the human eye can be detected and localized by the ear. Even noises whose sources are directly blocked by objects in between can be perceived by the human ear. Therefore, traffic information, such as honks or whistles and possible dangers, could be detected by a driver prematurely, after which the driver can prepare himself to avoid sudden or late reactions [Heb61, p. 48] [Ans11, p. 125].

The human is capable of localizing sound sources. There are binaural and monoaural cues. The left and the right hearing organ allow a differentiation in the direction of the coming acoustic wave and provides a spatial orientation through the interaural time difference (ITD) and the interaural level difference (ILD). At lower frequencies, the time difference between reaching one ear and the other is registered, where time intervals of $1/30000$ seconds are identifiable [Löh76, p. 34]. The reduction of intensities occurs only for high-frequency sounds, not for low-frequency sounds [Gol10, pp. 293–294] [Sch93, p. 40] [Ans11, p. 125].

The primary monoaural cue used for localization is called spectral cue. The information is contained in the differences in the distribution of frequencies from different locations. These differences originate from the reflections from the head and the various folds within the pinnae [Gol10, p. 295].

The normal mode of hearing is to listen to sounds in order to identify their cause and therefore, sounds provide information about the interaction of material at a specific location in the environment [Gav86, p. 169]. Functionally speaking, non-speech audio messages can be used to provide three general types of information: alarms and warnings, status and monitoring indicators, and encoded messages [Bux94, p. 1.5-1.6].

In vehicles, driving noises are present and consist of powertrain noises, rolling noises and wind noises. Their different components can be seen in Figure 4.5. Powertrain noises originate from the motor, transmission, accessories, intake- and outtake systems. The noises of the motor are dependent on the engine load and engine revolutions. The complete powertrain noise level in the interior of a sedan increases according to the power law with increasing revolutions [Zel09, pp. 158–159]. Rolling noises originate from the interaction between tires and roadway and they become louder with increasing speed. The intensity increases approximately with the second power with increasing speed, which corresponds to an increase in noises of $6\ dB$ with two times the speed [Zel09, p. 159].

Overall, it is possible to transmit a variety of signals and a huge amount of information through the acoustic channel. This channel combined with other perception channels can improve the driving task, the driver's attention and the feeling of presence [Neg07, p. 50] [Dem04, p. 21].

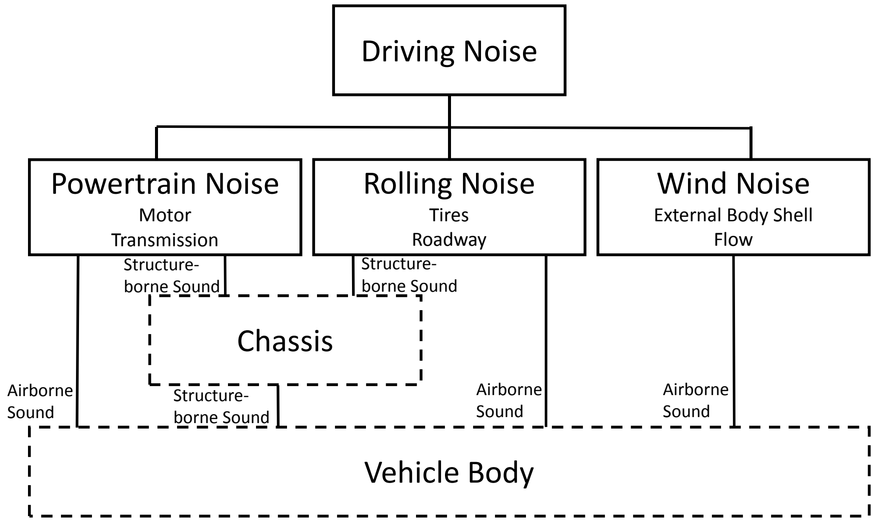

Figure 4.5: Components of driving noises (adapted from [Zel09, p. 159])

4.1.4.3 Haptic Sense

All the sensations related to vibration or force feedback from input devices are part of the haptical perception. A similar relation as in acoustic information can be found in feedback through vibrations: the higher the driven speed, the higher-frequency vibrations become. Additionally, information relevant to the perception of speed can be obtained through the position of the control devices, especially the accelerator. When driving on curves, force feedback is present in the steering wheel, whose amplitude depends on speed, steering wheel angle and road conditions [Bub77, p. 105]. This method of perception is of great help for the driver, since he can perceive information regarding speed and engine revolution through vibrations [Neg07, p. 91] and low-frequency vibrations that depend on speed are conducive for the perception of speed [Neg07, p. 105].

The haptic sense is an important sense for the driving task, since it provides information regarding the detection of approaching dynamic limits and feedback regarding contact between tires and road surface for safety and driving pleasure [Koc10, p. 20] [Bub01, p. 167]. Furthermore, the haptic channel possesses an advantage with respect to other channels, which is the presented benefits regarding reaction times [Hie11, p. 22].

It is therefore meaningful to include haptic feedback in a telepresence system, additionally to visual and acoustic feedback, especially when not only force feedback but also tactile feedback is included [Dem04, p. 27], which refers to the interaction between skin and surfaces and where deformations of the skin are perceived [Abe09, p. 6] [Hie11, pp. 73–74].

4.1.4.4 Vestibular Sense

The vestibular sense also contributes to the perception of speed and accelerations of one's own vehicle [Abe09, p. 6]. The information regarding change in position and posture on the driver's seat can be obtained from the vestibular channel. The driver uses the capabilities of the vestibular system and the gravitation to obtain the spatial position of the body [Ara82, p. 10] [Abe09, p. 6]. Through this system, horizontal and vertical linear accelerations and angular accelerations can be detected, even when the optical spatial orientation is not available [Heb61, p. 60]. This is made possible by the vestibular organs [Neg07, p. 14].

Nevertheless, the precise role of vestibular cues and its importance is still subject of ongoing research [Kem03, p. 33]. It was suggested that vestibular information had only little or no effect on steering performance and that it is not integrated with visual information [Wil05, p. 901]. However, it can be assumed that a missing acceleration simulation leads to a worse control of the vehicle, especially in highly dynamic situations, though the representation of accelerations involve great efforts and costs [Neg07, pp. 39–40].

4.2 Objective and Goals

The loss of situation awareness produces errors while performing the driving task [Jon96]. It is therefore essential to improve the conditions for the operator at the working station. Teleoperation is often problematic since it is common that the operator does not perceive the surroundings appropriately [Fon01b, p. 77]. Section 4.1.3 discussed the different aspects that influence the feeling of being there, or being "present".

When completely decoupled from the vehicle, the operator perceives only a limited amount of feedback information coming from the vehicle's surroundings. As mentioned in section 4.1.4, the ability to choose an appropriate speed plays an important role in the driving task. However, when the operator is deprived from these sources of information, the human senses are limited and it becomes harder to correctly estimate speeds.

Therefore, it is essential to improve the capabilities of the operator to properly estimate his own driving speed using different methods that make use of the human senses to influence their perception. This, on the other hand, greatly influences the operator's performance and the vehicle's safety. The actual driving speed could be directly displayed to the operator on a speedometer, however, from own experience, using only this method does not provide a proper feeling of speed. Whenever driving in a curve, it was not possible to assess if the current driving speed was appropriate or too fast only from the displayed speed on the speedometer. It was almost necessary to adapt the driving speed since usually a too high or too low speed was selected.

To develop the necessary methods that are capable of influencing the situation awareness and the speed perception of the human operator, the factors discussed in section 4.1 are taken into consideration. The developed methods, which include blur effects, artificial motor sound and vibrations at the driver's seat, are analyzed and studied in section 4.3. Ultimately, it is necessary to validate the effect of such methods. Using studies with test persons, the methods are studied and the effect analyzed.

4.3 Proposed Solutions to improve Speed Perception

The ability to perceive the speed correctly helps the human operator perform better in the driving task. With a better speed perception, the situation awareness is also improved. Since there are different human senses that are related to speed perception, there are multiple possibilities to influence it.

Section 4.1.4 discussed the senses that influence speed perception, being the optical sense the dominant one. Different factors that play an important role in the speed perception were presented, such as geometric field of view, image resolution, weather conditions and optical flow, among others.

An increase in the field of view increases the speed perception, therefore, the field of view could be theoretically further increased to achieve improvement. Nevertheless, the current field of view provided by the cameras in the experimental vehicle already fulfills the recommendation of a field of view of $180°$ [Ara82, p. 47] to provide a good speed perception and further increase would be difficult and costly. Reducing the field of view would only worsen the perception, which would in this case be senseless.

Similarly, the image resolution is directly related to the speed perception. Increasing the resolution would further improve perception and reducing it would worsen it. Theoretically, the image resolution could be increased, nevertheless, images are already transmitted in the highest possible resolution allowed by the bandwidth limitation.

On the other hand, weather conditions are not aspects that can be easily controlled at the operator working station. Lastly, the other factor that influences speed perception is the optical flow [Bub77, pp. 103–104]. Therefore, blur is proposed as a method to influence speed perception of the operator using the visual sense and is further explained in section 4.3.1.

The second sense involved in the speed perception in vehicles is the acoustic sense. There are many noises present when driving, such as powertrain noises, rolling noises and wind noises. Nevertheless, the engine revolution directly influences the perceived speed changes because of the change in the volume of the noises. The intensity of rolling noises originating from the contact between tires and road also influence the perceived speed. However, such noises would be difficult to reproduce artificially at the operator interface and therefore, an artificial motor sound determined by engine revolutions and load is used. This is further described in section 4.3.2.

The haptic sense helps the speed perception using feedback through vibrations. Similarly to the acoustic sense, the frequency of the vibrations increase with an increase in driven speed. Hence, a feedback using vibrations is used to study its influence at the working station. This is shortly described in section 4.3.3. Alternatively to vibrations at the seat, a force feedback at the steering wheel might be able to influence the speed perception.

4.3.1 Blur

Blur has been known since the advent of photography as being capable of producing a sense of speed. It is commonly used in video games to enhance the feeling of speed, as can be seen in Figure 4.6.

However, when used in the application of teleoperated road vehicles, it is undesirable that the complete picture becomes blurred due to the importance of keeping the visibility unobstructed. Therefore, the blur effect is only applied to the outer ranges of the picture and the middle part is kept unprocessed. The blur parameter [%] is used to determine the degree of blur and the position at which the blur effect starts. The higher this parameter is, the closer to the center of the image the effect of blur begins. Figure 4.7 shows an example of two different sets of blur parameters on the left section of the displayed image, 80% and 100% of blur, respectively.

(a) Blur effect on XNA Racing game [XNA14]

(b) Blur effect on Shift 2 computer game [Gam14]

Figure 4.6: Blur effect used in computer games to produce speed effect

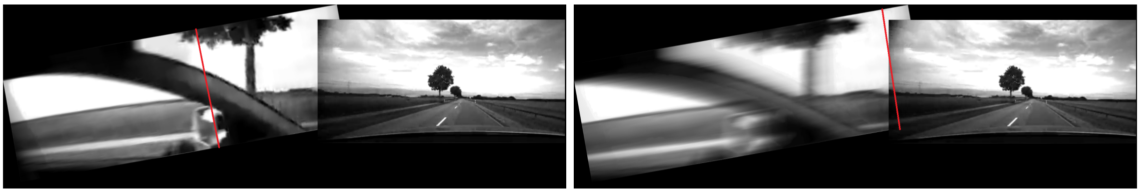

(a) Visualization of the left part of the images with a 80% blur parameter

(b) Visualization of the left part of the images with a 100% blur parameter

Figure 4.7: Visualization of the left part of the images using different sets of blur parameters

Motion Blur and *Zoom Blur* are two known methods to implement the blur effect on the images. For motion blur, two or more pictures (or frames) are superimposed and older pictures are blended in using transparency to minimize the transition between different frames. The biggest advantage of motion blur is that only moving objects become blurred. However, motion blur can only be achieved using multiple frames. Additionally, a higher frame rate is necessary to achieve smooth transitions, especially when driving at high speeds, where very strong differences between each frame are present. Compared to motion blur, zoom blur has the advantage that a single frame is capable of producing the blur effect. The idea is to take the same frame, slightly stretch it, overlay it on the original frame and cut its side margins. The complete process can be repeated to produce stronger effects. Using higher transparency, smoother transitions can be achieved. The degree of stretching and the number of stretched and overlayed frames determine the intensity of the blur effect. The biggest disadvantage of zoom blur is that everything in the side margins becomes blurred, regardless of being static or moving objects and regardless of their speed. Additionally, zoom blur can only be used to increase the perceived speed since the optical flow is intensified. Figures 4.8a and 4.8b show an example of motion and zoom blur, respectively.

It can be argued that zoom blur produces a blur that radiates to the margins from the center of the image, but it is also known that this type of blur produces a perceived forward motion into the image and this effect affects the amount of speed towards the center [GIM13].

Due to the application of teleoperated vehicles, only a limited bandwidth is currently available for the video transmission, and therefore, only a limited frame rate can be achieved. Considering this limitation and that smooth transitions at higher speed might not be possible to achieve, zoom blur was selected. The effect of zoom blur was created from the center of the image towards the sides in horizontal direction, making the direction of travel towards the center of the visual field. A frame rate of 25 frames per second (fps) was used since this frame rate is used as the PAL television standard. At a moving speed of $50\,{}^{\mathrm{km}}/_{\mathrm{h}}$, one

(a) Example of a real camera image using motion blur [Tan13c]

(b) Example of a real camera image using zoom blur [Tan13c]

Figure 4.8: Example of a real camera image using two different methods of blur [Tan13c]

frame could be captured every 0.56 meters, and when overlapping these to create motion blur, tests showed an unrealistic perception. Moreover, zoom blur is easy to implement and requires only a single image to achieve the effect.

4.3.2 Artificial Motor Sound

In order to address the acoustic sense, an artificial motor sound based on the current engine revolution and engine load is used. The engine behaviour is simulated by calculating increase and decrease in the revolution using fuzzy logic and making use of pre-recorded samples. These samples were taken at different revolutions and under different loads. Because of the samples taken with different vehicles, there is the possibility to choose from different types of vehicles.

The engine behaviour is simulated by calculating the increase and decrease load vector of the revolutions. The different loaded samples are looped and pitched according to the current revolution. Additionally, the volumes are adjusted between the samples to achieve the artificial motor sound experience.

The information of the current engine's revolution and load is obtained directly at the teleoperated vehicle and transmitted through the communications back to the operator working station. Using the current received data, the samples are adjusted to produce an artificial simulated motor sound and is then played using a conventional 5.1 surround sound system.

Even though the artificial motor sound does not provide a surround system, the transmission of real noises coming from the teleoperated vehicle could be possible using a surround recording system. This would allow the human operator at the working station to perceive surround noises and localizing objects in the surrounding, such as other traffic participants. This is however not considered in this dissertation.

4.3.3 Vibration at the Driver's Seat of Working Station

Additionally to the above mentioned senses, the haptic sense is addressed using bass-shakers installed in the driver's seat, one directly under the seat and the other one behind the backrest. The simulated artificial motor sound obtained from current engine revolution and engine load as described in section 4.3.2 is forwarded to an amplifier module *mivoc AM80* [Spe13] and low-frequency sounds are used to produce the vibrations.

Figure 4.9 shows the hardware components used for the reproduction of vibrations at the driver's seat.

(a) The amplifier module *mivoc AM80* used for the vibrations [Spe14]

(b) Bass shakers built in the driver's seat to reproduce vibrations [Ama14]

Figure 4.9: Components used for the reproduction of vibrations at the driver's seat

4.4 Results

In order to analyze the effects of the proposed solutions to improve the speed perception, a total of three different studies with test persons were conducted. The studies are presented in sections 4.4.1, 4.4.2 and 4.4.3 and later on, discussed in section 4.5.

4.4.1 Blur

A first study with test persons was conducted to analyze the effect of blur on the speed perception of an operator. A more detailed analysis can be found in [Tan13c], where also demographical aspects of the test subjects are discussed with regard to their influence to speed perception.

A tendency to under-estimate the speed can be seen as critical since the driver would tend towards increasing the current speed. On the other hand, over-estimation is seen as uncritical, because the driver would tend towards decreasing the speed, creating possible obstructions in traffic but without becoming safety-critical.

To analyze the estimation of speed, the following questions were used to address the problems:

(A) How good is the speed perception of the test subjects at the working station without practice?

(B) Does the "learning effect" at the working station influence speed perception?

(C) How does zoom blur effect at the side margins influence the test subjects?

(D) Which parameters are meaningful for the zoom blur effect?

During the experiment, the measured data is the assertion of the test subjects and results are additionally obtained from questionnaires. For the abovementioned questions, four hypotheses with corresponding Null Hypothesis "NH" and Alternative Hypothesis "AH" are defined:

Hypothesis A:

NH: The test subjects guess the speed correctly within a defined tolerance.

AH: The test subjects under-estimate or over-estimate the speed outside the defined tolerance.

Hypothesis B:

NH: The learning effect does not have any effect on the speed perception of the test subjects at the working station.

AH: The learning effect does have an effect on the speed perception of the test subjects at the working station.

Hypothesis C:

NH: Zoom blur does not have any effects or has negative effects on the perception of the test subjects at the working station.

AH: Zoom blur has positive effects on the speed perception of the test subjects at the working station.

Hypothesis D:

NH: Meaningful parameters for the zoom blur are the same for all test subjects.

AH: Meaningful parameters for the zoom blur are different for each test subject.

The hypotheses are analyzed through tests where test subjects are asked to guess the speed of a pre-determined sequence of videos. Pre-recorded videos were used in order to make the experiment reproducible and so that the seen velocity remained constant among all test subjects. The videos were recorded on the same test route, on the FS20 highway north of Munich between Dietersheim and Eching.

The selected speeds were measured in $1\,\text{km/h}$ intervals to avoid guesses rounded to multiples of $10\,\text{km/h}$.

The selected speed for the pre-recorded videos are based on the study by Bubb [Bub77]. In each of the shown videos, there is a ten second period where the previous speed in the cycle is driven, followed by a five second acceleration or deceleration period to achieve the speed to be guessed. This is done due to the effect that visual systems adapt to the prevailing image conditions, as explained in section 4.1.4, where a subject driving at a constant speed for a prolonged time may be subject to a reduction in the perceived speed [Hie08]. Figure 4.10 shows two different exemplary sequences of videos used for the study. Test subjects were asked to guess the speed only after the acceleration or deceleration was completed. Different cycles are used for different test groups, which are shown in table 4.2.

Even though the current application of teleoperated vehicles is limited to speeds of $60\,\text{km/h}$, speeds of up to $100\,\text{km/h}$ were also tested in order to avoid restricting the applicability of the results and to increase the effect size of the study.

The guess error is defined as the difference between the real speed and the guessed speed, where a positive error value means an under-estimation and consequently, a negative error value means an over-estimation.

A between subjects design was selected. The test subjects are split into two groups, A and B. Subjects belonging to group A receive no treatment, meaning that they do not see the videos with blur effect and are used for control purposes. Subjects from group B are given the option of parameterizing the zoom blur settings as deemed appropriate.

The complete study consists of five phases. During phase 1, the test subjects have to guess the speed without previous knowledge. In phase 2, the same videos as in phase 1 are shown to the subjects and the correct speed together with the guessed speed is communicated. Phase 3 consists of another guessing phase similar to phase 1, only with different speeds. In phase 4, the test subjects are split into two groups, A and B, with and without blur respectively. Subjects from group B can then use the keyboard to adjust the blur parameter to achieve a subjective perception of the correct speed. Subjects from group A are provided with other activities in order to keep the duration of the study equal for both groups. Finally, in phase 5 the subjects guess the speed similarly to phase 1 and 3, but with the videos in reverse order. Additionally to the guesses, the test subjects were asked to fill questionnaires regarding demographic characteristics and their subjective perception.

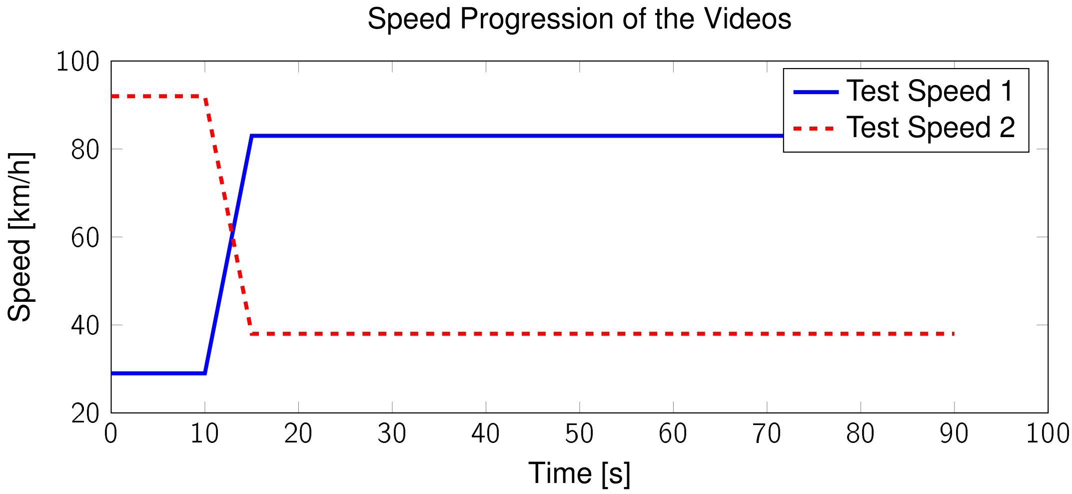

Figure 4.10: Examples of speed progression of the recorded videos for the study with test persons

Table 4.2: Speeds and cycles used in the study to evaluate speed perception of test subjects

All Speeds [km/h]	**0, 29, 38, 47, 56, 65, 74, 83, 92**
Cycle 1	(0)-29-83-29-65-47-83-65-47
Cycle 2	(65)-47-65-83-47-65-29-83-29
Cycle 3	(0)-56-38-74-92-38-92-56-74
Cycle 4	(56)-74-56-92-38-92-74-38-56

A total of 30 test subjects participated in the study, consisting of 26 male and 4 female participants with the youngest person being 19 years old and the eldest 41, with a mean of 23.3 and standard deviation of 4 years. The prerequisite was the possession of a class

B driving license. Test subjects held the driving license for a mean duration of 5.6 years and drive in average 8755 kilometers each year. No test subject had any aural disability or limited sight, however eight subjects were required to wear glasses when driving and were asked to do so during the study.

For the analysis of results, "good guessing" is defined when the guessing error was $\pm 4\,{}^{km}/_{h}$ based on the definition by BUBB [Bub77]. From the data obtained from the test subjects, a tendency towards under-estimation could be determined, confirming findings from other studies [Rec96, p. 301]. This is shown in Figure 4.11a. Due to the obtained results, the Null Hypothesis A is rejected and the Alternative Hypothesis A "The test persons under-estimate or over-estimate the speed outside the defined tolerance" is accepted.

To answer question B, the test subjects are split into groups according to their guess errors: good guessers, under-estimating guessers and over-estimating guessers, consisting of a total of 10, 12 and 8 subjects. The average guess errors at the beginning (phase 1) and after the learning phase (phase 3) is shown in Figure 4.11b and in table 4.3. An improvement in the error can be seen for the under- and over-estimating guessers. In each case, a t-test was conducted. The t-test can be used for the comparison of two means for dependent samples [Bor05, p. 143] and the assumption of a normal distribution can be made, when the sample is large enough [Sib12, p. 368]. From the results, the Null Hypothesis B is rejected and the Alternative Hypothesis B accepted, meaning that the learning effect influences the speed perception.

Table 4.3: Mean guess errors for hypotheses B and C

		Mean without treament	**Mean with treament**	**p-Value**
Learn Effect	Good guessers	-0.69	1.43	0.370
	Under-estimated Guessers	10.69	2.21	$9.887 \cdot 10^{-19}$ ***
	Over-estimated Guessers	-7.73	1.14	$1.613 \cdot 10^{-13}$ ***
Blur		3.44	-0.68	0.024 *

* significant ($p < 0.05$); ** very significant ($p < 0.01$); *** highly significant ($p < 0.001$)

To answer question C, groups A and B as divided in phase 4 are needed. First, it is important to clarify whether any differences between both groups exist. The variance analysis shows that there is no significant difference. 13 test subjects of 15 subjects in group B showed under-estimation in phase 1 and two of them never under-estimated. Therefore, these two subjects were considered with group A, since an additional blur treatment would be meaningless. Comparing the results shown in Figure 4.12a, a significant improvement (table 4.3) could be determined within both groups, even with a slight over-estimation. With these results, the Null Hypothesis C is also rejected and the Alternative Hypothesis C is accepted.

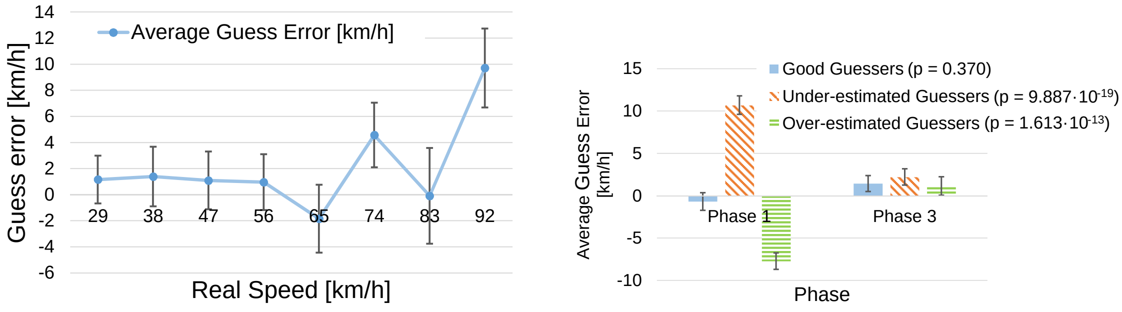

(a) Average guess error for different speeds with a linear approximation [Tan13c]

(b) Influence of learning effect on guess error of speed perception [Tan13c]

Figure 4.11: Results from the study regarding average guess error and the influence of learning effect [Tan13c]

An interesting aspect is that even though 8 of the subjects answered with "No" to the question if they thought zoom blur improved their speed perception, results showed a significant improvement.

Figure 4.12b shows the different blur parameters selected by the test subjects at different speeds. Since speed perception is subject to each subject's perception, it is not possible to generalize which parameters are meaningful without knowledge of the subject's specific guessing tendency. It cannot be concluded which parameter sets are the most meaningful and blur needs to be calibrated according to each person.

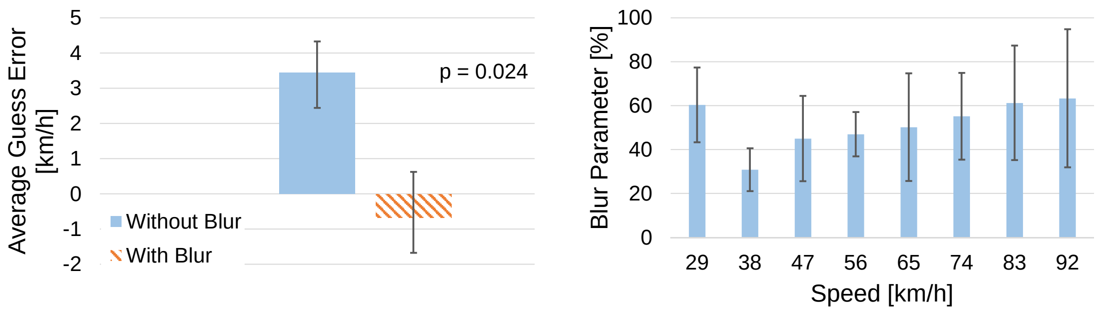

(a) Influence of zoom blur on the guess error [Tan13c]

(b) Average blur parameter for different speeds [Tan13c]

Figure 4.12: Guess error comparison between guessing with and without blur; average blur parameters [Tan13c]

4.4.2 Artificial Motor Sound, Vibration at the Driver's Seat, Blur

Similarly to the study for the effect of blur on speed perception, a further study with test persons was conducted to analyze the influence of artificial motor sounds and vibrations at the driver's seat. The study is mainly based on the described study above.

To analyze the effects of both proposed methods, the following questions were used:

(A) How good is the speed perception of the test subjects without any additional assistance?

(B) Does the additional playback of artificial motor sound improve the speed perception?

(C) Does additional vibration at the driver's seat improve the speed perception?

(D) Does the additional playback of artificial motor sound together with vibration at the driver's seat improve the speed perception?

(E) Does the effect of blur together with playback of artificial motor sound and vibration at the driver's seat improve the speed perception?

Again, the measured data is the assertion of the test subjects. For the abovementioned questions, corresponding hypotheses are defined:

Hypothesis A:

NH: The test subjects guess the speed correctly within a defined tolerance.

AH: The test subjects under-estimate or over-estimate the speed outside the defined tolerance.

Hypothesis B:

NH: The playback of artificial sound does not have any effects or has negative effects on the perception of the test subjects at the working station.

AH: The playback of artificial sound has positive effects on the speed perception of the test subjects at the working station.

Hypothesis C:

NH: Additional vibration at the driver's seat does not have any effects or has negative effects on the perception of the test subjects at the working station.

AH: Additional vibration at the driver's seat has positive effects on the speed perception of the test subjects at the working station.

Hypothesis D:

NH: Additional playback of artificial motor sound together with vibration at the driver's seat does not have any effects or has negative effects on the perception of the test subjects at the working station.

AH: Additional playback of artificial motor sound together with vibration at the driver's seat has positive effects on the speed perception of the test subjects at the working station.

Hypothesis E:

NH: Blur together with the playback of artificial motor sound and vibration at the driver's seat does not have any effects or has negative effects on the perception of the test subjects at the working station.

AH: Blur together with the playback of artificial motor sound and vibration at the driver's seat has positive effects on the speed perception of the test subjects at the working station.

The videos shown to the subjects to guess are based on the same principle described in section 4.4.1, with the additional information of engine revolution and load used for the calculation of the motor sound and vibrations. The speeds used are the same as shown in table 4.2. A between subjects design was selected.

The study is split into different phases. First, phase 1 consists of the test subjects guessing the speed without treatment. Then, the test subjects were split into groups A and B. Group A was required to guess the speed without any treatment throughout the study and was used as the control group. In phase 2, subjects from group B were asked to guess the speed with the playback of artificial motor sound. During phase 3, subjects were asked to guess the speed with only vibrations at the driver's seat and in phase 4, they were asked to guess the speed with a combination of artificial sound and vibrations. In phase 5, test subjects were asked to guess the speed with a combination of all proposed methods: blur, playback of artificial motor sound and vibrations at the driver's seat. At the end of the study, all subjects were asked to fill a questionnaire.

A total of 28 test subjects participated in the study, consisting of 20 male and 8 female participants. The possession of a class B driving license was a prerequisite. The youngest subject was 18 years old and the eldest 56, with a mean of 24.6 years and standard deviation of 8.5 years. In average, the test subjects held the driving license for 7.0 years and drive in average 11160 kilometers each year. Nine test subjects were required to wear glasses when driving and were asked to do so during the study. Two of the participants were excluded from the results since they showed little driving experience and a very low average driven kilometers each year when asked. In this case, one belonged to group A and the other one to group B.

Results from the study are presented in table 4.4 and Figure 4.13.

Table 4.4: Mean guess errors for hypotheses B, C, D and E

	Mean without treament	**Mean with treament**	**p-Value**
Motorsound	2.0769	0.5000	> 0.05
Vibration	1.8846	-0.6731	0.0446 *
Motorsound + Vibration	5.7596	-0.6635	$2.891 \cdot 10^{-7}$ ***
Motorsound + Vibration + Blur	6.9904	-2.9519	$4.551 \cdot 10^{-12}$ ***

* significant (p < 0.05); ** very significant (p < 0.01); *** highly significant (p < 0.001)

To answer question A, all subjects are asked to guess the speed without any treatment. From the data obtained, a tendency towards under-estimation could be determined, which agrees with the results from the first study and findings from other studies. This tendency can be seen in Figure 4.13a. Therefore, the alternative hypothesis that the subjects under- or over-estimate the speed outside the defined tolerance is accepted.

For questions B, C, D and E, it is again important to perform a variance analysis to determine if there is any significant difference between groups A and B. The analysis showed no significant difference between both groups.

From the results, even though there was an improvement in the mean error when using only artificial motor sound, the difference is not significant. When only using vibrations at the driver's seat, a significant reduction in the guess error was observed. Again, 7 out of 12 test subjects answered with "No" to the question if they felt that vibrations improved their

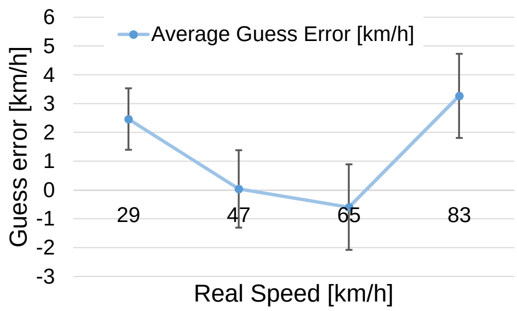

(a) Average guess error for different speeds

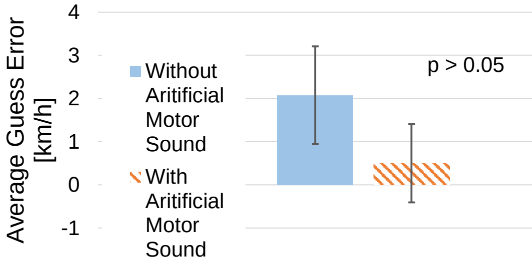

(b) Influence of artificial motor sound on the guess error

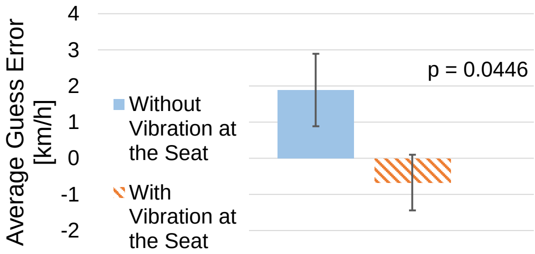

(c) Influence of vibration at the driver's seat on the guess error

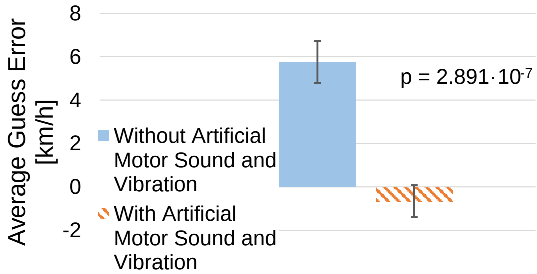

(d) Influence of artificial motor sound combined with vibration at the driver's seat on the guess error

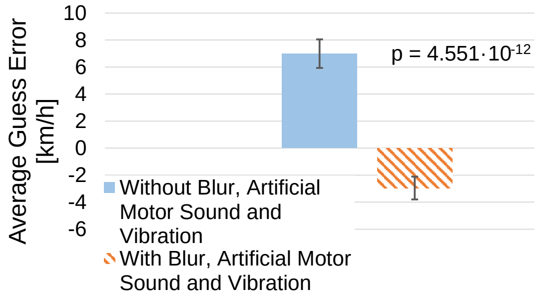

(e) Influence of blur combined with artificial motor sound and vibration at the driver's seat on the guess error

Figure 4.13: Guess error comparison between guessing with and without different methods implemented to influence speed perception

speed perception. When using artificial motor sound and vibrations at the driver's seat, a highly significant improvement was determined. When combining all methods (blur, artificial motor sound and vibrations at the driver's seat), a highly significant improvement could be observed.

Therefore, the null hypothesis B cannot be rejected, but the null hypotheses C, D and E are rejected.

4.4.3 Artificial Motor Sound, Vibration at the Driver's Seat, Blur while Driving

A further study with test subjects was conducted to understand if the abovementioned results obtained from previous studies are similar when the subject is not only looking at prerecorded videos but rather driving. For this purpose, the framework DYNA4 was used in combination with DYNAanimation3.

Two routes were developed for the purpose of exploring the effects of the methods while driving. Both routes consist of straight line segments, curves, and clothoids as connecting segments. The different sections of one route are repeated on the other route for purposes of comparison, but in different sequences to avoid the effect of test subjects memorizing the different velocities or curves. Both of the routes include road signs as velocity limits. However, for the purposes of the study, the test subjects were asked to drive at the shown speed instead of not exceeding the shown speed limit.

The test subjects were asked to drive along the courses using the same interface at the working station as when driving the real vehicle and the same that was used for the previous studies. Virtual cameras that correspond to the field of view and the position of the real cameras in the experimental vehicle are defined and the videos of the surroundings are sent to the operator. Figure 4.14 shows an example of the seen image by the test subjects during the study.

Figure 4.14: Interface at the working station showing the scenario used in the study with test subjects using DYNAanimation3

For the two routes, different sequences of speed were selected. These speeds are defined according to the segment they are traveling. Table 4.5 shows the speed sequences corresponding to the 14 different segments in each route.

The study was conducted with the help of the simulation environment because of practical and safety reasons. There was no testing ground available in which the developed routes could be safely driven.

Table 4.5: Speeds used in the study to evaluate speed perception of test subjects while driving

All Speeds [km/h]	**30, 40, 50, 70, 90**
Route 1	40-30-90-30-70-50-70-30-90-50-30-90-40-70
Route 2	30-50-70-90-30-70-40-30-50-90-70-30-90-40

In order to understand the effects of the proposed methods while driving, following questions were defined:

(A) How good is the speed perception of the test subject while driving without any additional assistance?

(B) Does blur improve the speed perception while driving?

(C) Does the additional playback of artificial motor sound together with vibration at the driver's seat improve the speed perception while driving?

(D) Does blur together with playback of artificial motor sound and vibration at the driver's seat improve the speed perception while driving?

In this case, the measured data is the own assertion of the test subjects. It is to be mentioned that the error in this study is defined as the difference between the driven speed of the test subjects and the target speed. A positive error would correspond to the test subject driving too fast, which indicates an under-estimation, whereas a negative error would correspond to driving too slow, indicating an over-estimation. The error is defined in this way to keep the error signs consistent for over- and under-estimation to the previous studies. For the abovementioned questions, corresponding hypotheses are defined:

Hypothesis A:

NH: The test subjects guess the speed correctly within a defined tolerance.

AH: The test subjects under-estimate or over-estimate the speed outside the defined tolerance.

Hypothesis B:

NH: Blur does not have any effects or has negative effects on the perception of the test subjects at the working station while driving.

AH: Blur has positive effects on the perception of the test subjects at the working station while driving.

Hypothesis C:

NH: The additional playback of artificial motor sound together with vibration at the driver's seat does not have any effects or has negative effects on the perception of the test subjects at the working station while driving.

AH: The additional playback of artificial motor sound together with vibration at the driver's seat has positive effects on the perception of the test subjects at the working station while driving.

Hypothesis D:

NH: Blur together with the additional playback of artificial motor sound and vibration at the driver's seat does not have any effects or has negative effects on the perception of the test subjects at the working station while driving.

AH: Blur together with the additional playback of artificial motor sound and vibration at the driver's seat has positive effects on the perception of the test subjects at the working station while driving.

The test subjects are greeted at the beginning of the study. The project of teleoperated vehicles is introduced and a description of the working station is made. The test subjects are asked to answer the first part of the questionnaire and are allowed to drive in the presented setup until they become familiar with the task at hand. It is additionally explained that driving at the working station is achieved through selecting a target speed. This means, that the accelerator pedal is used to increase the target speed and the brake pedal is used to reduce it. When no pedal is actuated, the selected target speed is kept constant and the vehicle travels at this speed. Additionally, it is explained to the test subjects that the velocity limit road signs are used in this study to determine the speed to be driven and not as the upper speed limit. Test subjects are to drive as close as possible to the shown speed.

A between subjects design is selected. Next, the test subjects belonging to the test group are allowed to drive while blur parameters are set. They are presented with a route where the speed is held constant at $60\ \mathrm{km/h}$. The person conducting the test study varies the parameters until the test subject perceives the speed as $60\ \mathrm{km/h}$. This parameter configuration is then used in the study.

Each test person completes each of the abovementioned two routes twice in random order. For the control group, the four runs are completed without any treatment. Test subjects in the test group complete the runs with different combinations: without assistance, blur, artificial motor sound with vibrations at the driver's seat and blur combined with artificial motor sound and vibrations at the driver's seat. These combinations are also permuted for each test subject.

After the completion of the four runs, the test subjects are asked to fill the remaining questions of the questionnaire. Figure 4.15 shows an example of the procedure of the study.

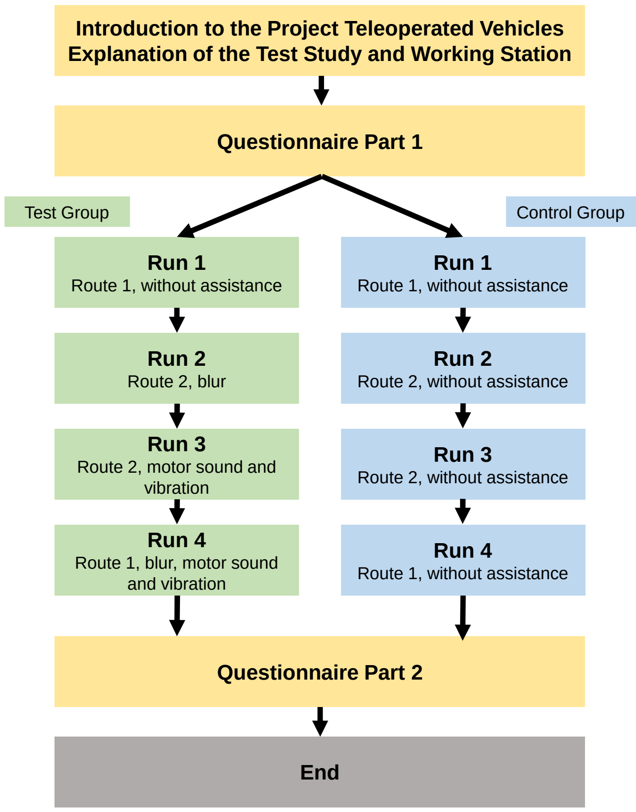

Figure 4.15: Exemplary procedure for the study with test subjects

A total of 32 test subjects participated in the study, consisting of 19 male and 13 female participants. The possession of a class B driving license was a prerequisite. The youngest subject was 19 years old and the eldest 34, with a mean of 23.56 years and standard deviation of 3.18 years. In average, the test subjects held the driving license for 5.5 years and drive in average 5106.6 kilometers each year. 13 test subjects were required to wear glasses when driving and were asked to do so during the study. One of the test persons was excluded from the results since the system crashed during the execution of the test resulting in the incompletion of the test. Nine subjects were assigned to the control group and 22 subjects to the test group.

The results of the comparison between the control group with the test group can be seen in table 4.6 and Figure 4.16.

Table 4.6: Mean guess errors for hypotheses B, C and D (between subjects design)

	Mean without treament	**Mean with treament**	**p-Value**
Blur	6.1230	5.7468	0.6327
Motorsound + Vibration	6.1230	1.4351	$2.503 \cdot 10^{-13}$ ***
Motorsound + Vibration + Blur	6.1230	0.4123	$< 2.2 \cdot 10^{-16}$ ***

* significant (p < 0.05); ** very significant (p < 0.01); *** highly significant (p < 0.001)

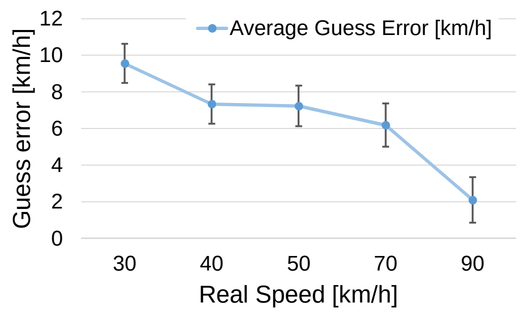

(a) Hypothesis A: Average guess error for different speeds

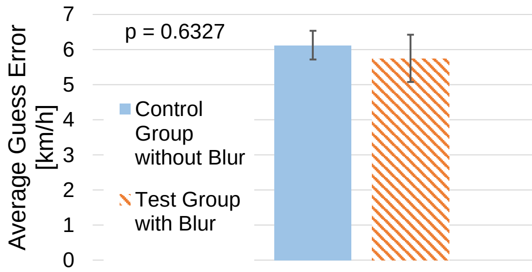

(b) Hypothesis B: Influence of blur on the guess error

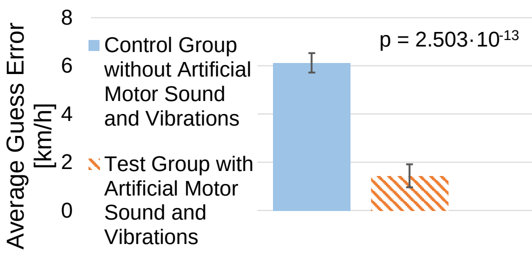

(c) Hypothesis C: Influence of artificial motor sound and vibration at the driver's seat on the guess error

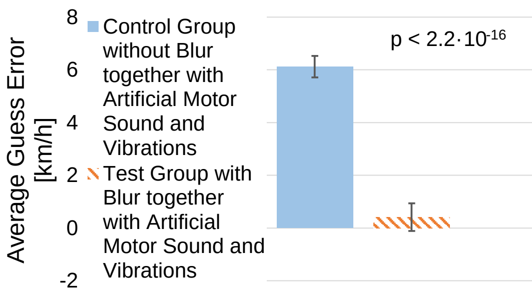

(d) Hypothesis D: Influence of blur combined with artificial motor sound and vibration at the driver's seat on the guess error

Figure 4.16: Guess error comparison between guessing with and without different treatment implemented to influence speed perception (between subjects design)

The tendency towards under-estimating can again be clearly seen in Figure 4.16a for the different speeds. Since this is the case, the null-hypothesis is rejected and the alternative hypothesis that the subjects under- or over-estimate the speed outside the defined tolerance is accepted. This result further corroborates the findings from the previous studies.

In order to compare both groups, a variance analysis is performed to determine if there is a significant difference between the control and the test group. The analysis showed no significant difference between both groups.

According to the results, even though a slight improvement in the speed perception could be seen when using only blur, the improvement is not significant, and therefore, the null hypothesis B cannot be rejected. For both cases where artificial motor sound was used with vibration and where all methods were used, a highly significant improvement could be seen. Thus, the null hypothese C and D are both rejected.

When only looking at the test group to determine the influence of the implemented methods using the comparison between driving with and without treatment (within-subjects design), similar results are obtained. These are shown in table 4.7 and Figure 4.17.

Table 4.7: Mean guess errors for hypotheses B, C and D (within subjects design)

	Mean without treament	**Mean with treament**	**p-Value**
Blur	7.3442	5.7468	0.1021
Motorsound + Vibration	7.3442	1.4351	$1.213 \cdot 10^{-11}$ ***
Motorsound + Vibration + Blur	7.3442	0.4123	$1.55 \cdot 10^{-14}$ ***

* significant (p < 0.05); ** very significant (p < 0.01); *** highly significant (p < 0.001)

Figure 4.17a shows the average guess error of the test subjects without any assistance method, also with a tendency to under-estimate. Results lead to not being able to reject the null hypothesis B because a significant improvement could not be determined. Null hypotheses C and D are rejected, since using artificial motor sound with vibrations and the combination of all methods showed a significant improvement.

With respect to the answers from the questionnaires regarding subjective perception of the influence of the presented methods, only 6 of the 22 test subjects belonging to the test group answered with yes to the question if blur improved their perception. To the other two questions if artificial motor sound combined with vibrations at the driver's seat and if the combination of blur, artificial motor sound and vibrations improved their speed perception, 15 and 18 out of 22 test subjects answered with yes, respectively.

4.5 Discussion

Multiple studies with test persons were conducted to analyze the influence of the proposed methods to improve speed perception of a human operator at the working station. The first conducted study addressed the human visual sense, where test subjects were asked to guess the speed according to pre-recorded videos. Several questions with their corresponding hypotheses were used to analyze the effects. Results showed that there is a tendency to

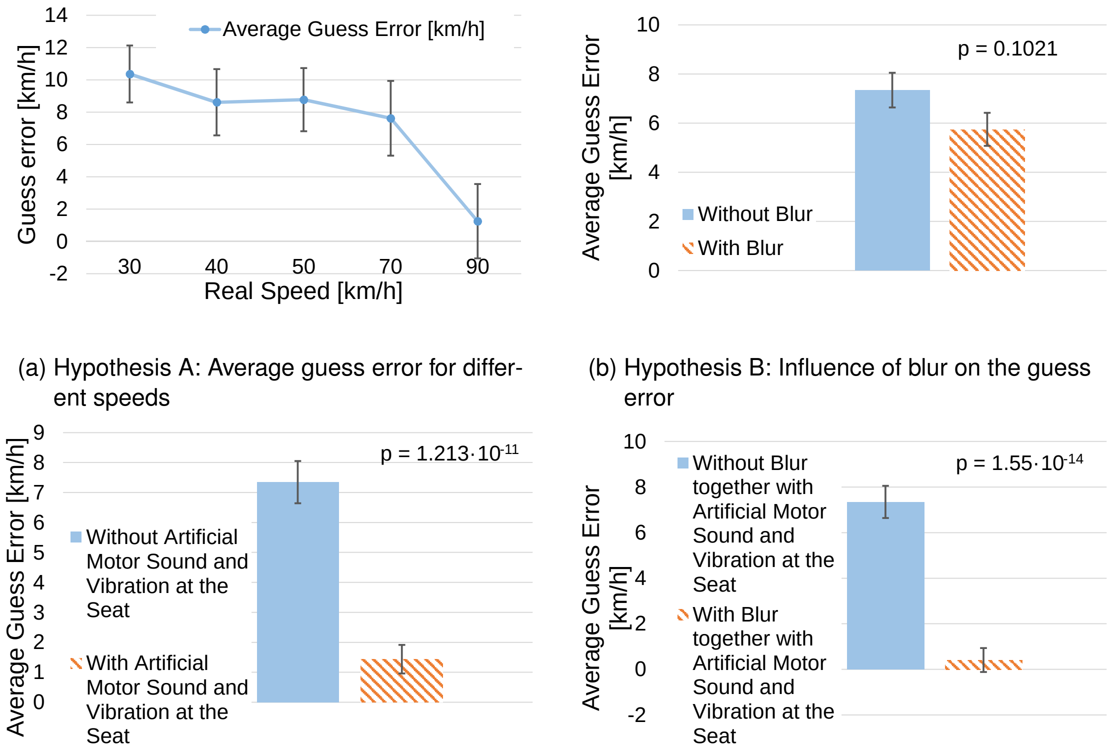

(a) Hypothesis A: Average guess error for different speeds

(b) Hypothesis B: Influence of blur on the guess error

(c) Hypothesis C: Influence of artificial motor sound and vibration at the driver's seat on the guess error

(d) Hypothesis D: Influence of blur combined with artificial motor sound and vibration at the driver's seat on the guess error

Figure 4.17: Guess error comparison between guessing with and without different treatment methods implemented to influence speed perception (within-subjects design)

under-estimate the speed at the working station. It was also possible to quantify the guess error through this study. Furthermore, it was obtained that it is possible to influence speed perception through the learning effect, at least temporarily. This could be of advantage since operators could be taught and especially trained for the application of teleoperated vehicles. This training could be compared to a driving school, where aspirants would have to pass an exam before being allowed to drive teleoperated vehicles. Since the training process would imply practice, it can be expected that certified operators would have a better perception of speed.

Furthermore, it was determined that zoom blur can be further used to improve speed perception. However, it is important to understand the operator's individual perception since at least from the results, no common blur parameters could be determined. So as not to negatively influence the operator, a previous calibration could be done to allow choosing meaningful blur parameters. The usage of zoom blur to influence the speed perception could also be trained before becoming a certified operator. An alternative solution would be establishing the parameters for blur as constants and instruct or train the operators to adapt to these parameters. Since it could be seen that a learning effect is also present, a possibility would be to allow the operators to learn the effect of blur with constant parameters and through enough exercise, improve the speed perception. Nevertheless, caution should be exercised when using blur, since images on the outer ranges will become unclear and could lead to dangerous situations, such as other traffic participants appearing suddenly in these areas.

A second study was conducted in order to address two further human senses that are important for the speed perception, namely the acoustic and haptic senses. Again, questions and corresponding hypotheses were used to study the effects of the proposed methods. A tendency towards under-estimation at the working station could be corroborated. The use of artificial motor sound showed a tendency towards reduction in guessing error, however, from this study, this improvement was not significant. Therefore, it would be advantageous to further analyze the real effect of artificial motor sound on the speed perception. Unfortunately, using only artificial motor sound does not provide information regarding the surroundings of the teleoperated vehicle, such as noises coming from other traffic participants. Transmitting information through a surround recording system in the teleoperated vehicle could further improve the awareness of the operator, since it would be possible to use the acoustic channel to interact with other traffic participants. However, by only providing acoustic information of the own vehicle, it can be expected to provide a better awareness at the working station.

When addressing the haptical sense through vibrations at the driver's seat, a significant improvement could be seen. Through bass shakers it was possible to use a further human sense to improve the awareness of the operator. However, such method presents limitations, since it does not reproduce completely the vehicle's environments. Information such as centrifugal forces, accelerations in longitudinal and lateral direction, etc., cannot be reproduced with only bass shakers.

Furthermore, when combining both human senses through feedback using artificial motor sound and vibrations, and also when combining blur with artificial motor sound and vibrations, highly significant improvements could be determined, showing that these methods can be all combined together and used to improve speed perception.

Since the methods presented have shown a positive influence in the speed perception of the test subjects when looking at the videos, it is important to determine the influence while the test subjects perform the driving task. This was studied in a third study with test persons, where the subjects were asked to drive at specific speeds. Results were presented in section 4.4.3 and showed that the proposed methods are capable of improving the speed perception while driving. When only using blur, however, no significant improvements could be determined. Since a tendency towards a reduction in guess error could be seen, it can be expected that it also has a positive effect. A further study could be conducted where more emphasis is put into parameterizing blur so that each subject has individual parameters throughout the complete spectrum of the driven speeds. Furthermore, some test subjects mentioned that the effect of blur could not be recognized easily since it was applied at the edges. This might be a reason why the results showed no significant improvement, compared to the first study conducted and described in section 4.4.1. When combining artificial motor sound with vibrations and using all presented methods, a significant improvement could be determined, both objectively and subjectively.

An interesting characteristic can be seen in the average guess errors for different speeds when only looking at the videos (figures 4.11a and 4.13a) and when driving (figures 4.16a and 4.17a). It can be noticed that at higher speeds, the guess error becomes smaller when driving. This could be compared to the results in the study conducted by BUBB [Bub77, p. 107]. In the study, speed estimation was compared between drivers and passengers. It was shown that drivers slightly over-estimated the speed at higher speeds. Similar results can be found in the study by RECARTE [Rec96, p. 295], where the error was reduced with increasing speed.

These results showed that the driver highly benefits from the additional information provided through the human senses. Even though the proposed methods are simple and do not completely depict the feedback a normal driver would perceive when physically present in the vehicle, they are still able to help the operator better guess the speed. This is of great importance and would allow the operator to perform his task more accurately.

Furthermore, during the studies, the subjects were asked to estimate the speed without being showed the real speed at any time. During the first study, the learning effect was studied. Test subjects were shown the correct driven speed between subsequent estimations. Results showed that at least temporarily, speed perception could be improved. Therefore, it can be expected that during teleoperation of road vehicles, if the real speed is constantly shown to the operator additionally to the developed methods, the operator would be able to constantly correct himself by looking at the real speed from time to time.

The situation awareness of the operator could probably be further improved through additional feedback. While currently the haptic senses are addressed through vibrations at the driver's seat, it can be expected that a force feedback at the steering wheel would further improve the operator's awareness. This force feedback is normally present due to steering torques, which unfortunately are not available at the working station. However, an artificial force feedback could be implemented according to the vehicle's state [Koc10].

5 Discussion

Sections 3.9 and 4.5 presented a discussion regarding the development of an emergency contingency strategy in case of connection loss and a discussion regarding methods implemented to improve the situation awareness at the operator working station, respectively. Both aspects are important methods to improve the control of teleoperated vehicles and increase the safety. The first aspect mainly addresses problems related to the teleoperated vehicle that is in motion and interacting with the environment, while the second aspect addresses problems related to the human operator sitting at a fixed position detached from the vehicle.

The following sections further discuss aspects relevant to teleoperated vehicles and possible factors that influence the above proposed methods.

5.1 Influence of Emergency Braking Reaction Time

An important aspect to be considered when calculating the "free corridor" is the influence of the time needed to detect the connection loss. Since it is not possible to predict when a connection loss will occur, a possibility for detection is to check for a constant arrival of commands at the vehicle coming from the working station. Nevertheless, some packets could get lost in the transmission, hence using the loss of one single packet to determine if the connection has been lost or not could be critical.

In the current system configuration and implementation, the non-arrival of five subsequent packets are determined as a connection loss. The system has an auto-repeat time of 40 milliseconds, producing a total delay of 200 milliseconds before a loss of connection can be determined. Taking this into consideration, the braking distance increases by an amount of:

$$s_{b,r} = t_r \cdot v \tag{5.1}$$

where $s_{b,r}$ is the braking distance caused by the time t_r until connection loss is detected. The total braking distance then becomes:

$$s_b = \frac{1}{2\kappa} \arcsin({v_0}^2 \cdot \frac{\kappa}{g \cdot \mu_{\max}}) + t_r \cdot v \tag{5.2}$$

and at the maximal allowed curve speed, the braking distance becomes

$$s_b = \frac{v^2}{g \cdot \mu_{\max}} \cdot \frac{\pi}{4} + t_r \cdot v \tag{5.3}$$

When considering the correction factor because of actuator limitations, equations (5.2) and (5.3) become

$$s_b = \frac{1}{K_{\text{actuator}}} \cdot \frac{1}{2\kappa} \arcsin({v_0}^2 \cdot \frac{\kappa}{g \cdot \mu_{\max}}) + t_r \cdot v \tag{5.4}$$

$$s_b = \frac{1}{K_{\text{actuator}}} \cdot \frac{v^2}{g \cdot \mu_{\max}} \cdot \frac{\pi}{4} + t_r \cdot v \tag{5.5}$$

respectively. This should be taken into account when calculating the displayed corridor. Not considering the time needed to detect the connection loss could lead to the vehicle overshooting the predicted braking point, bringing the teleoperated vehicle to a unsafe state.

5.2 Functional Safety Assessment

The "free corridor" is further discussed here using the International Standard ISO 26262, which addresses the functional safety features. This standard is based and adapted from the functional safety standard IEC 61508 for automotive electric and electronic systems. The ISO 26262 is a risk-based safety standard, where the risk of dangerous operational situations is assessed. Further, measures are found to avoid or control the systematic failure and to detect or control random hardware failures and mitigate their effects [Int11]. It basically provides an automotive-specific risk-based approach to determine the integrity levels (Automotive Safety Integrity Levels ASIL) [Int11, p. V Part 3].

In order to perform such an assessment, a detailed description is given and the system boundaries are specified. Through the definition of operation modes and operational situations, relevant combinations of scenarios are developed. Using the previously identified malfunctioning behaviors, hazardous events can be defined. These events are then evaluated using the classes shown in table 5.1, which are divided into three categories: Severity, Probability of Exposure and Controllability.

According to the classes assigned to each of the hazardous events, the ASIL is determined, which ranges from A to D, with A as the lowest and D as the highest safety integrity level. Additionally to the four ASILs, a class QM (quality management) denotes no requirement to comply with ISO 26262 [Int11, p. 10 Part 3]. For a more detailed description and examples of the classes, part 3 of the ISO 26262 provides a good overview [Int11].

The boundaries for the "free corridor" are specified as urban traffic only, since the application of teleoperated road vehicles is set for this scenario. Velocities higher than $50\,\mathrm{km/h}$ are not considered and the analysis is performed using the current configuration of the experimental

Table 5.1: Classes of severity, probability of exposure and controllability used to determine ASIL

Severity **S**		
	S0	No injuries
	S1	Light and moderate injuries
	S2	Severe and life-threatening injuries (survival probable)
	S3	Life-threatening injuries (survival uncertain), fatal injuries
Probability of Exposure **E**		
	E0	Incredible
	E1	Very low probability
	E2	Low probability
	E3	Medium probability
	E4	High probability
Controllability **S**		
	C0	Controllable in general
	C1	Simply controllable
	C2	Normally controllable
	C3	Difficult to control or uncontrollable

vehicle. The assessment was conducted among students and research associates involved in the project. Five operation modes were defined: stand, acceleration, constant velocity, braking, driving on curves. Several malfunctioning behaviors were defined and discussed:

- ESP failure, leading to implausible values used for the calculation of the "free corridor".
- Incorrect estimation or measurement of the coefficient of friction.
- Autobox failure.
- Steering actuator failure.
- Braking actuator (pneumatic system) failure.
- Steering wheel angle sensor failure, giving implausible values.
- ABS failure.
- Insufficient power supply.
- All braking lights defective.
- Following vehicle's distance is too small.
- Cameras failure.
- Operating elements at the working station failure.
- Loss of connection.

The assessment produced an ASIL B for the failure of the autobox and having the following vehicle's distance too small. In the case of autobox failure, probable solutions would be to implement redundant components that are capable of monitoring the functionality of the autobox and if necessary, start an emergency braking. When the following vehicle's distance is too small, that an emergency braking with maximal deceleration could produce a collision, it is important to provide the possibility to calculate the "free corridor" and brake with a smaller deceleration, if the conditions allow it. This is also a reason why ACC systems limit the maximal deceleration [Win09b, pp. 480–482] [Bau02, p. 43]. This could be achieved either manually through the operator when perceiving the vehicle to be too close or automatically, through additional sensors built in the back of the teleoperated vehicle.

With a lower assessment, ASIL A, were the failure of pneumatic braking actuator, the insufficient power supply, all braking lights being defective, the failure of cameras, failure of operating elements at the working station and the loss of connection. Here, solutions would be the introduction of a redundant emergency braking system, the monitoring of the voltage level, using warning lights and providing acoustic signals for other traffic participants, redundant cameras, possibility to simulate a connection loss manually to activate the "free corridor", and redundant mobile connections, respectively.

The results of the functional safety assessment only gives a rough general understanding of the current system combined with the "free corridor". A more extensive and detailed analysis should be conducted to achieve a more complete overview of the system and its functional safety aspects.

5.3 Risk Awareness

Additionally to speed perception, it is important for the operator to be able to recognize the limits of the system. As presented before, the "free corridor" shows limitations in its application, especially noticeable when driving in suboptimal environment conditions. For the operator, it is difficult if not impossible to accurately know the current road conditions, especially the coefficient of friction that determines the maximal possible deceleration. Therefore, a possibility would be to provide the operator with additional information that helps him to better assess these conditions. The limitations of the safety concept are known and whenever the driver exceeds them, a warning could be issued. This excess could be from driving at too high velocities or from increasing the steering wheel angle too fast. Furthermore, a constant feedback could be always provided so that the operator is capable of adapting his driving behavior constantly. A possible implementation could be as shown in 5.1. The operator drives along a road, however, road conditions may vary but remain unknown to the driver. For the same driving states (e.g. velocity, lateral acceleration, steering wheel angle or rate, etc.), two possibilities are shown in figures 5.1a and 5.1b depending on current available coefficient of friction. For the case of a dry road surface, the indicators would remain in the green area, showing no over-crossing of the limits (Figure 5.1a). On the other hand, because of humid or wet surfaces, the indicators could show a critical situation where the "free corridor" would not be able to guarantee a controlled braking (5.1b). This could induce the driver to notice the high risk and correspondingly, reduce the driving speed. This information or awareness could not be obtained or deduced only from driving states by the driver.

Furthermore, an interesting question would be to analyze if showing the trajectory that the vehicle would follow in the near future rather than the braking trajectory would help the oper-

(a) Operator interface with additional information for the operator for a non-critical situation

(b) Operator interface with additional information for the operator for a critical situation

Figure 5.1: Operator interface with additional information for the operator to assess current driving situations

ator complete the driving task better or not. It could be calculated for example for a constant amount of time. This idea could be compared to the concept presented by CHUCHOLOWSKI [Chu15], where the position of the vehicle is predicted according to the current time delay. This produces a better orientation and helps the driver to further improve the situation awareness.

5.4 Integration in the Research Group

Sections 2.5.2 and 2.5.3 presented two different approaches developed at the Institute of Automotive Technology to address the problem regarding time delays in the communications [Gna15] [Gna12b] [Chu15] [Chu13b] [Chu13a], which was described in section 3.2. Each of the two concepts possesses advantages and disadvantages.

On one hand, trajectory-based driving also provides an emergency concept for the case of a connection loss. This is because the vehicle would come to a stop at the end of the already planed and confirmed trajectory if no new segment was added afterwards. However, a large visual range is needed due to the anticipatory planing of the following segments and a highly-accurate positioning system, such as the RT3003, or a good odometry is needed to guarantee the correct control of the vehicle's position relative to the planed trajectory.

On the other hand, driving with predictive display also allows overcoming time delays. For the prediction of the vehicle's position, no additional sensors apart from the ones used in standard series vehicles are needed. Due to the slighter anticipatory planing needed, the visual range needed is not critical. However, no emergency concept is provided in the case of a connection loss.

The "free corridor" in its current state does not directly address the problem with time delays in the communication. Therefore, a combination of "Predictive Display" and "free corridor" would be meaningful. The predicted states of the vehicle are used for the calculation of the "free corridor". Both approaches would then complement each other, since time delays and an emergency concept would be present. A combination between trajectory-based driving and the "free corridor" would at this point be of no great meaning, since trajectory-based driving already includes an emergency concept. Figure 5.2 shows an idea of how the combination of predictive display and "free corridor" could look like. The predictive display is displayed using a frame to depict the current position of the front bumper. It is additionally complemented with ovals representing the tire contact points. Attached to the predictive display, the "free corridor" can be seen. It is calculated using the predicted vehicle states under the influence of time delays.

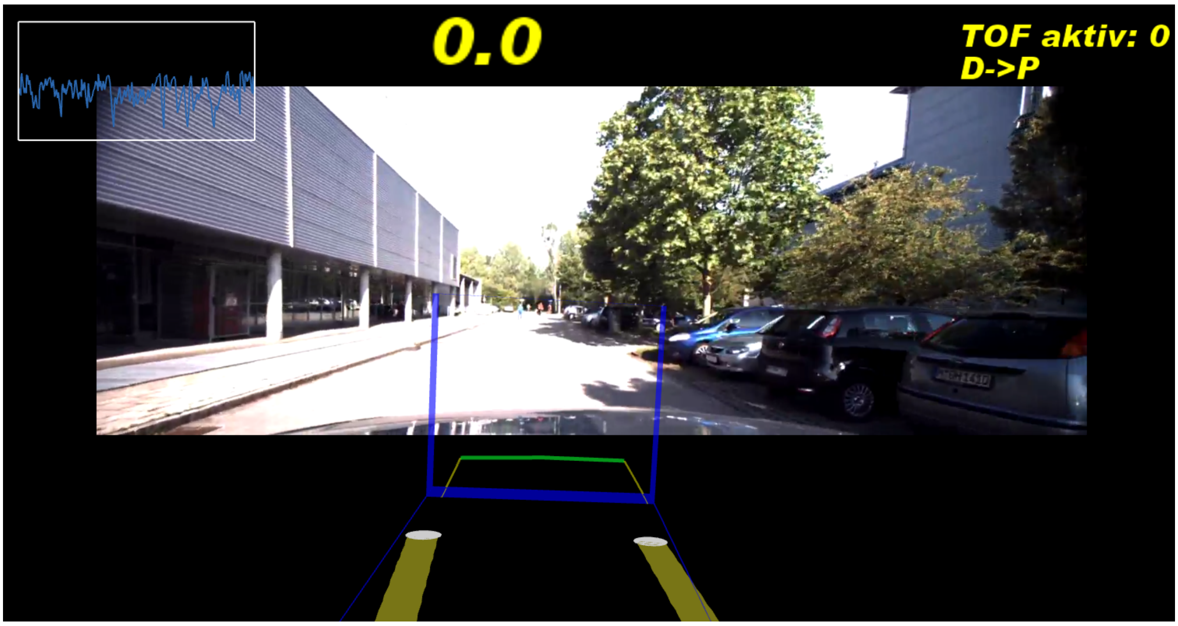

Figure 5.2: Interface at the working station showing the free corridor in combination with predictive display

However, it is still to be analyzed to what extent this combination is helpful for the operator and if it would cause any negative effects.

6 Summary and Outlook

6.1 Summary

The dream to achieve unmanned road vehicles is not a recent one. The individual mobility is changing and new concepts such as car-sharing and provision of vehicles are becoming more and more common in the society. Not only providers of such services could profit from unmanned vehicles, but also society itself. A higher efficiency and safety could be achieved through such ideas. Autonomous vehicles that are capable of moving completely independent of a human driver pose an attractive way to achieve this dream. Even though great progress has been made in the last decades towards autonomous vehicles, there are still limitations that prevent the deployment of such vehicles in public traffic.

The teleoperation of road vehicles proposes a solution to this problem in the near future. Teleoperation is known from the field of robotics and has been proven to be meaningful in situations where the task was too complex for complete automation but where the human being should not or could not be physically present [Win00, p. 148]. Autonomous vehicles in urban scenarios can be categorized as such a scenario. For teleoperated systems, different control concepts can be used, such as the concept for indirect control proposed by GNATZIG [Gna15], or the conventional direct control, where the signals are used directly to control the teleoperated system and the operator receives real-time feedback.

The goal of this dissertation was to develop and analyze methods to improve the control of teleoperated systems using direct control. To achieve this, two fundamental problems when dealing with teleoperated systems were addressed: First, the possibility of a connection loss between the working station and the teleoperated vehicle and therefore, the necessity to develop an emergency contingency concept to ensure the safe state of the vehicle at all times. Secondly, the physical separation of the operator at the working station and the teleoperated vehicle, which greatly restricts the available information as feedback, thus showing the necessity to provide a better situation awareness to improve performance.

An emergency strategy concept was presented, analyzed and discussed. This concept is called the "free corridor" and consists of a predicted trajectory which the vehicle would follow when a loss of connection is detected and an emergency braking maneuver was initiated. The operator is responsible of keeping this corridor free of obstacles at all times, thus guaranteeing a controlled braking of the vehicle to a safe state. This corridor is calculated according to the present vehicle states, relying on standard vehicle sensors. The concept is implemented in the simulation using the framework DYNA4 and tested in different scenarios using different control strategies. After validation of the concept in the simulation, the concept was carried over to the experimental vehicle. Again, it was tested in different scenarios using multiple control strategies. On the working station, the trajectory was shown directly to the operator. Results showed the feasibility of this concept and the possibility to guarantee a safe state of the vehicle in case of a connection loss. However, there are some aspects to be considered: The "free corridor" calculates the braking distance using the maximal possible deceleration, as described in section 3.5.4. According to the actuators available in the experimental vehicle, an actuator correction factor might be needed to determine the braking distance, as explained in section 3.8.1.2. Furthermore, the time to detect the connection loss needs to be considered, as discussed in section 5.1. This needed time would increase the length of the corridor, and if not considered, it could lead to an unsafe state, since the braking distance would not be realistic. Considering all these points, a safe braking can be achieved so that teleoperated vehicles can be driven safely reducing the possibility of accidents.

Additionally, to address the problem of lack of situation awareness at the working station, simple methods were implemented and studied so as to influence the operator's speed perception. Three human senses that influence speed perception were addressed: visual, acoustic and haptic senses. The commonly used blur method to create a feeling of speed was implemented and studied through test persons. For the acoustic and the haptic senses, an artificial motor sound was created using current engine load and revolutions. This source was used in combination with an amplifier module and two bass-shakers integrated in the driver's seat to produce vibrations. Again, the influence of these methods on speed perception was studied with test persons. These methods were tested both for test persons only seeing pre-recorded videos taken at specific speeds and for test persons driving themselves. Results showed an improvement in the speed perception of the test subjects. These studies showed the possibility to positively influence the driver and, therefore, improving the operator's own situation awareness. However, it is important to keep in mind that these simple methods do not provide information regarding the direct environment, such as sounds coming from other traffic participants, or centrifugal forces and therefore, these methods are to be used with care.

Teleoperation using direct control provides a temporary solution to unmanned vehicles. However, teleoperation could be difficult and often problematic for the operator. This work proposes solutions to increase the performance and safety of teleoperated vehicles, providing the operator with ways of completing the driving task in a successful way.

6.2 Outlook

The present dissertation presented two important aspects to improve the control of teleoperated road vehicles. These two concepts were studied and discussed separately. However, the impact on the driving performance when applying both simultaneously is still to be examined. It would be interesting to test and evaluate how much better the operators would drive when having the assistance of the "free corridor" together with the methods proposed for the improvement of situation awareness.

Additionally, the free corridor was developed with the assumption that after connection loss, the teleoperated vehicle would follow a predetermined trajectory. It was assumed that no other dynamic obstacles, such as pedestrians or other traffic participants, will enter this trajectory after connection loss, thus, guaranteeing that a safe state can be reached. Nevertheless, this is not always the case. It will be necessary to develop systems that are able to support the free corridor in such cases, acting autonomously. Such systems would theoretically be easier to implement compared to other assistance systems, since the exact trajectory that the vehicle would follow is already known.

Here in this work, the concept of teleoperated road vehicles was developed and tested on an experimental vehicle on restricted areas, where no other traffic participants were present. A detailed analysis regarding requirements and problems for such a concept is essential before it can be made available and approved for public roads. Further testings regarding the safety concept are also important to ensure its functionality. Especially a more detailed analysis of the complete system and the "free corridor" should be completed regarding functional safety, as explained in section 5.2. The proposed representation of the predicted trajectory at the working station could be further studied regarding ergonomics and driver's load when presented with extra information. Speed perception is only one of the factors that influence the situation awareness of an operator. Other aspects could be analyzed and solutions proposed to help the operator.

Finally, there are legal aspects that need to be clarified before teleoperated vehicles can become part of daily traffic, such as liability or redundancy of components. Requirements need to be clearly defined and kept. Some important legal aspects regarding teleoperated and autonomous vehicles are discussed in [Lut12b] [Lut13].

List of Figures

List of Tables

Bibliography

[AKK14] AKKA RESEARCH: *Link & Go*. URL: http://research.akka.eu/innovation/linkandgo.php, retrieved on 2014/12/04.

[Abe09] ABENDROTH, B. and BRUDER, R.: *Die Leistungsfähigkeit des Menschen für die Fahrzeugführung: Chapter 1*. In: *Handbuch Fahrerassistenzsysteme: Grundlagen, Komponenten und Systeme für aktive Sicherheit und Komfort*. Ed. by WINNER, H.; HAKULI, S., and WOLF, G. ATZ/MTZ-Fachbuch. Vieweg + Teubner, 2009, pp. 4–14.

[Ack11] ACKER, A.: *Anwendungspotential von Telepräsenz- und Teleaktionssystemen für die Präzisionsmontage*. PhD thesis. München: Technische Universität München, 2011.

[Ama14] AMAZON: *Lautsprecher Bodyshaker 100 Watt*. URL: http://www.amazon.de/Zisaline-Lautsprecher-Bodyshaker-100-Watt/dp/B002LQAHPE, retrieved on 2014/11/06.

[Ans11] ANSORGE, U. and LEDER, H.: *Wahrnehmung und Aufmerksamkeit*. VS Verlag fur Sozialwissenschaften GmbH, 2011.

[Ant90] ANTSAKLIS, P. J.; PASSINO, K. M., and WANG, S. J.: *An Introduction to Autonomous Control Systems*. In: *Intelligent Control, 1990. Proceedings., 5th IEEE International Symposium on*. Philadelphia, PA, 1990, 21–26 vol.1. DOI: 10.1109/ISIC.1990.128434.

[App10] APPELQVIST, P.; KNUUTTILA, J., and AHTIAINEN, J.: *Mechatronics Design of an Unmanned Ground Vehicle for Military Applications: Chapter 15*. In: *Mechatronic Systems Applications*. Ed. by DONATO DI PAOLA, ANNALISA MILELLA and CICIRELLI, G. Helsinki: InTech, 2010. DOI: 10.5772/8919.

[Ara82] ARAND, W. and KUPKE, P.: *Anforderungen an Fahrsimulatoren zur Untersuchung des Fahrer-Fahrzeug-Verhaltens sowie der verkehrstechnisch relevanten Eigenschaften von Straßenentwürfen*. Forschung Straßenbau und Straßenverkehrstechnik. Bundesminister für Verkehr, Abt. Straßenbau, 1982.

[Arn63] ARNOLD, J. E. and BRAISTED, P. W.: *Design and evaluation of a predictor for remote control systems operating with signal transmission delays*. Washington, D.C: National Aeronautics and Space Administration, 1963.

[Aud13] AUDI: *Elektroniktrends des kommenden Jahrzehnts - Audi auf der CES 2013*. URL: https://www.audi-mediaservices.com/publish/ms/content/de/public/hintergrundberichte/2013/01/08/audi_praesentiert.-download.gid-oeffentlichkeit.acq/qual-DownloadFileList.Single.DownloadFile.0001.File/BasisInfoCES0113.pdf, retrieved on 2014/02/26.

[BMW13] BMW: *Mit dem BMW hochautomatisiert auf den Autobahnen Europas*. URL: https://www.press.bmwgroup.com/deutschland/download.html?textId=168141&textAttachmentId=208915, retrieved on 2014/02/26.

[Bau02] BAUER, H., ed.: *Adaptive Fahrgeschwindigkeitsregelung ACC*. 1st ed. Gelbe Reihe Ausgabe 2002. Technische Unterrichtung. Sicherheits- und Komfortsysteme. Stuttgart: Robert Bosch GmbH, 2002.

[Bau06] BAUMANN, M. R. K.; PETZOLDT, T., and KREMS, J. F.: *Situation Awareness beim Autofahren als Verstehensprozess*. In: MMI Interaktiv 2006.

[Ben14] BENGLER, K. et al.: *Three Decades of Driver Assistance Systems: Review and Future Perspectives*. In: Intelligent Transportation Systems Magazine, IEEE 4, pp. 6–22, 2014.

[Ber04] BERESTESKY, P.; CHOPRA, N., and SPONG, M. W.: *Discrete Time Passivity in Bilateral Teleoperation over the Internet*. In: *Robotics and Automation, 2004. Proceedings. ICRA '04. 2004 IEEE International Conference on*. Vol. 5. New Orleans, LA, USA, 2004, 4557–4564 Vol.5. DOI: 10.1109/ROBOT.2004.1302436.

[Ber08] BERGER, C. and RUMPE, B.: *Autonomes Fahren – Erkenntnisse aus der DARPA Urban Challenge (Autonomous Driving – Insights from the DARPA Urban Challenge)*. In: it - Information Technology 4, pp. 258–264, 2008.

[Ber75] BERTHOZ, A.; PAVARD, B., and YOUNG, L. R.: *Perception of linear horizontal self-motion induced by peripheral vision (linearvection) basic characteristics and visual-vestibular interactions*. In: Experimental Brain Research 5, pp. 471–489, 1975.

[Bir05] BIRAL, F.; DA LIO, M., and BERTOLAZZI, E.: *Combining safety margins and user preferences into a driving criterion for optimal control-based computation of reference maneuvers for an ADAS of the next generation*. In: *Intelligent Vehicles Symposium, 2005. Proceedings. IEEE*. Las Vegas, NV, 2005, pp. 36–41. DOI: 10.1109/IVS.2005.1505074.

[Boe06] BOERNER, M.: *Modellierung, Analyse und Simulation der Fahrzeugquerdynamik: Chapter 3*. In: *Fahrdynamik-Regelung: Modellbildung, Fahrerassistenzsysteme, Mechatronik*. Ed. by ISERMANN, R. Wiesbaden: Vieweg, 2006, pp. 47–70.

[Bor05] BORTZ, J.: *Statistik für Human- und Sozialwissenschaftler*. 6., vollst. überarb. und aktualisierte Aufl. Springer-Lehrbuch. Berlin, Heidelberg, and New York: Springer, 2005.

[Bou10] BOUZOURAA, S.; REICHEL, M.; HOFMANN, M.; SIEDERSBERGER, K.-H., and SIEGEL, A.: *Grundlegende Architekturentscheidungen für hochautomatisierte Fahrerassistenzsysteme am Beispiel einer Aktiven Gefahrenbremsung*. In: *4. Tagung Sicherheit durch Fahrerassistenz*. München, 2010.

[Bou13] BOUGUET, J.-Y.: *Camera Calibration Toolbox for Matlab*. URL: http://www.vision.caltech.edu/bouguetj/calib_doc/index.html, retrieved on 2014/02/27.

[Bub01] BUBB, H.: *Haptik im Kraftfahrzeug: Chapter 10*. In: *Kraftfahrzeugführung*. Ed. by JÜRGENSOHN, T. and TIMPE, K.-P. Springer, 2001, pp. 155–175.

[Bub03] BUBB, H.: *Fahrerassistenz primär ein Beitrag zum Komfort oder für die Sicherheit*. In: *Der Fahrer im 21. Jahrhundert. Anforderungen, Anwendungen, Aspekte für Mensch-Maschine-Systeme*. Braunschweig, 2003, pp. 25–46.

[Bub75] BUBB, H.: *Untersuchung über die Anzeige des Bremsweges im Kraftfahrzeug*. PhD thesis. München: Technische Universität München, 1975.

[Bub77] BUBB, H.: *Analyse der Geschwindigkeitswahrnehmung im Kraftfahrzeug*. In: Zeitschrift für Arbeitswissenschaft 2, pp. 103–112, 1977.

[Bun13] BUNDESMINISTERIUM DER JUSTIZ: *Straßenverkehrs-Ordnung (StVO)*. 2013. URL: http://www.gesetze-im-internet.de/bundesrecht/stvo_2013/gesamt.pdf.

[Bux94] BUXTON, W.; GAVER, W., and BLY, S.: *Auditory Interfaces: The Use of Non-Speed Audio at the Interface*. URL: http://www.billbuxton.com/Audio.TOC.html, retrieved on 2014/02/20.

[Can09] CANZLER, W. and KNIE, A.: *Grüne Wege aus der Autokrise: Vom Autobauer zum Mobilitätsdienstleister ; ein Strategiepapier*. Berlin: Heinrich-Böll-Stiftung, 2009.

[Cav01] CAVALLO, V.; COLOMB, M., and DORÉ, J.: *Distance Perception of Vehicle Rear Lights in Fog*. In: Human Factors: The Journal of the Human Factors and Ergonomics Society 3, pp. 442–451, 2001.

[Cha03] CHATZIASTROS, A.: *Visuelle Kontrolle der Lokomotion*. PhD thesis. Tübingen: Justus-Liebig-Universität Gießen, 2003.

[Cha92] CHARWAT, H. J.: *Lexikon der Mensch-Maschine-Kommunikation*. München: Oldenbourg, 1992.

[Cho03] CHOPRA, N.; SPONG, M. W.; HIRCHE, S., and BUSS, M.: *Bilateral teleoperation over the internet: the time varying delay problem*. In: *American Control Conference, 2003. Proceedings of the 2003*. Vol. 1. Denver, CO, USA, 2003, pp. 155–160. DOI: 10.1109/ACC.2003.1238930.

[Chu13a] CHUCHOLOWSKI, F.; SAUER, M., and LIENKAMP, M.: *Evaluation of Display Methods for the Teleoperation of Road Vehicles*. In: *9th International Conference on Intelligent Unmanned Systems*. Jaipur, 2013.

[Chu13b] CHUCHOLOWSKI, F.; BUECHNER, S.; REICHENEDER, J., and LIENKAMP, M.: *Prediction Methods for Teleoperated Road Vehicles*. In: *Conference on Future Automotive Technology*. Ed. by LIENKAMP, M. München, 2013.

[Chu13c] CHUCHOLOWSKI, F.; GNATZIG, S.; TANG, T.; HOSSEINI, A., and LIENKAMP, M.: *Teleoperiertes Fahren Aktuelle Entwicklungen*. In: *6. Tagung Fahrerassistenz*. München, 2013.

[Chu14] CHUCHOLOWSKI, F.; TANG, T., and LIENKAMP, M.: *Teleoperiertes Fahren Sichere und robuste Datenverbindungen*. In: ATZelektronik 1, pp. 60–63, 2014.

[Chu15] CHUCHOLOWSKI, F.: *Eine vorausschauende Anzeige zur Teleoperation von Straßenfahrzeugen - Beseitigung von Zeitverzögerungseffekten im Fahrer-Fahrzeug Regelkreis*. (expected to be published in 2015). PhD thesis. München: Technische Universität München, 2015.

[Coh91] COHEN, A. S. and HIRSIG, R.: *The Role of Foveal Vision in the Process of Information Input*. In: *Vision in vehicles III*. Ed. by GALE, A. G. Amsterdam, New York, and New York, N.Y., U.S.A: North-Holland and Sole distributors for the U.S.A. and Canada, Elsevier Science Pub. Co., 1991.

[Con06] CONCHILLO, A.; RECARTE, M. A.; NUNES, L., and RUIZ, T.: *Comparing speed estimations from a moving vehicle in different traffic scenarios: absence versus presence of traffic flow*. In: The Spanish journal of psychology 1, pp. 32–37, 2006.

[Con13] CONTINENTAL: *Continental und BMW Group entwickeln gemeinsam hochautomatisiertes Fahren für die Autobahn*. URL: https://www.conti-online.com/www/presseportal_com_de/themen/pressemitteilungen/1_topics/pr_2013_02_26_bwm_de.html, retrieved on 2014/02/27.

[Cor04] CORRIDORI, C. and ZANIN, M.: *High curvature two-clothoid road model estimation*. In: *Intelligent Transportation Systems, 2004. Proceedings. The 7th International IEEE Conference on*. Washington, D.C: IEEE, 2004, pp. 630–635. DOI: 10.1109/ITSC.2004.1398974.

[Dar99] DARKEN, R. P.; BERNATOVICH, D.; LAWSON, J. P., and PETERSON, B.: *Quantitative Measures of Presence in Virtual Environments: The Roles of Attention and Spatial Comprehension*. In: CyberPsychology & Behavior 4, pp. 337–347, 1999.

[Dee14] DEEP OCEAN ENGINEERING: URL: http://www.deepocean.com/index.php, retrieved on 2014/03/25.

[Dem04] DEML, B.: *Telepräsenzsysteme: Gestaltung der Mensch-System-Schnittstelle*. PhD thesis. Neubiberg: Universität der Bundeswehr München, 2004.

[Deu94] DEUTSCHES INSTITUT FÜR NORMUNG E.V.: *DIN 70000*. 1994.

[Dic05] DICKMANNS, E. D.: *Vision: Von Assistenz zum Autonomen Fahren*. In: *Fahrerassistenzsysteme mit maschineller Wahrnehmung*. Ed. by MAURER, M. and STILLER, C. Berlin: Springer, 2005, pp. 203–237.

[Dic95] DICKMANNS, E. D.: *Performance improvements for autonomous road vehicles*. In: *Proceedings of International Conference on Intelligent Autonomous Systems (IAS-4)*. Karlsruhe, 1995, pp. 2–14.

[Die09] DIELS, C. and PARKES, A. M.: *Geometric Field Of View Manipulations Affect Perceived Speed in Driving Simulators*. In: *Road Safety and Simulation 2009*. Paris, 2009.

[Die11] DIERMEYER, F.; GNATZIG, S.; CHUCHOLOWSKI, F.; TANG, T., and LIENKAMP, M.: *Der Mensch als Sensor - Der Weg zum teleoperierten Fahren*. In: *11. Braunschweiger Symposium AAET*. Braunschweig, 2011.

[Dol05] DOLLENTE, T.: *Cell Breathing*. URL: http://searchmobilecomputing.techtarget.com/definition/cell-breathing, retrieved on 2014/03/27.

[Don82] DONGES, E.: *Aspekte der Aktiven Sicherheit bei der Führung von Personenkraftwagen.pdf*. In: Automobil-Industrie pp. 183–190, 1982.

[Don99] DONGES, E.: *A Conceptual Framework for Active Safety in Road Traffic*. In: Vehicle System Dynamics 2-3, pp. 113–128, 1999.

[End01] ENDSLEY, M. R.: *Designing for Situation Awareness in Complex System*. In: *Proceedings of the 2nd international workshop on symbiosis of humans, artifacts and environment*. Kyoto, 2001.

[End12] ENDSLEY, M. R. and JONES, D. G.: *Designing for Situation Awareness: An Approach to User-Centered Design*. 2nd ed. CRC Press, 2012.

[End88] ENDSLEY, M. R.: *Situation awareness global assessment technique (SAGAT)*. In: *Aerospace and Electronics Conference, 1988. NAECON 1988., Proceedings of the IEEE 1988 National*. Dayton, OH, 1988, 789–795 vol.3.

[End95] ENDSLEY, M. R.: *Toward a theory of situation awareness in dynamic systems*. In: Human Factors: The Journal of the Human Factors and Ergonomics Society 1, pp. 32–64, 1995.

[End97] ENDSLEY, M. R. and JONES, W. M.: *Situation Awareness Information Dominance & Information Warfare*. 1997. URL: http://oai.dtic.mil/oai/oai?verb=getRecord&metadataPrefix=html&identifier=ADA347166.

[Eva70] EVANS, L.: *Speed Estimation from a Moving Automobile*. In: Ergonomics 2, pp. 219–230, 1970.

[Fen04] FENNER, W.; NAUMANN, P., and TRINCKAUF, J.: *Bahnsicherungstechnik*. 2nd ed. Erlangen: Publicis Publishing, 2004.

[Fer64] FERRELL, W. R.: *Remote manipulation with transmission delay*. PhD thesis. Massachusetts Institute of Technology, 1964.

[Fer67] FERRELL, W. R. and SHERIDAN, T. B.: *Supervisory control of remote manipulation*. In: Spectrum, IEEE 10, pp. 81–88, 1967.

[Fis09] FISCHER, T.; BUTZ, T.; EHMANN, M., and IRMSCHER, M.: *Fahrermodellierung für Fahrdynamik und Verbrauchsberechnungen*. In: *Fahrermodellierung in Wissenschaft und Wirtschaft, Fortschritt-Berichte VDI, Reihe 22 Mensch-Maschine-Systeme, Nr. 28*. Mensch-Maschine-Systeme. 2009.

[Fit51] FITTS, P. M., ed.: *Human Engineering for an Effective Air-Navigation and Traffic-Control System*. 1951.

[Fle11] FLEMISCH, F. et al.: *Design of Human Computer Interfaces for Highly Automated Vehicles in the Eu-project HAVEit*. In: *Proceedings of the 6th International Conference on Universal Access in Human-computer Interaction: Context Diversity - Volume Part III*. UAHCI'11. Berlin, Heidelberg: Springer-Verlag, 2011, pp. 270–279.

[Fon01a] FONG, T.: *Collaborative Control: A Robot-Centric Model for Vehicle Teleoperation*. PhD thesis. Pittsburg, PA: Carnegie Mellon University, 2001.

[Fon01b] FONG, T.; THORPE, C. E., and BAUR, C.: *Advanced Interfaces for Vehicle Teleoperation: Collaborative Control, Sensor Fusion Displays, and Remote Driving Tools*. In: Autonomous Robots 1, pp. 77–85, 2001.

[Fon01c] FONG, T. and THORPE, C. E.: *Vehicle Teleoperation Interfaces*. In: Autonomous Robots 1, pp. 9–18, 2001.

[GIM13] GIMP: *Motion Blur - GIMP User Manual: Chapter 2.5*. URL: http://docs.gimp.org/en/plug-in-mblur.html, retrieved on 2013/04/02.

[Gam14] GAME REACTOR: *Shift 2*. URL: http://www.gamereactor.de/media/93/shift2_239378b.jpg, retrieved on 2014/11/06.

[Gas12] GASSER, T. M. et al.: *Rechtsfolgen zunehmender Fahrzeugautomatisierung*. Bergisch Gladbach, 2012. URL: http://trid.trb.org/view.aspx?id=1217277.

[Gav86] GAVER, W.: *Auditory Icons: Using Sound in Computer Interfaces*. In: Human-Computer Interaction 2, pp. 167–177, 1986.

[Gen14] GENERAL ATOMICS AERONAUTICALS: *Predator UAS*. URL: http://www.ga-asi.com/products/aircraft/predator.php, retrieved on 2014/03/25.

[Ger02] GERSTER, B.; WALZ, F.; MUSER, M., and NIEDERER, P.: *Aktive und passive Fahrzeugsicherheit - Teilprojekt zu den Grundlagen für eine Strassenverkehrssicherheitspolitik des Bundes (VESIPO)*. Bern, 2002. URL: http://www.bfu.ch/German/strassenverkehr/viasicura/Documents/Fahrzeugsicherheit.pdf.

[Gib38] GIBSON, J. J. and CROOKS, L. E.: *A Theoretical Field-Analysis of Automobile-Driving*. In: The American Journal of Psychology 3, p. 453, 1938.

[Gib79] GIBSON, J. J.: *The Ecological Approach to Visual Perception*. Houghton Mifflin Company, 1979.

[Gna12a] GNATZIG, S.; HAAS, E., and LIENKAMP, M.: *Die Teleoperation als Ansatz zur fahrerlosen Fahrzeugführung*. In: *5. Tagung Fahrerassistenz*. München, 2012.

[Gna12b] GNATZIG, S.; SCHULLER, F., and LIENKAMP, M.: *Human-machine interaction as key technology for driverless driving - A trajectory-based shared autonomy control approach*. In: *2012 IEEE RO-MAN: The 21st IEEE International Symposium on Robot and Human Interactive Communication*. Paris: IEEE, 2012, pp. 913–918. DOI: 10.1109/ROMAN.2012.6343867.

[Gna13] GNATZIG, S.; CHUCHOLOWSKI, F.; TANG, T., and LIENKAMP, M.: *A System Design for Teleoperated Road Vehicles*. In: *ICINCO2013, 10th International Conference on Informatics in Control, Automation and Robotics*. Vol. 2. Reykjavik, 2013, pp. 231–238.

[Gna15] GNATZIG, S.: *Trajektorienbasierte Teleoperation von Straßenfahrzeugen auf Basis eines Shared-Control-Ansatzes*. (expected to be published in 2015). PhD thesis. München: Technische Universität München, 2015.

[Goe08] GOEBL, M. et al.: *Design and capabilities of the Munich Cognitive Automobile*. In: *Intelligent Vehicles Symposium (IV), 2008 IEEE*. Eindhoven, 2008, pp. 1101–1107.

[Goe09] GOEBL, M.: *Eine realzeitfähige Architektur zur Integration kognitiver Funktionen*. PhD thesis. München: Technische Universität München, 2009.

[Gol02] GOLDSTEIN, E. B.: *Wahrnehmungspsychologie*. 2. dt. Aufl., 6. amerikanische Auflage. Spektrum Lehrbuch. Heidelberg [u.a.]: Spektrum, Akad. Verl., 2002.

[Gol10] GOLDSTEIN, E. B.: *Sensation and perception*. 8th ed. PSY 385 Perception Series. Wadsworth Cengage Learning, 2010.

[Goo07] GOODRICH, M. A. and SCHULTZ, A. C.: *Human-Robot Interaction: A Survey*. In: Foundations and Trends in Human-Computer Interaction 3, pp. 203–275, 2007.

[Gri09] GRIP, H. F.; IMSLAND, L.; JOHANSEN, T. A.; KALKKUHL, J. C., and SUISSA, A.: *Vehicle Sideslip Estimation: Design, Implementation, and Experimental Validation*. In: Control Systems, IEEE 5, pp. 36–52, 2009.

[Gro13] GROVER, C. et al.: *Automated emergency brake systems: Technical requirements, costs and benefits*. In: TRL Limited 2013.

[Hac82] HACKENBERG, U. and HEISSING, B.: *Die fahrdynamischen Leistungen des Fahrer-Fahrzeug-Systems im Straßenverkehr.pdf*. In: ATZ - Automobiltechnische Zeitschrift pp. 341–345, 1982.

[Ham00] HAMMETT, S. T.; THOMPSON, P. G., and BEDINGHAM, S.: *The dynamics of velocity adaptation in human vision*. In: Current Biology 18, pp. 1123–1126, 2000.

[Han11] HANNING, T.: *High Precision Camera Calibration*. Wiesbaden: Vieweg + Teubner Verlag, 2011.

[Har06] HART, S. G.: *Nasa-Task Load Index (NASA-TLX); 20 Years Later*. In: Proceedings of the Human Factors and Ergonomics Society Annual Meeting 9, pp. 904–908, 2006.

[Heb61] HEBENSTREIT, B.: *Grundzüge Einer Verkehrspsychologie*. Berlin, Heidelberg: Springer Berlin Heidelberg, 1961. DOI: 10.1007/978-3-642-47659-4.

[Hee05] HEERS, R.: *"Being There" Untersuchungen zum Wissenserwerb in virtuellen Umgebungen*. PhD thesis. Tübingen: Eberhard-Karls-Universität Tübingen, 2005.

[Hei08] HEISSING, B. and ERSOY, M., eds.: *Fahrwerkhandbuch: Grundlagen, Fahrdynamik, Komponenten, Systeme, Mechatronik, Perspektiven*. 2nd ed. Vieweg + Teubner Verlag, 2008.

[Hei11] HEISSING, B.; ERSOY, M., and GIES, S., eds.: *Fahrwerkhandbuch: Grundlagen, Fahrdynamik, Komponenten, Systeme, Mechatronik, Perspektiven*. 3rd ed. ATZ/MTZ-Fachbuch. Vieweg + Teubner Verlag, 2011.

[Hel06] HELMS, E.: *Roboterbasierte Bahnführungsunterstützung von industriellen Handhabungs - und Bearbeitungsprozessen*. PhD thesis. Stuttgart: Universität Stuttgart, 2006.

[Hen79] HENRICI, P.: *Zur numerischen Berechnung der Fresnelschen Integrale*. In: Zeitschrift für angewandte Mathematik und Physik ZAMP 2, pp. 209–219, 1979.

[Hen94] HENDRIX, C. M.: *Exploratory Studies on the Sense of Presence in Virtual Environments as a Function of Visual and Auditory Display Parameters: Master Thesis*. Seattle, 1994. URL: http://citeseerx.ist.psu.edu/viewdoc/summary?doi=10.1.1.6.2562.

[Hie08] HIETANEN, M. A.; CROWDER, N. A., and IBBOTSON, M. R.: *Differential changes in human perception of speed due to motion adaptation*. In: Journal of Vision 11, 2008.

[Hie11] HIESGEN, G.: *Effiziente Entwicklung eines menschzentrierten Querführungsassistenzsystems mit einem Fahrsimulator*. PhD thesis. Essen: Universität Duisburg-Essen, 2011.

[Hig96] HIGUCHI, M.; KUSAKA, K.; SHIBUSAWA, K.; HIRATA, H., and TSUKAGOSHI, M.: *Handling Analysis and Prediction During Cornering*. In: *Proceedings of the International Symposium on Advanced Vehicle Control*. Aachen, 1996, pp. 1027–1036.

[Hir05] HIRCHE, S. and BUSS, M.: *Human Perception Oriented Control Aspects of Networked Telepresence and Teleaction Systems*. In: *SICE Annual Conference - International Conference on Instrumentation, Control and Information Technology*. Okayama, 2005.

[Hoe11] HOERWICK, M.: *Sicherheitskonzept für hochautomatisierte Fahrerassistenzsysteme*. PhD thesis. München: Technische Universität München, 2011.

[Hol04] HOLT, V. v. and MAURER, M.: *Aktive Sicherheitssysteme mit maschineller Wahrnehmung - Anforderungen, Potentiale und Einführungshemmnisse*. In: *Aktive Sicherheit durch Fahrerassistenz*. 2004.

[Hua03] HUANG, P.-s.: *Regelkonzepte zur Fahrzeugführung unter Einbeziehung der Bedienelementeigenschaften*. PhD thesis. München: Technische Universität München, 2003.

[Int11] INTERNATIONAL ORGANIZATION FOR STANDARDIZATION: *ISO 26262*. 2011.

[Ise06] ISERMANN, R.: *Fault-Diagnosis Systems: An Introduction from Fault Detection to Fault Tolerance*. London: Springer Verlag, 2006.

[Jam00] JAMSON, H.: *Driving Simulator Validity: Issues of Field of View and Resolution*. In: *Driving Simulation Conference DSC*. Paris, 2000, pp. 57–64.

[Jan02] JANSSON, J.; JOHANSSON, J., and GUSTAFSSON, F.: *Decision Making for Collision Avoidance Systems*. In: Society of Automotive Engineers Technical Paper 2002.

[Jan05] JANSSON, J.: *Collision Avoidance Theory with Applilcation to Automotive Collision Mitigation*. PhD thesis. Linköping University, 2005.

[Jet14] JET PROPULSION LABORATORY, CALIFORNIA INSTITUTE OF TECHNOLOGY: *Mars Exploration Rovers*. URL: http://marsrover.nasa.gov/home/index.html, retrieved on 2014/03/25.

[Jon96] JONES, D. G. and ENDSLEY, M. R.: *Sources of situation awareness errors in aviation*. In: Aviation Space and Environmental Medicine 6, pp. 507–512, 1996.

[Jun05] JUNGMANN, T.: *Grand Challenge 2005, die Rallye der Rechner*. In: ATZ Online 2005.

[Jür01] JÜRGENSOHN, T. and TIMPE, K.-P., eds.: *Kraftfahrzeugführung*. Springer, 2001.

[Jür97] JÜRGENSOHN, T.: *Hybride Fahrermodelle*. PhD thesis. Berlin: Institut für Fahrzeugtechnik, 1997.

[KFZ14] KFZ.DE: *Sicherheitsabstand laut Straßenverkehrs-Ordnung (StVO)*. 2014/02/06.

[Kae07] KAEMPCHEN, N.: *Feature-Level Fusion of Laser Scanner and Video Data for Advanced Driver Assistance Systems: Dissertation*. PhD thesis. Ulm: Universität Ulm, 2007.

[Kam08] KAMMEL, S. et al.: *Team AnnieWAY's autonomous system for the 2007 DARPA Urban Challenge*. In: Journal of Field Robotics 9, pp. 615–639, 2008.

[Kau10] KAUER, M.; SCHREIBER, M., and BRUDER, R.: *How to conduct a car? A design example for maneuver based driver-vehicle interaction*. In: *Intelligent Vehicles Symposium (IV), 2010 IEEE*. San Diego, 2010, pp. 1214–1221.

[Kay95] KAY, J. S. and THORPE, C. E.: *Operator Interface Design Issues In A Low-Bandwidth And High-Latency Vehicle Teleoperation System*. In: *International Conference on Environmental Systems*. San Diego, CA, 1995.

[Kay97] KAY, J. S.: *STRIPE: Remote Driving Using Limited Image Data*. PhD thesis. Pittsburg, PA: Carnegie Mellon University, 1997.

[Kem03] KEMENY, A. and PANERAI, F.: *Evaluating perception in driving simulation experiments*. In: Trends in Cognitive Sciences 1, pp. 31–37, 2003.

[Kis13] KISHIYAMA, Y.; BENJEBBOUR, A.; NAKAMURA, T., and ISHII, H.: *Future steps of LTE-A: evolution toward integration of local area and wide area systems*. In: Wireless Communications, IEEE 1, pp. 12–18, 2013.

[Kiv04] KIVRIKIS, A. and TJERNSTRÖM, J.: *Development and Evaluation of Multiple Objects Collision Mitigation by Braking Algorithms: Master Thesis*. 2004. URL: http://www.openthesis.org/documents/Development-Evaluation-Multiple-Objects-Collision-415109.html.

[Koc10] KOCH, T.: *Untersuchungen zum Lenkgefuehl von Steer-by-Wire Lenksystemen*. PhD thesis. München: Technische Universität München, 2010.

[Kra08] KRAMER, U.: *Kraftfahrzeugführung: Modelle, Simulation, Regelung*. Fahrzeugtechnik. München: Carl Hanser, 2008.

[Kra12] KRAUS, S.: *Fahrverhaltensanalyse zur Parametrierung situationsadaptiver Fahrzeugfuehrungssysteme*. PhD thesis. München: Technische Universität München, 2012.

[Kre08] KRENIK, B.: *4G wireless technology: When will it happen? What does it offer?* In: *Solid-State Circuits Conference, 2008. A-SSCC '08. IEEE Asian*. Fukuoka, 2008, pp. 141–144. DOI: 10.1109/ASSCC.2008.4708715.

[Kri12] KRITAYAKIRANA, K. and GERDES, J. C.: *Autonomous vehicle control at the limits of handling*. In: International Journal of Vehicle Autonomous Systems 4, p. 271, 2012.

[Lag01] LAGES, U.: *Untersuchungen zur aktiven Unfallvermeidung von Kraftfahrzeugen*. PhD thesis. Universität der Bundeswehr Hamburg, 2001.

[Lap99] LAPPE, M.; BREMMER, F., and VAN DEN BERG, A. V.: *Perception of self-motion from visual flow*. In: Trends in Cognitive Sciences 9, pp. 329–336, 1999.

[Lee70] LEE, D. N.: *Spatio-temporal integration in binocular-kinetic space perception*. In: Vision Research 1, pp. 65–78, 1970.

[Lun08] LUNZE, J.: *Regelungstechnik 1: Systemtheoretische Grundlagen, Analyse und Entwurf einschleifiger Regelungen*. 7., neu bearb. Aufl. Berlin and Heidelberg: Springer, 2008.

[Lut12b] LUTZ, L.; TANG, T., and LIENKAMP, M.: *Analyse der rechtlichen Situation von teleoperierten (und autonomen) Fahrzeugen*. In: *5. Tagung Fahrerassistenz*. München, 2012.

[Lut13] LUTZ, L.; TANG, T., and LIENKAMP, M.: *Die rechtliche Situation von teleoperierten und autonomen Fahrzeugen*. In: Neue Zeitschrift für Verkehrsrecht 2, pp. 57–63, 2013.

[Löh76] LÖHR, R. W.: *Ergonomie. Grundlagen der Wechselbeziehungen zwischen Mensch, Technik und Umwelt*. Kamprath-Reihe kurz und bündig. Technik. Würzburg: Vogel Verlag, 1976.

[Mar12] MARINE TECHNOLOGY SOCIETY: *Remotely Operated Vehicles Commitee of the Marine Technology Society*. URL: http://www.rov.org, retrieved on 2012/09/01.

[Mat80] MATTHEWS, M. L. and COUSINS, L. R.: *The influence of vehicle type on the estimation of velocity while driving*. In: Ergonomics 12, pp. 1151–1160, 1980.

[Mau00] MAURER, M.: *Flexible Automatisierung von Straßenfahrzeugen mit Rechnersehen*. PhD thesis. Neubiberg: Universität der Bundeswehr München, 2000.

[Mau09] MAURER, M.: *Entwurf und Test von Fahrerassistenzsystemen*. In: *Handbuch Fahrerassistenzsysteme: Grundlagen, Komponenten und Systeme für aktive Sicherheit und Komfort*. Ed. by WINNER, H.; HAKULI, S., and WOLF, G. ATZ/MTZ-Fachbuch. Vieweg + Teubner, 2009, pp. 43–54.

[McG89] MCGOVERN, D. E.: *Experiences in teleoperation of Land Vehicles*. In: NASA, Ames Research Center, Spatial Displays and Spatial Instruments pp. 1–12, 1989.

[Mei12] MEINEL, C. and SACK, H.: *Internetworking: Technische Grundlagen und Anwendungen*. X.media.press. Berlin, Heidelberg: Springer-Verlag Berlin Heidelberg, 2012.

[Mil88] MILLER, D. P.: *Evaluation of Vision Systems for Teleoperated Land Vehicles*. In: Control Systems Magazine, IEEE 3, pp. 37–41, 1988.

[Mit04] MITSCHKE, M. and WALLENTOWITZ, H.: *Dynamik der Kraftfahrzeuge*. 4th ed. VDI-Buch. Berlin, Heidelberg: Springer Berlin Heidelberg, 2004.

[Mou07] MOURANT, R. R.; AHMAD, N.; JAEGER, B. K., and LIN, Y.: *Optic flow and geometric field of view in a driving simulator display*. In: Displays 3, pp. 145–149, 2007.

[Mui09] MUIGG, A.: *Implizites Workloadmanagement - Konzept einer zeitlich-situativen Informationsfilterung im Automobil*. PhD thesis. Technische Universität München, 2009.

[NAS12] NASA: *Mars Science Laboratory/Curiosity*. URL: http://www.jpl.nasa.gov/news/fact_sheets/mars-science-laboratory.pdf, retrieved on 2012/09/23.

[Nef05] NEFF, J.: *DARPA Grand Challenge won by Stanford's Stanley*. URL: http://www.autoblog.com/2005/10/11/darpa-grand-challenge-won-by-stanfords-stanley/, retrieved on 2013/03/28.

[Neg07] NEGELE, H. J.: *Anwendungsgerechte Konzipierung von Fahrsimulatoren für die Fahrzeugentwicklung*. PhD thesis. München: Technische Universität München, 2007.

[Nga11] NGAI, C. K. and YUNG, NELSON H. C.: *DAQL-Enabled Autonomous Vehicle Navigation in Dynamically Changing Environment: Chapter 21*. In: *Advances in Reinforcement Learning*. Ed. by MELLOUK, A. InTech, 2011, pp. 385–410. DOI: 10.5772/13743.

[Nie07] NIELSEN, C. W.; GOODRICH, M. A., and RICKS, R. W.: *Ecological Interfaces for Improving Mobile Robot Teleoperation*. In: Robotics, IEEE Transactions on 5, pp. 927–941, 2007.

[Oxf11] OXFORD TECHNICAL SOLUTIONS LIMITED: *RT Intertial and GPS Measurement System User Manual*. 2011.

[Pas94] PASTORE, T. H.: *Improved Operator Awareness of Teleoperated Land Vehicle Attitude*. 1994. URL: http://www.ntis.gov/search/product.aspx?ABBR=ADA290443.

[Pin12] PINTO, C.: *How Autonomous Vehicle Policy in California and Nevada Addresses Technological and Non-Technological Liabilities*. In: Intersect: The Stanford Journal of Science, Technology and Society 2012.

[Pon08] PONGRAC, H.: *Gestaltung und Evaluation von virtuellen und Telepräsenzsystemen an Hand von Aufgabenleistung und Präsenzempfinden*. PhD thesis. Neubiberg: Universität der Bundeswehr München, 2008.

[Pud11] PUDENZ, K.: *Forschungsfahrzeug fährt autonom durch das Zentrum von Berlin*. In: ATZ Online 2011.

[Rad12] RADI, M.: *Workspace Scaling and Haptic Feedback for Industrial Telepresence and Teleaction Systems with Heavy-Duty Teleoperators*. PhD thesis. München: Technische Universität München, 2012.

[Ras04] RASSL, R.: *Ablenkungswirkung tertiärer Aufgaben im Pkw Systemergonomische Analyse und Prognose*. PhD thesis. München: Technische Universität München, 2004.

[Ras83] RASMUSSEN, J.: *Skills, rules, and knowledge; signals, signs, and symbols, and other distinctions in human performance models*. In: Systems, Man and Cybernetics, IEEE Transactions on 3, pp. 257–266, 1983.

[Rat07] RATTEI, F.; GOEBL, M., and FAERBER, G.: *Beitrag zur Robustheitssteigerung videobasierter Fahrerassistenzsysteme durch frühe Rückkopplungen zur Sensorebene*. In: *Bildverarbeitung in der Mess- und Automatisierungstechnik*. VDI Bericht. VDI Verlag, 2007.

[Rau09] RAUCH, N.: *Ein verhaltensbasiertes Messmodell zur Erfassung von Situationsbewusstsein im Fahrkontext*. PhD thesis. Würzburg: Julius-Maximiliams-Universität Würzburg, 2009.

[Rau12] RAUCH, S.; AEBERHARD, M.; ARDELT, M., and KAEMPCHEN, N.: *Autonomes Fahren auf der Autobahn- Eine Potentialstudie für zukünftige Fahrerassistenzsysteme*. In: *5. Tagung Fahrerassistenz*. München, 2012.

[Rec96] RECARTE, M. A. and NUNES, L. M.: *Perception of speed in an automobile: Estimation and production*. In: Journal of Experimental Psychology: Applied 4, pp. 291–304, 1996.

[Reg08] REGAN, M. A.; LEE, J. D., and YOUNG, K. L., eds.: *Driver Distraction: Theory, Effects, and Mitigation*. CRC Press, 2008.

[Rie40] RIEKERT, P. and SCHUNCK, T. E.: *Zur Fahrmechanik des gummibereiften Kraftfahrzeugs*. In: Ingenieur-Archiv 3, pp. 210–224, 1940.

[Rob10] ROBUFFO GIORDANO, P.: *Visual-Vestibular Feedback for Enhanced Situational Awareness in Teleoperation of UAVs*. In: *AHS International 66th Annual Forum, 66th American Helicopter Society International Annual Forum 2010*. Phoenix, AZ, 2010, pp. 2809–2818.

[Ros07] ROSENBLUM, M.: *DARPA Urban Challenge 2007 Team Urbanator Technical Description*. 2007. URL: http://archive.darpa.mil/grandchallenge/TechPapers/Team_Urbanator.pdf.

[Ryu07] RYU, J.-H. and PREUSCHE, C.: *Stable Bilateral Control of Teleoperators Under Time-varying Communication Delay: Time Domain Passivity Approach*. In: *Robotics and Automation, 2007 IEEE International Conference on*. Rome, 2007, pp. 3508–3513. DOI: 10.1109/ROBOT.2007.364015.

[SEN14] SENSODRIVE: *SENSO-Wheel SD-LC*. URL: http://www.sensodrive.de/EN/Produkte/Force-Feedback-Wheels/Senso-Wheel-SD-LC.php, retrieved on 2014/03/27.

[Sch03] SCHWEIGERT, M.: *Fahrerblickverhalten und Nebenaufgaben*. PhD thesis. München: Technische Universität München, 2003.

[Sch06] SCHORN, M.: *Modelle zur Beschreibung des Fahrzeugverhaltens: Chapter 2*. In: *Fahrdynamik-Regelung: Modellbildung, Fahrerassistenzsysteme, Mechatronik*. Ed. by ISERMANN, R. Wiesbaden: Vieweg, 2006, pp. 27–46.

[Sch08] SCHEDEL, R.: *Darpa Urban Challenge 2007*. In: ATZ - Automobiltechnische Zeitschrift 1, pp. 28–30, 2008.

[Sch09] SCHALLER, T.: *Stauassistenz — Längs- und Querführung im Bereich niedriger Geschwindigkeit*. PhD thesis. München: Technische Universität München, 2009.

[Sch77] SCHMIDT, R. F. and THEWS, G., eds.: *Physiologie des Menschen*. 19., überarb. Aufl. Berlin and New York: Springer-Verlag, 1977.

[Sch93] SCHMIDTKE, H. and BERNOTAT, R.: *Ergonomie*. 3., neubearb. und erw. Aufl. München [u.a.]: Hanser, 1993.

[Sec03] SECCHI, C.; STRAMIGIOLI, S., and FANTUZZI, C.: *Digital Passive Geometric Telemanipulation*. In: *Robotics and Automation, 2003. Proceedings. ICRA '03. IEEE International Conference on*. Vol. 3. Taipei, 2003, 3290–3295 vol.3. DOI: 10.1109/ROBOT.2003.1242098.

[See06] SEECK, A. and GASSER, T. M.: *Klassifizierung und Würdigung der rechtlichen Rahmenbedingungen im Zusammenhang mit der Einführung moderner FAS*. In: *2. Tagung Aktive Sicherheit durch Fahrerassistenz*. München, 2006.

[She02] SHERIDAN, T. B.: *Humans and Automation: System Design and Research Issues*. Vol. 3. HFES issues in human factors and ergonomics series. Santa Monica, CA, USA: Human Factors and Ergonomics Society, 2002.

[She92] SHERIDAN, T. B.: *Telerobotics, Automation, and Human Supervisory Control*. Cambridge, MA, USA: MIT Press, 1992.

[She93] SHERIDAN, T. B.: *Space teleoperation through time delay: review and prognosis*. In: IEEE Transactions on Robotics and Automation 5, pp. 592–606, 1993.

[She94] SHERIDAN, T. B.: *Further Musings on the Psychophysics of Presence*. In: *Systems, Man, and Cybernetics, 1994. Humans, Information and Technology., 1994 IEEE International Conference on*. Vol. 2. San Antonio, TX, 1994, pp. 1073–1077. DOI: 10.1109/ICSMC.1994.399986.

[Sib12] SIBBERTSEN, P. and LEHNE, H.: *Statistik: Einführung für Wirtschafts- und Sozialwissenschaftler*. SpringerLink : Bücher. Berlin, Heidelberg: Springer, 2012.

[Ski91] SKIBA, R.: *Taschenbuch Arbeitssicherheit*. 7th ed. Erich Schmidt Verlag, 1991.

[Smi87] SMITH, A. T.: *Velocity perception and discrimination: Relation to temporal mechanisms*. In: Vision Research 9, pp. 1491–1500, 1987.

[Spe13] SPEAKER TRADE: *mivoc AM 80 - Owners Manual*. 2013. URL: http://mivoc.de/shop/de/mivoc/details-verstaerker.html?marke=mivoc&artikel=AM80schwarz.

[Spe14] SPEAKER TRADE: *mivoc AM 80*. URL: http://mivoc.de/homepage/de/mivoc/xxl/am80_front_xxl.jpg, retrieved on 2014/11/12.

[Sta08] STAEMPFLE, M. and BRANZ, W.: *Kollisionsvermeidung im Längsverkehr - die Vision vom unfallfreien Fahren rückt näher*. In: *3. Tagung Aktive Sicherheit durch Fahrerassistenz*. München, 2008.

[Sta11] STATISTISCHES BUNDESAMT: *Unfallentwicklung auf deutschen Straßen 2010*. 2011. URL: https://www.destatis.de/DE/Publikationen/Thematisch/TransportVerkehr/Verkehrsunfaelle/Unfallentwicklung5462401109004.pdf?__blob=publicationFile.

[Sta14] STATISTISCHES BUNDESAMT: *Verkehrsunfälle*. Wiesbaden, 2014.

[Ste04] STEINFELD, A.: *Interface Lessons for Fully and Semi-Autonomous Mobile Robots*. In: *Robotics and Automation, 2004. Proceedings. ICRA '04. 2004 IEEE International Conference on*. Vol. 3. New Orleans, LA, USA, 2004, pp. 2752–2757.

[Ste92] STEUER, J.: *Defining Virtual Reality: Dimensions Determining Telepresence*. In: Journal of Communication 4, pp. 73–93, 1992.

[Sti05] STILLER, C.: *Fahrerassistenzsysteme - Von realisierten Funktionen zum vernetzt wahrnehmenden, selbstorganisierenden Verkehr*. In: *Fahrerassistenzsysteme mit maschineller Wahrnehmung*. Ed. by MAURER, M. and STILLER, C. Berlin: Springer, 2005. DOI: 10.1007/3-540-27137-6_1.

[Sti09] STILLER, C.; BACHMANN, A., and DUCHOW, C.: *Maschinelles Sehen: Chapter 15*. In: *Handbuch Fahrerassistenzsysteme: Grundlagen, Komponenten und Systeme für aktive Sicherheit und Komfort*. Ed. by WINNER, H.; HAKULI, S., and WOLF, G. ATZ/MTZ-Fachbuch. Vieweg + Teubner, 2009, pp. 198–222.

[Stu04] STUEKER, D.: *Heterogene Sensordatenfusion zur robusten Objektverfolgung im automobilen Straßenverkehr*. PhD thesis. Universität Oldenburg, 2004.

[Suo01] SUOMELA, J.: *Tele-presence aided teleoperation of semi-autonomous work vehicles: Licentiate Thesis*. 2001. URL: http://automation.tkk.fi/attach/AS-84-3147/LisuriJS.pdf.

[Swi74] SWIK, R.: *Optimales Abbremsen eines Fahrzeuges bei Kurvenfahrt*. In: Vehicle System Dynamics 4, pp. 193–215, 1974.

[Söh01] SÖHNITZ, I.: *Querregelung eines autonomen Straßenfahrzeugs*. PhD thesis. Braunschweig: Technische Universität Braunschweig, 2001.

[Tan13a] TANG, T.; CHUCHOLOWSKI, F.; YAN, M., and LIENKAMP, M.: *A Novel Study on Data Rate by the Video Transmission for Teleoperated Road Vehicles*. In: *9th International Conference on Intelligent Unmanned Systems*. Jaipur, 2013.

[Tan13b] TANG, T.; VETTER, P.; FINKL, S.; FIGEL, K., and LIENKAMP, M.: *Teleoperated Road Vehicles - The "Free Corridor" as a safety strategy approach*. In: *ICCMA2013, International Conference on Control, Mechatronics and Automation*. Sydney, 2013.

[Tan13c] TANG, T.; KURKOWSKI, J., and LIENKAMP, M.: *Teleoperated Road Vehicles: A Novel Study on the Effect of Blur on Speed Perception*. In: International Journal of Advanced Robotic Systems 2013.

[Tan14a] TANG, T.; VETTER, P.; FINKL, S.; FIGEL, K., and LIENKAMP, M.: *Teleoperated Road Vehicles – The "Free Corridor" as a Safety Strategy Approach*. In: Applied Mechanics and Materials pp. 1399–1409, 2014.

[Tan14b] TANG, T.; CHUCHOLOWSKI, F., and LIENKAMP, M.: *Teleoperiertes Fahren Grundlagen und Systementwurf*. In: ATZ - Automobiltechnische Zeitschrift 2, pp. 30–33, 2014.

[Tay64] TAYLOR, D. H.: *Driver's Galvanic Skin Response and the Risk of Accident*. In: Ergonomics 4, pp. 439–451, 1964.

[Ten10] TENORIO, S.; EXADAKTYLOS, K.; MCWILLIAMS, B., and LE PEZENNEC, Y.: *Mobile broadband field network performance with HSPA+*. In: *Wireless Conference (EW), 2010 European*. Lucca, 2010, pp. 269–273. DOI: 10.1109/EW.2010.5483428.

[Tes11] TESIS DYNAWARE GMBH: *DYNAanimation 2.0 User Manual*. 2011.

[Tes12] TESIS DYNAWARE GMBH: *DYNA4 Documentation*. 2012.

[The04] THE EUROPEAN PARLIAMENT AND THE COUNCIL: *2003/97/EG*. 2004.

[The77] THE EUROPEAN PARLIAMENT AND THE COUNCIL: *77/649/EWG*. 1977.

[Thr06] THRUN, S. et al.: *The Robot that Won the DARPA Grand Challenge*. In: Journal of Field Robotics pp. 661–692, 2006.

[Thu08] THUY, M. et al.: *Kognitive Automobile - Neue Konzepte und Ideen des Sonderforschungsbereiches / TR-28*. In: *3. Tagung Aktive Sicherheit durch Fahrerassistenz*. München, 2008.

[Thu09] THUY, M. and LEON, F. P.: *Non-Linear, Shape Independent Object Tracking based on 2D Lidar Data*. In: *Intelligent Vehicles Symposium (IV), 2009 IEEE*. Xi'an, 2009, pp. 532–537.

[Tra06] TRABIA, M. B.; SHI, L. Z., and HODGE, N. E.: *A Fuzzy Logic Controller for Autonomous Wheeled Vehicles: Chapter 10*. In: *Mobile Robotics, Moving Intelligence*. Ed. by BUCHLI, J. InTech, 2006, pp. 175–200. DOI: 10.5772/4721.

[Tza06] TZAFESTAS, C. S.: *Virtual and Mixed Reality in Telerobotics: A Survey: Chapter 23*. In: *Industrial Robotics: Programming, Simulation and Applications*. Ed. by HUAT, L. K. InTech, 2006, pp. 437–470.

[Uni11] UNITED NATIONS: *World Urbanization Prospects: The 2011 Revision*. 2011. URL: http://esa.un.org/unup/.

[Wal14] WALLNER, J.; TANG, T., and LIENKAMP, M.: *Development of an Emergency Braking System for Teleoperated Vehicles Based on Lidar Sensor Data*. In: *ICINCO2014, 11th International Conference on Informatics in Control, Automation and Robotics*. Vol. 2. Vienna, 2014, pp. 569–576.

[Wan96] WANG, J.-S.; KNIPLING, R. R., and GOODMAN, M. J.: *The Role of Driver Inattention in Crashes; New Statistics from the 1995 Crashworthiness Data System*. In: *40th Annual Proceedings: Association for the Advancement of Automotive Medicine*. Vancouver, 1996, pp. 377–392.

[Web12] WEBER, D.: *Untersuchung des Potenzials einer Brems-Ausweich-Assistenz*. PhD thesis. Karlsruher Institut für Technologie, 2012.

[Weg05] WEGSCHEIDER, M. and PROKOP, G.: *Modellbasierte Komfortbewertung von Fahrerassistenzsystemen*. In: VDI Berichte pp. 17–36, 2005.

[Wei03] WEISSE, J.: *Beitrag zur Entwicklung eines optimierten Bremsassistenten*. PhD thesis. Technische Universität Darmstadt, 2003.

[Wel09] WELTONLINE: *Ein frontaler Crash kann das Glück im Unglück sein*. URL: http://www.welt.de/motor/article4313773/Ein-frontaler-Crash-kann-das-Glueck-im-Unglueck-sein.html, retrieved on 2014/02/13.

[Wic95] WICKENS, C. D.: *Situation Awareness: Impact of Automation and Display Technology*. In: *Agard Conference Proceedings 575. Situation Awareness: Limitations and Enhancement in the Aviation Environment*. Brussels, 1995, K2.1–K2.13.

[Wil05] WILKIE, R. M. and WANN, J. P.: *The Role of Visual and Nonvisual Information in the Control of Locomotion*. In: Journal of Experimental Psychology: Human Perception and Performance 5, pp. 901–911, 2005.

[Wil12] WILLE, J. M.: *Manöverübergreifende autonome Fahrzeugführung in innerstädtischen Szenarien am Beispiel des Stadtpilotprojekts*. PhD thesis. Braunschweig: Technische Universität Carolo-Wilhelmina zu Braunschweig, 2012.

[Win00] WINFIELD, A. F. T.: *Future Directions in Tele-operated Robotics*. In: *Telerobotic Applications*. Ed. by SCHILLING, T. London: Professional Engineering Pub, 2000, pp. 147–163.

[Win09a] WINNER, H.: *Frontalkollisionsschutzsysteme: Chapter 33*. In: *Handbuch Fahrerassistenzsysteme: Grundlagen, Komponenten und Systeme für aktive Sicherheit und Komfort*. Ed. by WINNER, H.; HAKULI, S., and WOLF, G. ATZ/MTZ-Fachbuch. Vieweg + Teubner, 2009, pp. 522–542.

[Win09b] WINNER, H.; DANNER, B., and STEINLE, J.: *Adaptive Cruise Control: Chapter 32*. In: *Handbuch Fahrerassistenzsysteme: Grundlagen, Komponenten und Systeme für aktive Sicherheit und Komfort*. Ed. by WINNER, H.; HAKULI, S., and WOLF, G. ATZ/MTZ-Fachbuch. Vieweg + Teubner, 2009, pp. 478–521.

[Win09c] WINNER, H. and WOLF, G.: *Quo vadis, FAS? Chapter 44*. In: *Handbuch Fahrerassistenzsysteme: Grundlagen, Komponenten und Systeme für aktive Sicherheit und Komfort*. Ed. by WINNER, H.; HAKULI, S., and WOLF, G. ATZ/MTZ-Fachbuch. Vieweg + Teubner, 2009, pp. 664–673.

[Wit14] WITTMANN, D.; CHUCHOLOWSKI, F., and LIENKAMP, M.: *Improving Lidar Data Evaluation for Object Detection and Tracking Using a Priori Knowledge and Sensorfusion*. In: *ICINCO2014, 11th International Conference on Informatics in Control, Automation and Robotics*. Vol. 1. Vienna, 2014, pp. 794–801.

[Wit98] WITMER, B. G. and SINGER, M. J.: *Measuring Presence in Virtual Environments: A Presence Questionnaire*. In: Presence: Teleoperators and Virtual Environments 3, pp. 225–240, 1998.

[XNA14] XNA GAME STUDIO: *XNA Racing Game*. URL: http://xbox.create.msdn.com/assets/cms/images/XNA_Racing-Game_02_large.jpg, retrieved on 2014/11/06.

[Yan04] YANCO, H. A. and DRURY, J.: *Classifying Human-Robot Interaction: An Updated Taxonomy*. In: *Systems, Man and Cybernetics, 2004 IEEE International Conference on*. Vol. 3. The Hague, 2004, 2841–2846 vol.3. DOI: 10.1109/ICSMC.2004.1400763.

[Yok99] YOKOKOHJI, Y.; IMAIDA, T., and YOSHIKAWA, T.: *Bilateral Teleoperation under Time-Varying Communication Delay*. In: *Intelligent Robots and Systems, 1999. IROS '99. Proceedings. 1999 IEEE/RSJ International Conference on*. Vol. 3. Kyongju, 1999, 1854–1859 vol.3. DOI: 10.1109/IROS.1999.811748.

[Zel09] ZELLER, P., ed.: *Handbuch Fahrzeugakustik: Grundlagen, Auslegung, Berechnung, Versuch*. SpringerLink : Bücher. Wiesbaden: Vieweg + Teubner Verlag, 2009.

[Zie42] ZIEGLER, J. G. and NICHOLS, N. B.: *Optimum Settings for Automatic Controllers*. In: Transactions of ASME pp. 759–768, 1942.

Student Research Projects

Multiple student research theses were supervised during the completion of this dissertation. Listed below are the student research theses relevant to this dissertation. Many thanks to all the involved persons for their extensive support in this research project.

Student Research Projects

[Ank11] ANKENBAUER, T.: *Implementierung eines Algorithmus in Simulink zur pneumatischen Regelung eines Bremssystems für teleoperiertes Fahren: Semesterarbeit*. München, 2011.

[Bad13] BADBANCHI, S.: *Erzeugung eines realistischen Fahrens durch Erhöhung des Risikobewusstseins am Operatorarbeitsplatz: Semesterarbeit*. München, 2013.

[Dia13] DIAZ, J. L.: *Umsetzung und experimentelle Untersuchung des Sicherheitskonzepts "Freier Korridor" bei teleoperierten Fahrzeugen: Masterarbeit*. München, 2013.

[Du12] DU, Y.: *Entwicklung und Bewertung von Fahrzustsandsschätzer für das Sicherheitskonzept "Freier Korridor" bei teleoperierten Fahrzeugen: Semesterarbeit*. München, 2012.

[Fig12] FIGEL, K.: *Optimierung des Sicherheitskonzepts "Freier Korridor" bei ferngesteuerten Fahrzeugen: Bachelorarbeit*. München, 2012.

[Fin12] FINKL, S.: *Optimierung und Erweiterung des Konzepts "Freier Korridor" als Notfallstrategie bei teleoperierten Fahrzeugen für Spurwechselmanöver: Diplomarbeit*. München, 2012.

[Fra13] FRANKE, J.: *Anbindung und Ansteuerung von Eingabegeräten eines Operatorarbeitsplatzes für teleoperierte Fahrzeuge: Semesterarbeit*. München, 2013.

[Fri14] FRIEDRICH, P.: *Weiterentwicklung und Optimierung eines Regelungssystems für das Sicherheitskonzept „Freier Korridor“ bei teleoperierten Fahrzeugen: Bachelorarbeit*. München, 2014.

[Gu12] GU, P.: *Untersuchung von Notfallstrategien für semi-autonome Fahrzeuge: Bachelorarbeit*. München, 2012.

[Hir13] HIRCHE, B.: *Aufbau einer Model-in-the-Loop Simulationsumgebung für hochautomatisierte Fahrerassistenzsysteme auf Basis von DYNA4: Bachelorarbeit*. München, 2013.

[Hir14] HIRSCHMANN, H.: *Erweiterung des Regelungssystems für das Sicherheitskonzept "Freier Korridor" bei teleoperierten Fahrzeugen: Bachelorarbeit*. München, 2014.

[Kle12] KLEMENT, T.: *Konstruktion und Realisierung eines "Shift-by-wire" Systems für den Versuchsträger Audi Q7: Semesterarbeit*. München, 2012.

[Kur12] KURKOWSKI, J.: *Untersuchung des Geschwindigkeitsempfinden beim Teleoperierten Fahren durch Probandenversuche: Bachelorarbeit*. München, 2012.

[Lut12a] LUTZ, L.: *Analyse von rechtlichen Aspekten des teleoperierten Fahrens: Diplomarbeit*. München, 2012.

[Mac14] MACIUGA, T.: *Experimentelle Untersuchung des Geschwindigkeitsempfindens beim Teleoperierten Fahren durch Probandenversuche: Bachelorarbeit*. München, 2014.

[Mil14] MILLE, L.: *Entwicklung und Umsetzung von realistischem Lenkgefühl am Operatorarbeitsplatz bei teleoperierten Fahrzeugen: Bachelorarbeit*. München, 2014.

[Mti13] MTIR, N.: *Entwicklung eines Konzeptes zur Erhöhung des Risikobewusstseins am Operatorarbeitsplatz: Semesterarbeit*. München, 2013.

[Mue13] MUELLER, M.: *Entwicklung eines Regelungssystems für das Sicherheitskonzept "Freier Korridor" bei teleoperierten Fahrzeugen: Diplomarbeit*. München, 2013.

[Rap12] RAPP, F.: *Erhöhung des Risikobewusstseins am Operatorarbeitsplatz beim teleoperierten Fahren durch auditive und haptische Rückmeldungen: Bachelorarbeit*. München, 2012.

[Rei13] REICH, M.: *Konstruktion und Aufbau eines Operatorarbeitsplatzes für teleoperierte Straßenfahrzeuge: Bachelorarbeit*. München, 2013.

[Rie13] RIES, Y. O.: *Konstruktive Lösung eines Notbremssystems unter Betrachtung einer Risikoanalyse eines Elektrofahrzeugs: Semesterarbeit*. München, 2013.

[Spi14] SPIESS, C.: *Untersuchung des Sicherheitskonzepts "Freier Korridor" durch einen Probandenversuch: Semesterarbeit*. München, 2014.

[Uen13] UENAL, G.: *Untersuchung des Mobilfunks anhand eines entwickelnden Tools zur Prädiktion eines Verbindungsabbruchs für teleoperierte Fahrzeuge: Semesterarbeit*. München, 2013.

[Wal13a] WALLNER, J.: *Entwicklung eines Notbremsassistenten für teleoperierte Fahrzeuge basierend auf Lidar-Sensor-Daten: Masterarbeit*. München, 2013.

[Wal13b] WALTHER, L.: *Simulative Untersuchung des Sicherheitskonzeptes "Freier Korridor" mit Berücksichtigung von Zeitverzögerungen bei der Übertragung: Bachelorarbeit*. München, 2013.

[Wei13] WEINMANN, G.: *Experimentelle Untersuchung des Geschwindigkeitsempfindens beim Teleoperierten Fahren hinsichtlich auditive und haptische Rückmeldungen am Operatorarbeitsplatz: Bachelorarbeit*. München, 2013.

[Xu12] XU, Y.: *Literaturrecherche zur Umgebungswahrnehmung bei intelligenten Straßenfahrzeugen: Semesterarbeit*. München, 2012.

[Yan12] YAN, M.: *Spezifikation von nötigen visuellen Informationen zur Reduzierung der Datenrate bei teleoperierten Fahrzeugen: Masterarbeit*. München, 2012.

Student Research Projects Supervised by Colleagues

[Gol11] GOLD, C.: *Spezifikation zusätzlicher Informationen für den Operator-Arbeitsplatz eines teleoperierten Fahrzeugs: Semesterarbeit*. München, 2011.

[Vet11] VETTER, P.: *Simulative Untersuchung des Sicherheitskonzeptes "Freier Korridor" bei teleoperierten Fahrzeugen: Semesterarbeit*. München, 2011.

A special thanks to Mathias **Ptacek** for the support and provision of the software used for the reproduction of artificial motor sound. This software came into being as an university project in 2012.

Own Publications in Context of this Thesis

[Chu13c] CHUCHOLOWSKI, F.; GNATZIG, S.; TANG, T.; HOSSEINI, A., and LIENKAMP, M.: *Teleoperiertes Fahren Aktuelle Entwicklungen*. In: *6. Tagung Fahrerassistenz*. München, 2013.

[Chu14] CHUCHOLOWSKI, F.; TANG, T., and LIENKAMP, M.: *Teleoperiertes Fahren Sichere und robuste Datenverbindungen*. In: ATZelektronik 1, pp. 60–63, 2014.

[Die11] DIERMEYER, F.; GNATZIG, S.; CHUCHOLOWSKI, F.; TANG, T., and LIENKAMP, M.: *Der Mensch als Sensor - Der Weg zum teleoperierten Fahren*. In: *11. Braunschweiger Symposium AAET*. Braunschweig, 2011.

[Gna13] GNATZIG, S.; CHUCHOLOWSKI, F.; TANG, T., and LIENKAMP, M.: *A System Design for Teleoperated Road Vehicles*. In: *ICINCO2013, 10th International Conference on Informatics in Control, Automation and Robotics*. Vol. 2. Reykjavik, 2013, pp. 231–238.

[Lut12b] LUTZ, L.; TANG, T., and LIENKAMP, M.: *Analyse der rechtlichen Situation von teleoperierten (und autonomen) Fahrzeugen*. In: *5. Tagung Fahrerassistenz*. München, 2012.

[Lut13] LUTZ, L.; TANG, T., and LIENKAMP, M.: *Die rechtliche Situation von teleoperierten und autonomen Fahrzeugen*. In: Neue Zeitschrift für Verkehrsrecht 2, pp. 57–63, 2013.

[Tan13a] TANG, T.; CHUCHOLOWSKI, F.; YAN, M., and LIENKAMP, M.: *A Novel Study on Data Rate by the Video Transmission for Teleoperated Road Vehicles*. In: *9th International Conference on Intelligent Unmanned Systems*. Jaipur, 2013.

[Tan13b] TANG, T.; VETTER, P.; FINKL, S.; FIGEL, K., and LIENKAMP, M.: *Teleoperated Road Vehicles - The "Free Corridor" as a safety strategy approach*. In: *ICCMA2013, International Conference on Control, Mechatronics and Automation*. Sydney, 2013.

[Tan13c] TANG, T.; KURKOWSKI, J., and LIENKAMP, M.: *Teleoperated Road Vehicles: A Novel Study on the Effect of Blur on Speed Perception*. In: International Journal of Advanced Robotic Systems 2013.

[Tan14a] TANG, T.; VETTER, P.; FINKL, S.; FIGEL, K., and LIENKAMP, M.: *Teleoperated Road Vehicles – The "Free Corridor" as a Safety Strategy Approach*. In: Applied Mechanics and Materials pp. 1399–1409, 2014.

[Tan14b] TANG, T.; CHUCHOLOWSKI, F., and LIENKAMP, M.: *Teleoperiertes Fahren Grundlagen und Systementwurf*. In: ATZ - Automobiltechnische Zeitschrift 2, pp. 30–33, 2014.

[Wal14] WALLNER, J.; TANG, T., and LIENKAMP, M.: *Development of an Emergency Braking System for Teleoperated Vehicles Based on Lidar Sensor Data*. In: *ICINCO2014, 11th International Conference on Informatics in Control, Automation and Robotics*. Vol. 2. Vienna, 2014, pp. 569–576.

Appendix

A. Questionnaire for Study with Test Subjects using Blur

Demographischer Fragebogen:

Personenfragebogen
zur Versuchsreihe
Geschwindigkeitsempfinden beim teleoperierten Fahren

Vielen Dank für Ihre Teilnahme an den Versuchen. Lesen Sie die Fragen bitte gut durch und beantworten sie so genau wie möglich. Ihre Daten werden selbstverständlich anonymisiert und vertraulich behandelt sowie nur zur Auswertung dieser Versuchsreihe verwendet.

1.) Wie alt sind Sie? ________ Jahre

2.) Sind Sie weiblich oder männlich? ☐ weiblich ☐ männlich

3.) Seit wie vielen Jahren besitzen sie den Führerschein Klasse B? ________ Jahre

4.) Wie viele Kilometer fahren Sie pro Jahr Auto? ________ Kilometer

5.) Welches Fahrzeug fahren Sie am häufigsten selbst? ________ [Marke]
________ [Modell]
________ [Baujahr]

6.) Kreuzen Sie bitte in der folgenden Skala an, wie Sie ihren Fahrstil einschätzen:

sportlich ... langsam
Ich fahre in der Regel gerne schnell und sportlich. ☐ ☐ ☐ ☐ ☐ Ich fahre eher langsam und vorsichtig.

☐ keine Angabe

7.) Wie verhalten Sie sich Geschwindigkeitsbeschränkungen gegenüber?

streng ... nicht
An Geschwindigkeits-beschränkungen halte ich mich streng. ☐ ☐ ☐ ☐ ☐ Geschwindigkeitsbe-schränkungen beachte ich nur, wenn ich von ihrer Notwendigkeit überzeugt bin.

☐ keine Angabe

8.) Sind sie beim Autofahren verpflichtet, eine Sehhilfe zu verwenden? ☐ ja ☐ nein
Wenn ja, dann verwenden Sie die Sehhilfe bitte auch im Versuch.

9.) Ist Ihr Sichtfeld eingeschränkt? ☐ ja ☐ nein

10.) Ist Ihr Hörvermögen beeinträchtigt? ☐ ja ☐ nein

- 1 -

11.) Wie häufig spielen Sie Videospiele, bei denen es um Lenken von Fahrzeugen geht?

☐ nie ☐ selten ☐ monatlich ☐ wöchentlich ☐ täglich

12.) Haben Sie schon einmal an einem Fahrversuch teilgenommen? ☐ ja ☐ nein

Die Fragen 6 und 7 stammen aus einer Dissertation von Assmann[1].

Fragebogen zur Selbsteinschätzung

Fragebogen zur Selbsteinschätzung
zur Versuchsreihe
Geschwindigkeitsempfinden beim teleoperierten Fahren
(auszufüllen durch den Versuchsleiter während Befragung der Versuchspersonen)

1.) Wie sicher waren Sie sich bei Ihren Schätzungen?

Phase 1:	☐ sehr sicher	☐ sicher	☐ neutral	☐ unsicher	☐ sehr unsicher
(nach Phase 1)					
Phase 3:	☐ sehr sicher	☐ sicher	☐ neutral	☐ unsicher	☐ sehr unsicher
(nach Phase 3)					
Phase 5:	☐ sehr sicher	☐ sicher	☐ neutral	☐ unsicher	☐ sehr unsicher
(nach Phase 5)					

2.) Finden Sie, dass sich ihr Einschätzungsvermögen für die Geschwindigkeit im Lauf der Versuche verbessert hat?

☐ja ☐nein

Für Probanden, die Blur im letzten Versuch haben:

3.) Finden Sie, dass die Unschärfe Ihr Geschwindigkeitsempfinden verbessert hat?

☐ja ☐nein

[1] Assmann, Ernst: Untersuchung über den Einfluss einer Bremsweganzeige auf das Fahrverhalten. München, Technische Universität München, Institut für Ergonomie. Dissertation.

- 2 -

B. Questionnaire for Study with Test Subjects using Artificial Motor Sound, Vibration at the Driver's Seat, Blur

Fragebogen

Vielen Dank, dass Sie sich für den Versuch zur Verfügung stellen. Ihre Daten werden selbstverständlich anonym behandelt.

Bitte lesen Sie sich die Fragen genau durch und beantworten Sie diese so genau wie möglich.

Bitte beantworten Sie VOR dem Versuch nur die erste Seite des Fragebogens.

1) Wie alt sind Sie? …………………..

2) Sind Sie männlich oder weiblich? ☐ männlich ☐ weiblich

3) Seit wie vielen Jahren besitzen Sie einen Führerschein der Klasse B? …………………..

4) Wie viele Kilometer fahren Sie pro Jahr? …………………..

5) Müssen Sie eine Sehhilfe beim Autofahren tragen? ☐ Ja ☐ Nein

6) Ist Ihr Hörvermögen beeinträchtigt? ☐ Ja ☐ Nein

7) Hören Sie regelmäßig Musik/Radio im Auto? ☐ Ja ☐ Nein

8) Wie schätzen Sie Ihren Fahrstil ein? Bitte kreuzen Sie an.

Sportlich ☐ ☐ ☐ ☐ ☐ langsam und vorsichtig

9) Wie verhalten Sie sich gegenüber Geschwindigkeitsbegrenzungen?

Ich halte mich streng an sie ☐ ☐ ☐ ☐ ☐ Ich beachte sie nur, wenn ich von ihrer Notwendigkeit überzeugt bin.

10) Haben Sie schon einmal an einem Fahrversuch teilgenommen? ☐ Ja ☐ Nein

11) Als wie sicher würden Sie Ihr Einschätzungsvermögen betrachten?

Sehr sicher ☐ ☐ ☐ ☐ ☐ Sehr unsicher

i

12) Glauben Sie, dass Ihr Einschätzungsvermögen im Laufe des Versuchs verbessert wurde?

☐ Ja ☐ Nein

Nur für Teilnehmer der Testgruppe:

13) Glauben Sie, dass der Einsatz von Ton Ihr Einschätzungsvermögen verbessert hat?

☐ Ja ☐ Nein

14) Glauben Sie, dass der Einsatz von Vibration Ihr Einschätzungsvermögen verbessert hat?

☐ Ja ☐ Nein

15) Glauben Sie, dass die Kombination von Ton und Vibration Ihr Einschätzungsvermögen verbessert hat?

☐ Ja ☐ Nein

16) Glauben Sie, dass die Kombination von Ton, Vibration und Blur Ihr Einschätzungsvermögen verbessert hat?

☐ Ja ☐ Nein

C. Questionnaire for Study with Test Subjects using Artificial Motor Sound, Vibration at the Driver's Seat, Blur while Driving

Fragebogen

Vielen Dank, dass Sie sich für den Versuch zur Verfügung stellen. Ihre Daten werden selbstverständlich anonym behandelt.

Bitte lesen Sie sich die Fragen genau durch und beantworten Sie diese so genau wie möglich.

Bitte beantworten Sie VOR dem Versuch nur die erste Seite des Fragebogens.

1) Wie alt sind Sie? …………………..

2) Sind Sie männlich oder weiblich? ☐ männlich ☐ weiblich

3) Seit wie vielen Jahren besitzen Sie einen Führerschein der Klasse B? …………………..

4) Wie viele Kilometer fahren Sie pro Jahr ca.? …………………..

5) Müssen Sie eine Sehhilfe beim Autofahren tragen? ☐ Ja ☐ Nein

6) Ist Ihr Hörvermögen beeinträchtigt? ☐ Ja ☐ Nein

7)Wie schätzen Sie Ihren Fahrstil ein? Bitte kreuzen Sie an.
Sportlich langsam und vorsichtig

Sportlich ☐ ☐ ☐ ☐ ☐ langsam und vorsichtig

8) Wie verhalten Sie sich gegenüber Geschwindigkeitsbegrenzungen?

Ich halte mich streng an sie ☐ ☐ ☐ ☐ ☐ Ich beachte sie nur, wenn ich von ihrer Notwendigkeit überzeugt bin.

9) Haben Sie schon einmal an einem Fahrversuch teilgenommen? ☐ Ja ☐ Nein

-Seite 1-

10) Als wie sicher würden Sie Ihr Einschätzungsvermögen betrachten?
Sehr sicher Sehr unsicher

Sehr sicher ☐ ☐ ☐ ☐ ☐ Sehr unsicher

11) Glauben Sie, dass Ihr Einschätzungsvermögen im Laufe des Versuchs verbessert wurde?

☐ Ja ☐ Nein

Nur für Teilnehmer der Testgruppe:

12) Glauben Sie, dass der Einsatz von Ton und Vibration Ihr Einschätzungsvermögen verbessert hat?

☐ Ja ☐ Nein

13) Glauben Sie, dass der Einsatz von Blur Ihr Einschätzungsvermögen verbessert hat?

☐ Ja ☐ Nein

14) Glauben Sie, dass die Kombination von Ton, Vibration und Blur Ihr Einschätzungsvermögen verbessert hat?

☐ Ja ☐ Nein

-Seite 2-